

INFORMATION TO USERS

This manuscript has been reproduced from the microfilm master. UMI films the text directly from the original or copy submitted. Thus, some thesis and dissertation copies are in typewriter face, while others may be from any type of computer printer.

The quality of this reproduction is dependent upon the quality of the copy submitted. Broken or indistinct print, colored or poor quality illustrations and photographs, print bleedthrough, substandard margins, and improper alignment can adversely affect reproduction.

In the unlikely event that the author did not send UMI a complete manuscript and there are missing pages, these will be noted. Also, if unauthorized copyright material had to be removed, a note will indicate the deletion.

Oversize materials (e.g., maps, drawings, charts) are reproduced by sectioning the original, beginning at the upper left-hand corner and continuing from left to right in equal sections with small overlaps. Each original is also photographed in one exposure and is included in reduced form at the back of the book.

Photographs included in the original manuscript have been reproduced xerographically in this copy. Higher quality 6" x 9" black and white photographic prints are available for any photographs or illustrations appearing in this copy for an additional charge. Contact UMI directly to order.

UMI

**A Bell & Howell Information Company
300 North Zeeb Road, Ann Arbor MI 48106-1346 USA
313/761-4700 800/521-0600**



Université d'Ottawa • University of Ottawa

A Continuous Thermodynamics Model for Multicomponent Droplet Vaporization

Jihane Tamim

**A thesis presented to The School of Graduate Studies and Research
in partial fulfilment of the requirements for the
degree of
Master of Applied Science
in the Department of Chemical Engineering
University of Ottawa**

December 1996

Jihane Tamim, 1996.



**National Library
of Canada**

**Acquisitions and
Bibliographic Services**

**395 Wellington Street
Ottawa ON K1A 0N4
Canada**

**Bibliothèque nationale
du Canada**

**Acquisitions et
services bibliographiques**

**395, rue Wellington
Ottawa ON K1A 0N4
Canada**

Your file Votre référence

Our file Notre référence

The author has granted a non-exclusive licence allowing the National Library of Canada to reproduce, loan, distribute or sell copies of his/her thesis by any means and in any form or format, making this thesis available to interested persons.

The author retains ownership of the copyright in his/her thesis. Neither the thesis nor substantial extracts from it may be printed or otherwise reproduced with the author's permission.

L'auteur a accordé une licence non exclusive permettant à la Bibliothèque nationale du Canada de reproduire, prêter, distribuer ou vendre des copies de sa thèse de quelque manière et sous quelque forme que ce soit pour mettre des exemplaires de cette thèse à la disposition des personnes intéressées.

L'auteur conserve la propriété du droit d'auteur qui protège sa thèse. Ni la thèse ni des extraits substantiels de celle-ci ne doivent être imprimés ou autrement reproduits sans son autorisation.

0-612-20955-5

ACKNOWLEDGEMENTS

I express deep gratitude to Professor William L. H. Hallett for his guidance and encouragement, for providing a comfortable working atmosphere, for always being available for discussions and for his patience during these past two years. His quick and careful editing of the manuscript and his comments contributed significantly to the quality of this thesis.

I would also like to thank my family for their constant morale support, help and encouragement.

ABSTRACT

For mixtures containing many components, as in the case of commercial fuels and polymer solutions for example, it is practically impossible to have a complete listing of all the components. A method known as continuous thermodynamics has recently been developed for use when dealing with such mixtures. Continuous thermodynamics describes the composition of the mixture by a probability density function with respect to one or more variable, such as molecular mass, boiling point or any other physical property.

This method is used here to study the vaporization of multicomponent fuel droplets. Liquid droplet vaporization plays an important role in the formation of the fuel/air mixture necessary for combustion, and the fuel composition has an effect on the performance of combustion equipment such as Diesel engines.

Transport equations are developed, which describe species diffusion in terms of the parameters of the distribution function. These equations are developed for “fuel” vapour as a whole and for the mean and second moment of the distribution. A continuous thermodynamics form of the energy equation is also developed. These general equations are then applied to the vaporizing droplet problem.

A gamma distribution function, with molecular mass as the characterizing variable has been chosen. The transport equations in continuous form have been incorporated into a finite difference model of droplet vaporization. Physical property correlations have also been developed in terms of the characterizing variable chosen and integrated in the model.

The numerical solution of these equations and the equations of conservation of mass

and species at the droplet surface gives the droplet vaporization rate, the mixture composition field in the vapour phase surrounding the droplet and the change of the liquid composition with time.

SOMMAIRE

Pour les mélanges qui contiennent plusieurs composants comme pour les carburants commerciaux et les solutions de polymères, il est presque impossible d'obtenir la liste complète de tous les composants présents. Une méthode connue sous le nom de "thermodynamique continue" a récemment été développée pour étudier ces mélanges complexes. La "thermodynamique continue" décrit la composition du mélange à l'aide d'une fonction de probabilité en fonction d'une ou plusieurs variables comme par exemple la masse moléculaire, le point d'ébullition ou tout autre propriété physique. Cette méthode est utilisée, ici, pour étudier la vaporisation d'une goutte d'un mélange de carburant contenant un nombre inconnu de composants. La vaporisation des gouttes de carburant joue un rôle important dans la formation du mélange air/carburant nécessaire pour la combustion. De plus, la composition du carburant a une grande influence sur la performance des systèmes à combustion comme les moteurs Diesel.

Les équations qui décrivent la diffusion des composants et le transport d'énergie sont développées en fonction des paramètres de la fonction de distribution choisie. Dans ce cas-ci, la fonction de distribution gamma a été choisie avec comme variable la masse moléculaire. Les équations de transport, dérivées en terme de la thermodynamique continue, ont été incorporées dans un modèle numérique décrivant la vaporisation d'une goutte de carburant. Les propriétés physiques ont également été modélisées en fonction de la variable de la distribution et intégrées dans le modèle.

La solution numérique de ces équations et des équations de conservation de masse et de concentration à la surface de la goutte permet d'obtenir le taux de vaporisation, la composition du

mélange dans la phase vapeur autour de la goutte et le changement de composition dans la phase liquide.

NOMENCLATURE

A	droplet surface area, (m^2)
c	vapour molar density, ($kmol/m^3$)
c_L	liquid molar density, ($kmol/m^3$)
\bar{C}_p	mixture specific heat, ($kJ/kmol K$)
D	diffusion coefficient, (m^2/s)
D_{im}	effective diffusivity of component i in the mixture, (m^2/s)
$\bar{D}, \hat{D}, \tilde{D}$	average diffusivities weighted with respect to the mol fraction, the mean of the distribution and the variance of the distribution, (m^2/s)
$f(I)$	probability density function
h_{fg}	heat of vaporization, ($kJ/kmol$)
\bar{h}_i	partial molal enthalpy of component i , ($kJ/kmol K$)
I	distribution parameter
J_i^*	molar flux, ($kmol/m^2s$)
N	molar flux from the droplet, ($kmol/m^2s$)
P	total pressure, (kPa)
P_v	vapour pressure, (kPa)
q	heat flux to the droplet surface by conduction, (W/m^2)
r	radial position, (m)
R	droplet radius, (m)
\dot{R}	$=dR/dt$
S_{fg}	entropy of vaporization, ($kJ/kmol K$)
t	time, (sec)
T	temperature, (K)
T_B	boiling point, (K)
V	droplet volume, (m^3)
\bar{v}^*	molar average velocity, (m/s)

w	velocity relative to ξ coordinate
y, x	vapour and liquid mol fraction respectively

Greek Letters

α, β	parameters of the Gamma distribution
γ	origin of the distribution
Γ	gamma function
θ, θ_L	mean molecular mass of the vapour and liquid phase distribution respectively, (kg/kmol)
λ	thermal conductivity, (W/m K)
$\xi = r/R$	dimensionless coordinate
ρ_L	mass density of the liquid, (kg/m ³)
σ, σ_L	standard deviation of the vapour and liquid distribution respectively
$\psi = \theta^2 + \sigma^2$	second moment about the origin of the density function (vapour phase)
ψ_L	second moment about the origin of the density function (liquid phase)

Subscripts:

A, F	refers to air and fuel respectively
E, W	eastern and western grid point respectively
i	chemical species
L	liquid
m	mixture
N	number of grid points in the vapour phase
P	grid point
R	droplet surface
T_{cr}	critical temperature, (K)
∞	ambient condition

Superscripts

- $^{\circ}$ previous time step
- $'$ trial value

Linearization Coefficients:

- a constant of the linearization
- b slope

- a_B, b_B linear variation coefficients in the equation for T_B
- a_C, b_C linear variation coefficients in the equation for $C_p(T)$
- a_{cr}, b_{cr} linear variation coefficients in the equation for T_{cr}
- a_K, b_K linear variation coefficients in the equation for λ thermal conductivity
- a_L, b_L, c_L linear variation coefficients in the equation for the liquid specific heat C_{pL}

TABLE OF CONTENTS

ACKNOWLEDGEMENT	i
ABSTRACT	ii
SOMMAIRE	iv
NOMENCLATURE	vi
TABLE OF CONTENTS	ix
LIST OF FIGURES	xi
LIST OF TABLES	xiv
1. INTRODUCTION	1
1.1 Multicomponent fuels	1
1.2 Droplet Evaporation and Ignition	4
1.3 Previous Work	6
1.4 Objectives	7
2. LITERATURE REVIEW	9
2.1 Introduction	9
2.2 Droplet Evaporation	9
2.2.1 Basic Processes	9
2.2.2 Multicomponent Droplets	11
2.2 Continuous Thermodynamics	13
2.3 Conclusion	18
3. MATHEMATICAL MODEL	20
3.1 Introduction	20
3.2 Transport Equations for the Vapour Phase	21
3.2.1 Vapour Phase Basic Equations	21
3.2.2 Species Transport Equation In Continuous Form	22
3.2.3 Energy Equation in Continuous Form	30
3.3 Liquid Phase Balance Equations	32
3.4 Enthalpy of vaporization	39
3.5 Vapour Liquid Equilibrium	39
3.6 Distribution Function	44

4. NUMERICAL MODEL	46
4.1 Numerical Solution	46
4.1.1 Finite Volume Solution	46
4.1.2 Computational Grid and Time Step	51
4.2 Transport Property Correlations	53
4.2.1 Reference State	53
4.2.2 Enthalpy of vaporization	54
4.2.3 Heat Capacity for Vapour Phase	62
4.2.4 Heat Capacity for Liquid Phase	62
4.2.5 Thermal Conductivity of Vapour Phase:	66
4.2.6 Vapour Phase Diffusivity	68
5. RESULTS AND DISCUSSION	72
5.1 Simulation of a single-component fuel	72
5.2 Selection of distribution functions for commercial fuels	76
5.3 Simulation of a gasoline fuel	81
5.4 Simulation of a Diesel fuel	93
6. CONCLUSIONS AND RECOMMENDATIONS	98
6.1 Conclusions	98
6.2 Recommendations	99
LIST OF REFERENCES	101
APPENDIX A	105
APPENDIX B	107
APPENDIX C	108
APPENDIX D	109
APPENDIX E	115

LIST OF FIGURES

Figure 1.1:	Typical ASTM D86 distillation curve for gasoline	3
Figure 1.2:	Temperature and fuel concentration profiles near a vaporizing droplet ..	5
Figure 3.1:	Temporal variation of the average volatile molar fractions for mixtures of hexadecane with tetradecane, dodecane, and decane.	34
Figure 3.2:	Normal boiling points of n-alkanes in terms of molecular mass	43
Figure 4.1:	Diagram of cell around droplet	49
Figure 4.2:	Flow chart of computer program	51
Figure 4.3:	Exponentially spaced grid	52
Figure 4.4:	Heat of vaporization at normal boiling point as a function of molecular mass	56
Figure 4.5:	Correlated and actual molar heat of vaporization at normal boiling point with respect to molecular mass	57
Figure 4.6:	Variation of the critical temperature with molecular mass for n-alkanes	61
Figure 4.7:	Variations of n-alkane liquid heat capacity with molecular mass at two different temperatures: 250 and 300 K	64
Figure 4.8:	Comparison of Luria-Benson, Hadden and the present liquid heat capacity correlation at 300 K for n-alkanes	65
Figure 4.9:	Present correlation for vapour phase thermal conductivity compared to literature values	67
Figure 4.10:	Theoretical and calculated values for vapour phase diffusivities	71
Figure 5.1:	Comparison of the results obtained from single pure component calculations using the Antoine equation and the Clausius-Clapeyron ..	74

Figure 5.2:	Liquid Temperature T_L and mass fraction evaporated m/m_o versus time for 1.5 diameter n-dodecane droplet. Comparison of predictions from the continuous thermodynamics model with single pure component calculations.	75
Figure 5.3:	ASTM D86 curves predicted using continuous thermodynamics for gasoline and Diesel, compared to actual values (Kallio et al., 1985). ...	79
Figure 5.4:	Distribution curves for both gasoline and Diesel using the parameter values fitted to the ASTM curve.	80
Figure 5.5:	Distribution functions of the liquid phase and the vapour phase at the droplet surface for a 1.5 mm gasoline droplet.	85
Figure 5.6:	Time histories of liquid phase properties and of vapour phase mol fraction at the surface y_{FR} for a 0.1 mm gasoline droplet	86
Figure 5.7:	Time histories of liquid phase properties and of vapour phase mol fraction at the surface y_{FR} for a 1.5 mm gasoline droplet	87
Figure 5.8:	Vapour phase properties as a function of dimensionless radius (r/R) for a 0.1 mm "gasoline" droplet	88
Figure 5.9:	Vapour phase properties as a function of dimensionless radius (r/R) for a 1.5 mm "gasoline" droplet	89
Figure 5.10:	Vapour phase properties as a function of dimensionless radius (r/R) for a 1.5 mm "gasoline" droplet. Model run with all three average diffusivities set equal.	90
Figure 5.11:	Liquid temperature and boiling point temperature for a 1.5 mm "gasoline" droplet evaporating. Comparison of results obtained with a time step of 0.01 s with results obtained with a time step half time smaller.	91
Figure 5.12:	Liquid and boiling point temperatures for a 1.5 mm "gasoline" droplet. Comparison of the results obtained with a 20 and a 40 grid point model.	92
Figure 5.13:	Time histories of liquid phase properties and of vapour phase mol fraction at the surface y_{FR} for a 0.1 mm Diesel droplet.	94

Figure 5.14: Time histories of liquid phase properties and of vapour phase mol fraction at the surface y_{FR} for a 1.5 mm Diesel droplet.	95
Figure 5.15: Vapour phase properties as a function of dimensionless radius (r/R) for a 0.1 mm Diesel droplet	96
Figure 5.16: Vapour phase properties as a function of dimensionless radius (r/R) for a 1.5 mm Diesel droplet	97

LIST OF TABLES

Table 4.1:	Values of parameters for enthalpy of vaporization correlation	59
Table 5.1:	ASTM Distillation Test for Diesel Fuel	77
Table 5.2:	ASTM Distillation Test for gasoline	78

1. INTRODUCTION

1.1 Multicomponent fuels

The combustion of liquid fuel is of considerable practical importance since liquid petroleum constitutes a significant share of the total energy requirements of the world. Petroleum, synthetic fuels and other multicomponent mixtures have an exceedingly complex composition, consisting, in the case of petroleum, of many different hydrocarbons and some inorganic and other organic compounds. The number of carbon atoms in the components may range from five to more than 50, so that the compounds may exhibit atmospheric pressure boiling points from $65^{\circ}C$ to $300^{\circ}C$ or more. In a given boiling range, the number of different compounds that exhibit only small differences in volatility (e.g. isomers) multiplies rapidly with increasing boiling point.

In spite of the importance of mixtures of real fuels and the increasing utilization of synthetic fuels made of different mixtures, there is little information in the literature about the vaporization and combustion of multicomponent liquid fuel droplets. In most of the work done, single component or binary mixture droplets were considered; very few studies deal with more than two components. Commercial fuels, however, are usually mixtures of hundreds of components with different boiling points. It is practically impossible most of the time to have a complete listing of these components, which makes calculations for the design or operation of such systems difficult. During droplet combustion, these fuel

components undergo various chemical and physical changes that influence the rate of evaporation and combustion, which in turn have a great influence on the performance of combustion systems. Therefore, an understanding of how the chemical and physical processes affect the way mixtures evaporate is essential for efficient use of fuels in combustion. The present work introduces a model for the evaporation of droplets of complex liquid mixtures or mixtures with an indefinite number of components.

A simple method widely used in industry to characterize such mixtures is the ASTM D 86 distillation test. As described in Perry's Chemical Engineer's Handbook (1984), 100 ml of a sample is charged to a flask and heated at a sufficient rate to produce the first drop of distillate from the lower end of the condenser tube in from 5 to 15 min, depending on the nature of the sample. The temperature of the liquid at that instant is recorded as the initial boiling point (IBP). Heating is continued at a rate such that the time from the IBP to 5 volume percent recovered of the sample in the cylinder is 60 to 75 s. Again, the vapour temperature is recorded. Then successive vapour temperatures are recorded from 10 to 90 percent recovered in intervals of 10, and at 95 percent recovered, with the heating rate adjusted so that 4 to 5 ml are collected per minute. At 96 percent recovered, the burner flame is increased if necessary to achieve the maximum vapour temperature, referred to as the end point (EP), in from 3 to 5 additional min. The percent recovery is reported as the maximum percent recovered in the cylinder. Any residue remaining in the flask is reported as percent residue, and percent loss is reported as the difference between 100 ml and the sum of the percent recovery and percent residue. Fig. 1.1 shows the results of a typical ASTM distillation test for an automotive gasoline.

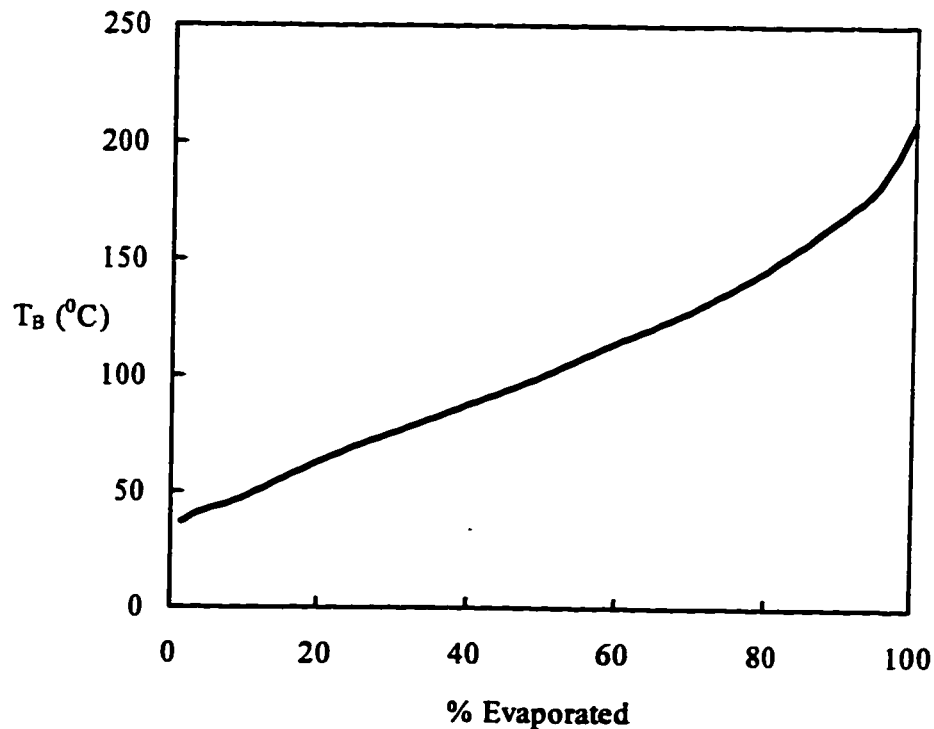


Figure 1.1: Typical ASTM D86 distillation curve for gasoline. (Data taken from Perry's Chemical Engineers Handbook, 1984)

The description of composition by mole fraction is very simple when the mixture contains two or three components but when a large number of very similar chemical species is involved, as in the case of polymers and commercial fuels, it becomes much more difficult. Mixtures such as these are called complex mixtures. Calculations for these mixtures are often done using the pseudo-component method, in which components are arbitrarily lumped together into groups and each group is considered as a pure component. This method's main disadvantage is its high sensitivity to the arbitrary choice of the pseudo-components. In recent years, a new method has been developed to describe mixtures containing large numbers of components, called *Continuous Thermodynamics*. Instead of

describing the mixture composition by mole fractions, as it is usually done in classical thermodynamics, when using the methods of continuous thermodynamics the mixture composition is represented by a continuous probability density function of a characterizing variable. This variable could be any relevant physical property, such as component molecular mass or boiling temperature.

Continuous thermodynamics is used in this work to model the vaporization of a single multicomponent droplet. The ASTM distillation curve will be used as the basis for choosing a continuous thermodynamics composition model to describe a commercial gasoline or Diesel fuel.

1.2 Droplet Evaporation and Ignition

Fuel and air must be well mixed to cause combustion. For better mixing of fuel and air, spray combustion is used in most liquid fuel systems, such as Diesel engines, gas turbines and industrial furnaces. The method of spraying is not particular to combustion systems but is used in many engineering processes. At injection in combustion systems, fuel is atomized to fine droplets to enlarge the surface area for faster evaporation. The subsequent processes are numerous, namely, mixing with air, heat transfer to the droplets, evaporation and mixing of fuel vapour with air, ignition, and burning of the vapour. The vaporization and burning of the droplets have a great influence on the performance of combustion systems. Because of the complexity of these processes, and the interaction of

the droplets and their vapours, much of the research on liquid combustion is done on single fuel droplets. Thus, in order to understand the process of spray combustion, a good knowledge of single droplet behaviour is required.

Since the droplet temperature at the surface is lower than the surroundings, heat is transferred towards the droplet by conduction (see Fig. 1.2). At the surface, part of this heat is transferred inside the droplet which begins to heat up, while the other part is used to vaporize the liquid at the surface. As the concentration of fuel is lower in the surroundings of the droplet, a concentration gradient occurs outwards and fuel is transported away from the droplet. The depletion of the fuel vapour at the surface makes it possible for more evaporation to take place. A liquid mass is continuously converted to vapour which is dispersed to the surroundings. The rate controlling processes are then mass and heat transfer.

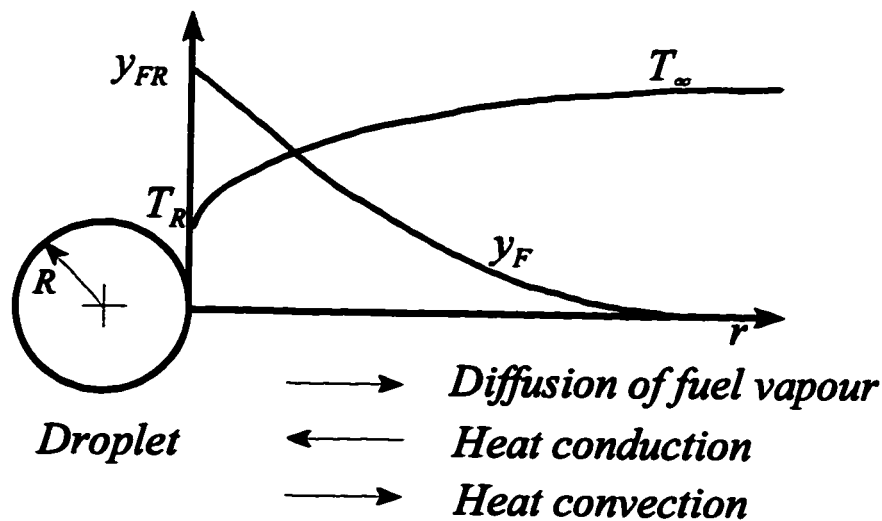


Figure 1.2: Temperature and fuel concentration profiles near a vaporizing droplet.

Droplet ignition consists of two steps. First, the droplet is subjected to a high temperature and starts evaporating. The vapour diffuses out and mixes with the air, and chemical reaction begins in the vapour phase. As more vapour diffuses out and the temperature rises, the reaction accelerates to thermal runaway - this is ignition.

1.3 Previous Work

This study builds on earlier work on droplet mixture processes at the University of Ottawa. Previous work done by Bergeron and Hallett (1989a, 1989b) described the ignition of liquid fuel at atmospheric pressure. A mathematical model was developed to predict the time required for evaporation and ignition of a single and a two-component droplet after sudden exposure to a hot air environment. The energy, diffusion and continuity equations were solved for time-varying conditions in the vapour phase surrounding the droplet using a finite volume method. Several assumptions were made to reduce computational effort: spherical symmetry, constant transport properties (constant with space), uniform droplet temperature and negligible chemical reaction effect on species concentrations prior to ignition. For two component fuels, the liquid diffusion equation was solved numerically, the combined effects of molecular diffusion and internal circulation being represented by an effective liquid diffusivity.

Ruszalo and Hallett (1991) extended the low pressure model to a high pressure model to simulate a Diesel engine environment. Some modifications were investigated and

added to suit the model for high pressure environment, such as a suitable vapour-liquid equilibrium calculation to describe the droplet surface, the effect of absorption and diffusion of air in the liquid phase, and appropriate correlations for transport properties at high pressures.

Hallett and Ricard (1992) applied the low pressure model developed by Bergeron and Hallett (1989b) to a number of seven-component hydrocarbon mixtures to test the effects of boiling curve and chemical composition on ignition. The model was based on the same assumptions: the liquid phase was assumed well-mixed and vapour-liquid equilibrium was modelled using Raoult's law with component vapour pressures from the Antoine's equation.

1.4 Objectives

The present work is a first step in studying the ignition and combustion of droplets of complex multicomponent mixtures, which will help in the modelling of the chemical and physical processes necessary for the design of combustion systems. The main objective is to apply the principles of continuous thermodynamics to model the evaporation of droplets of complex mixtures. In order to do this, transport equations in continuous formulation first had to be developed; these equations will be found to represent the diffusion and convection of species as the transport of the parameters of the distribution function describing the mixture composition. In previous work on multicomponent droplets, only two or three

component mixtures were considered; very few researchers have discussed more complex mixtures, and the method of continuous thermodynamics has never been used before to solve this or other combustion problems.

The numerical model developed is an extension of the single component droplet model developed by Ruzsalo and Hallett (1991). To apply the model to a multicomponent droplet using continuous thermodynamics substantial modifications were required:

- Formulation of numerical (finite volume) approximations to the transport equations.
- Selection of an appropriate distribution function to represent the fuel mixture.
- Selection of an appropriate characterizing variable for the distribution.
- Development of correlation equations for the transport properties in terms of the distribution characterizing variable.

The next chapter will give a brief review of the research done on droplet evaporation, especially for droplets of mixtures, as well as a literature survey of the methods of continuous thermodynamics. The mathematical model based on the principles of continuous thermodynamics is presented in chapter 3 along with the transport properties correlations developed to solve this problem. The numerical solution chosen to solve the problem is presented in chapter 4. Results and discussion are shown in chapter 5, followed by the conclusions and recommendations for further work in chapter 6.

2. LITERATURE REVIEW

2.1 Introduction

Liquid droplets undergoing vaporization or condensation are frequently encountered in many areas of technical importance employing liquid sprays. Liquid fuel combustion is one application in which the importance of the droplet is due to its role in the formation of the fuel/air mixture. There is extensive information in the literature about liquid fuel droplet vaporization and ignition but most of the studies consider single or two-component droplets. This chapter will briefly review the droplet evaporation process, especially for multicomponent fuel droplets, and the technique of continuous thermodynamics used in this work to solve the problem.

2.2 Droplet Evaporation

2.1.1 Basic Processes

If an isolated pure component droplet is suddenly subjected to a hot oxidizing environment, it starts evaporating. As the droplet temperature is lower than the surroundings, heat is transferred to the droplet through conduction. At the surface, part of this heat is used to heat up the liquid fuel and the other part is used to vaporize the liquid at the droplet surface. As the droplet continues to vaporize, the vapour diffuses away from the

surface to the less concentrated surroundings. The basic model describing droplet evaporation and the most often used one is the quasi-steady state model, in which the gas phase properties at any instant in time are assumed to be approximately at steady state. For a pure component droplet at constant liquid temperature, this means that the square of the droplet diameter varies linearly. For this reason, this model is also referred to as the “ d^2 Law”. Some of the major assumptions on which this model is based are:

- Spherical symmetry: forced and natural convection are neglected or treated as acting in a spherical symmetrical film;
- Constant gas phase properties, evaluated at an appropriate reference state;
- Gas phase quasi-steadiness: because of the density difference between liquid and gas, the liquid properties change at a very slow rate compared to the gas phase changes so that the boundary locations and conditions can be considered constant and the gas treated as at steady state; (Williams, 1973; Faeth, 1977; Law, 1982).
- Ideal liquid-vapour behaviour;

With these assumptions, the model becomes a steady, one dimensional flow governed by ordinary differential equations. Since the quasi-steady state theory was developed, many studies have included the transient terms in the model (Bergeron and Hallett, 1989b), the effects of forced and natural convection have been studied, and some work has also been done to evaluate the effects of variable properties compared to constant properties. As models become more and more complex, numerical solutions are required to solve the

equations. A complete review of droplet processes is given by Bergeron and Hallett (1989b), Williams (1973), Faeth (1977) and Law (1982).

2.2.2 Multicomponent Droplets

Multicomponent effects were originally not considered serious and most studies on droplet evaporation and combustion used pure fuels. However, hydrocarbon fuels consist of large numbers of components with a wide range of boiling points (e.g. $65^{\circ}C$ - $300^{\circ}C$ or more). More and more research is also being directed to the utilization of alternative fuels such as alcohol/oil, coal/oil or water/oil mixtures. The widely different physical and chemical properties of all these fuels necessitate the consideration of multicomponent effects.

According to Law (1982), three major factors have to be considered when trying to understand multicomponent fuel behaviour:

- The relative concentrations and volatilities of the liquid components;
- The miscibility of the liquid constituents, which controls the phase change characteristics;
- The intensity of liquid motion, which controls the rate at which the components are exposed to the surface of the droplet.

The last point is a major problem when dealing with multicomponent fuels. The liquid constituents can only vaporize once they are exposed to the surface. The degree of

mixedness of the liquid phase gave rise to two limiting theories when modelling the behaviour of a multicomponent fuel: the diffusion-limited model and the batch distillation model (also called the well-mixed model).

The diffusion-limited theory is based on the assumption that there is no circulation or liquid motion within the droplet so that the components are brought to the surface through diffusion only. Liquid phase diffusion, which limits the rate of supply of components to the surface, is a very slow process compared to the rate of surface area regression during rapid vaporization (Law, 1982), so that the relative volatilities, have less effect on the vaporization. In this case, the droplet temperature and concentration profiles are not uniform across the liquid phase (Williams, 1973; Faeth, 1977; Law, 1982).

The assumption in the batch distillation model is that in realistic situations some liquid motion always exists, induced either by the buoyant motion of air around the droplet or as a result of the droplet velocity acquired at injection (Law, 1982). As a result of the liquid motion, the temperature and composition of the droplet are considered to be uniform at each instant but vary with time. The vaporization of the droplet follows then the process of a batch distillation, in which the most volatile component vaporizes first (Hallett and Ricard, 1992).

Landis and Mills (1974) published one of the earliest papers on the evaporation of a two-component fuel droplet, in which they compared the results of a well-mixed model and a diffusion-limited model. Their conclusion was that a rigorous model of multicomponent droplet evaporation should account for internal liquid circulation.

Real droplets generally possess some degree of internal fluid motion and exhibit

behaviour intermediate between a well-mixed and a diffusion-limited; this has been modelled either as a vortex flow within the droplet (Tong and Sirignano, 1986), or more simply, as an increase in the effective radial diffusion rate (Randolph *et al.*, 1986; Talley and Yao, 1986; Bergeron and Hallett, 1989b).

Very little appears in the literature on mixtures with more than two components. One of the earliest works is that of Newbold and Amundson (1973) who developed a quasi-steady state model with a well-mixed droplet to solve the vaporization problem for a three-component mixture. The most complex mixture modelled to date is that of Hallett and Ricard (1992), in which a study of droplet ignition was done for a seven-component hydrocarbon mixture, and the results showed that ignition was controlled by the most volatile component in the mixture. A qualitative understanding of the behaviour of commercial petroleum fuels has been gained by the experiments of Chen and El-Wakil (1969) and of Braide *et al.* (1979), but modelling of these fuels has only been attempted on an empirical basis, using an ASTM distillation curve to describe the progress of droplet vaporization (Bardon *et al.*, 1990; Rah *et al.*; 1986). There are therefore no general models for the evaporation and combustion of complex mixtures.

2.2 Continuous Thermodynamics

The description of the chemical composition of multicomponent mixtures is a problem not only for liquid fuel combustion but also in many other processes such as

distillation, separation and fractionation of complex mixtures. Examples of such complex mixtures are higher petroleum fractions, coal-derived liquids and polymer solutions in which a large number of very similar chemical species occurs, in the order of hundreds or thousands. If a mixture contains 2 or 3 components, description of the composition by mole fraction usually is not a problem. But for complex mixtures, the mole fractions of the individual components are usually unknown, and even if they were known, managing a system of hundreds of equations for some hundreds of components would be very complicated. For such cases, instead of the mole fractions of individual components, the composition of these mixtures can be given by a continuous distribution function, hence the term describing this method: "*Continuous Thermodynamics*" or "*Thermodynamics of Continuous Mixtures*".

In classical thermodynamics, the quantities considered are functions depending on the mole fractions of the components. In complex mixtures, it is sometimes impossible to determine the number of components present and thus the mole fractions are unknown. For such mixtures, classical thermodynamics is difficult to apply. In continuous thermodynamics, the mole fraction is replaced by a continuous distribution function $F(I)$, where I is the characterizing variable for the mixture. The characterizing variable could be any physical property such as molecular mass, carbon number, boiling point or others.

The idea of describing complex mixtures using continuous functions dates back at least sixty years but it is only in the last 20 years that it has been used more extensively. Katz and Brown (1933) presented a method for calculating the vapour pressure of petroleum fractions. When dealing with complex mixtures, the authors suggested using the same

methods as for discrete mixtures but in differential form, with the composition of the mixture expressed in terms of the true boiling point obtained from an efficient distillation column. The assumption made was that the properties of the complex mixture have to be continuous throughout the range of composition to enable the use of the data and properties of the pure hydrocarbons for any point on the true boiling point curve. This is considered to be the first paper on continuous thermodynamics.

Most of the work in the literature about continuous thermodynamics deals with converting classical thermodynamics relations into a form adapted to the continuous distribution function (Kehlen and Rätzsch *et al.*, 1980, 1983, 1985, 1988, 1989; Briano and Glandt, 1983; Du and Mansoori, 1986; Willman and Teja, 1987; Ying *et al.*, 1989). The method has been applied to a number of processes, including distillation calculations, dew and bubble point calculations and flash calculations. These calculations have been done for hydrocarbon mixtures (Kehlen and Rätzsch *et al.*, 1983, 1985, 1988, 1989) and polymer solutions (Kehlen and Rätzsch *et al.*, 1983). Three major points have to be considered when solving a problem using continuous thermodynamics:

- The choice of the distribution function;
- The choice of the characterizing variable(s);
- The vapour-liquid equilibrium relation when necessary.

The choice of F , the probability distribution function, is determined primarily by its ability to represent reality to a sufficient degree of approximation. However, another

consideration in the choice of F is mathematical convenience. If an analytical solution is sought, some functions F are more suitable than others. The simplest distribution to use is the Gaussian distribution (Hoffman, 1968; Kehlen and Rätzsch, 1980, 1983, 1985, 1988, 1989). The main problem with the Gaussian distribution is that it is unbounded in both directions, which is unrealistic because molecular mass, carbon numbers and other distribution variables have a lower bound. One of the most used distribution functions is the Gamma (Γ) distribution function (Whitson, 1983; Cotterman, Prausnitz *et al.*, 1985; Chou and Prausnitz, 1986, Willman and Teja, 1987). It is reasonably simple, gives a good representation for petroleum fractions, and is bounded at the lower end. Other distributions have been successfully used by others: Peng *et al.* (1987) used the beta distribution, while Haynes and Matthews (1991), for a hydrocarbon mixture, used the experimental true boiling point distillation curve as the distribution function.

The distribution function chosen can be characterized by one or more variables. Although the literature states that real fluids are best represented by two or three characterizing variables (Gualtieri *et al.*, 1982; Briano and Glandt, 1983), most of the work on continuous systems has considered the simple situation of a single distributed variable I . This characterizing variable can be any physical or chemical property. Hoffman (1968), Cotterman and Prausnitz *et al.* (1985), Kehlen and Rätzsch (1980, 1983, 1985, 1988, 1989), and Haynes and Matthews (1991) used the normal boiling point of the mixture considered. Gal-Or *et al.* (1975), Whitson (1983), Cotterman and Prausnitz *et al.* (1985), Chou and Prausnitz (1986), and Ying *et al.* (1989) used the molecular mass as a characterizing variable. Willman and Teja (1987) used the carbon number as a characterizing variable to

calculate dew points of natural gas condensates.

The most important application of continuous thermodynamics deals with the vapour-liquid equilibrium relation (Kehlen and Rätzsch, 1983). Different approaches are discussed in the literature. An approach used by Kehlen and Rätzsch *et al.* in most of their work (1980, 1983, 1985, 1988, 1989), with good reported results, is the assumption of ideal solution behaviour in all the systems they have studied. Vapour-liquid equilibrium for the mixture was described using Raoult's law, and the Clausius-Clapeyron equation and Trouton's rule were used to express the component vapour pressure in terms of the distribution variable. The technique was applied to flash calculations for a crude oil (1988) and distillation calculations of hydrocarbon mixtures (1983, 1985, 1989).

Another approach using an equation of state for solving equilibrium problems in continuous mixtures has been developed by Gualtieri *et al.* (1982). They used the Van der Waals equation of state to solve for the fractionation of a polydisperse impurity dissolved in a solvent. Chou and Prausnitz (1986) performed flash calculations of continuous mixtures based on the Soave-Redlich-Kwong equation of state, while Du and Mansoori (1986) used the Peng-Robinson equation of state. Cotterman, Prausnitz *et al.* (1985) reported good agreement between calculated and experimental results for dew point calculations of a natural gas using the Soave-Redlich-Kwong equation of state. Willman and Teja (1987) also performed dew point calculations of a natural gas using the virial equation of state and compared their results to the ones obtained by Cotterman and Prausnitz *et al.* (1985). Their conclusion was that both methods were comparable, whether the Soave-Redlich-Kwong or the virial equation of state is used.

All of the applications of continuous thermodynamics cited have been to operations in which transport processes (diffusion and convection) are unimportant. However, continuous thermodynamics has great potential for modelling transport processes involving complex fluid mixtures in such areas as combustion and detailed modelling of refinery operations. So far, no solutions to such problems have been published, excepting the present work. The only paper which undertakes any steps towards the development of the necessary transport equations is that of Gal-Or *et al.* (1975), but in their derivations of the equations, they considered the diffusion coefficient as being independent of the molecular mass which is not normally true.

All the literature cited reports that the method of continuous thermodynamics provides a more accurate representation of complex mixtures than the pseudo-component method, and an important reduction in computer time is registered when running models using this method.

2.3 Conclusion

The conclusions that are drawn from the review of the literature done here are:

- There are no adequate models to describe the evaporation of droplets of complex mixtures;
- The technique of continuous thermodynamics has proven to be a successful model for complex mixtures calculations and has not yet been applied to droplets or other

evaporation and combustion problems. The method has not been applied to transport processes at all.

This report presents a model describing the vaporization of a single multicomponent fuel droplet using the method of continuous thermodynamics. The classical relations describing the process are converted in terms of the distribution function chosen to represent a hydrocarbon mixture of an indefinite number of components. Since there are no general transport properties correlations for mixtures, these have to be developed in terms of the distribution variable.

3. MATHEMATICAL MODEL

3.1 Introduction

The purpose of the model using continuous thermodynamics is to describe the vaporization process of a multicomponent liquid fuel droplet suddenly exposed to a hot environment. In this chapter, the governing equations describing the process are derived in a continuous form, while a numerical solution method is developed in chapter 4. The resulting solutions describe changes in liquid and vapour composition with time as well as the variation of the vapour composition in space. Raoult's law for the vapour pressure and the ideal gas law are used to represent the vapour-liquid equilibrium at the droplet surface. The choice of the distribution used is also discussed.

To simplify the model, the following assumptions were made:

- the droplet temperature is uniform in space but may vary in time;
- only the evaporation of the droplet is modelled; chemical reaction is not considered;
- transport properties are uniform in space but may vary in time;
- spherical symmetry of the droplet and surroundings is assumed, so that only radial transport is possible.

These same assumptions were used and justified by Bergeron and Hallett (1989a), and are standard in most droplet models.

3.2 Transport Equations for the Vapour Phase

For generality, the transport equations are developed in vector form. The fundamental equations derived here can thus be used for virtually any heat and mass transfer problem with complex mixtures in one, two or three dimensions. For the droplet problem, spherical coordinates will be used since spherical symmetry is assumed, and only the terms showing the changes in the radial direction will be kept.

3.2.1 Vapour Phase Basic Equations

The vector form of the basic governing equations necessary for solving the droplet vaporization problem are, for each single discrete component i ,

Continuity equation

$$\frac{\partial c}{\partial t} + \nabla \cdot c \mathbf{v}^* = 0 \quad (3-1)$$

where c is the molar density (kmol/m^3) and \mathbf{v}^* is the molar average velocity (m/s). Molar densities and mole fractions are used throughout instead of mass units to avoid the need to convert from mass to mole fraction and back again when dealing with phase equilibrium at the droplet surface. The equations therefore contain \mathbf{v}^* rather than the more usual mass average velocity \mathbf{v} . It is assumed that there is no chemical reaction, otherwise the right hand side would be non-zero.

Diffusion equation

One diffusion equation is required for each fuel component, plus one for the air or other ambient gas:

$$\frac{\partial}{\partial t}(cy_i) + \nabla \cdot (cv^*y_i) = \nabla \cdot (cD_{im} \nabla y_i) \quad (3-2)$$

where c is the molar density (kmol/m^3), y_i is the mol fraction of i in the vapour phase, and D_{im} is the diffusivity of component i in the mixture (m^2/s). Since in a complex mixture, the concentration of any individual fuel component will be small because of the large number of components, it has been assumed that multicomponent diffusion can be approximated by Fick's law, with D_{im} being the effective diffusivity of i in the mixture.

Energy equation

$$\bar{C}_p \frac{\partial}{\partial t}(cT) + \bar{C}_p \nabla \cdot (cv^* \cdot T) = \nabla \cdot \lambda \nabla T - \sum_{i=1}^n J_i^* \cdot \nabla \bar{h}_i \quad (3-3)$$

where \bar{C}_p is the mixture specific heat (kJ/kmol K), J_i^* is the molar flux of i ($\text{kmol/m}^2\text{s}$) and \bar{h}_i is the partial molal enthalpy (kJ/kmol) of species i .

3.2.2 Species Transport Equation In Continuous Form

The main task in developing a continuous thermodynamics model of this process is to describe the diffusion of the mixture vapour into the surrounding gas, which in this case is air. To solve the system of equations given in section (3.2.1) for a multicomponent

droplet, continuous thermodynamics equivalents to these three governing equations have to be developed.

First, a distribution function has to be chosen with a suitable characterizing variable. Then, the governing equations are written and derived in terms of this distribution. In this case, a single variable distribution function $f(I)$ was chosen to represent the molar concentrations of species of a continuous mixture, so that the mole fraction of a species i is given by

$$y_i = f(I)_i \Delta I_i \quad (3-4)$$

where ΔI_i is the interval in I centred about the value of I corresponding to species i . As discussed in chapter 2, the distribution variable I may be any physical property. In the present work, molecular mass was chosen as the distribution variable, although the derivation that follows is valid for any variable I . The distribution has the property that

$$\int_0^{\infty} f(I) dI = 1 \quad (3-5)$$

In the particular case of droplet evaporation, the evaporating substance is present with overall mol fraction y_F ($F = \text{“fuel”}$), the remainder being air (A) so that

$$y_A = 1 - y_F \quad (3-6)$$

and in the vapour phase the species mol fraction becomes

$$y_i = y_F f(I)_i \Delta I_i \quad (3-7)$$

The diffusion of the mixture is described by deriving transport equations for the distribution function. Substituting the component mol fraction y_i above in eq.(3-2) gives

$$\frac{\partial}{\partial t} (c y_F f(I)_i \Delta I_i) + \nabla \cdot (c v \cdot y_F f(I)_i \Delta I_i) = \nabla \cdot [c D_m(I) \nabla (y_F f(I)_i \Delta I_i)] \quad (3-8)$$

Note that the diffusivity $D_m(I)$ has been allowed to vary, reflecting the fact that species diffusivity depends on molecular mass and other properties. Allowing the interval ΔI_i to become infinitesimally small, and integrating over I from 0 to ∞ yields:

- first term of the left hand side of equation (3-8):

$$\begin{aligned} \int_0^{\infty} \frac{\partial}{\partial t} (c y_F f(I) dI) &= \int_0^{\infty} c y_F \frac{\partial}{\partial t} f(I) dI + \int_0^{\infty} f(I) dI \frac{\partial}{\partial t} (c y_F) \\ &= c y_F \frac{\partial}{\partial t} \int_0^{\infty} f(I) dI + \frac{\partial}{\partial t} (c y_F) \int_0^{\infty} f(I) dI \\ &= 0 + \frac{\partial}{\partial t} (c y_F) \end{aligned} \quad (3-9)$$

- second term of the left hand side of equation (3-8):

$$\begin{aligned} \int_0^{\infty} \frac{\partial}{\partial r} (r^2 c v \cdot y_F f(I) dI) &= \int_0^{\infty} r^2 c v \cdot y_F \frac{\partial}{\partial r} f(I) dI + \int_0^{\infty} f(I) \frac{\partial}{\partial r} (r^2 c v \cdot y_F) dI \\ &= r^2 c v \cdot y_F \frac{\partial}{\partial r} \int_0^{\infty} f(I) dI + \frac{\partial}{\partial r} (r^2 c v \cdot y_F) \int_0^{\infty} f(I) dI \quad (3-10) \\ &= 0 + \frac{\partial}{\partial r} (r^2 c v \cdot y_F) \end{aligned}$$

- right hand side term of equation (3-8) :

$$\begin{aligned}
\int_0^{\bar{r}} \frac{\partial}{\partial r} \left[r^2 c D_m(I) \frac{\partial}{\partial r} (y_F f(I) dI) \right] &= \frac{\partial}{\partial r} \int_0^{\bar{r}} r^2 c D_m(I) \frac{\partial}{\partial r} [y_F f(I) dI] \\
&= \frac{\partial}{\partial r} \left[\int_0^{\bar{r}} r^2 c D_m(I) y_F \frac{\partial f(I) dI}{\partial r} \right. \\
&\quad \left. + \int_0^{\bar{r}} r^2 c D_m(I) \frac{\partial y_F}{\partial r} f(I) dI \right] \\
&= \frac{\partial}{\partial r} \left[r^2 y_F \int_0^{\bar{r}} c D_m(I) \frac{\partial f(I) dI}{\partial r} \right. \\
&\quad \left. + \frac{\partial y_F}{\partial r} \int_0^{\bar{r}} r^2 c D_m(I) f(I) dI \right] \tag{3-11} \\
&= \frac{\partial}{\partial r} \left[r^2 y_F \int_0^{\bar{r}} \frac{\partial}{\partial r} (c D_m(I) f(I)) dI \right. \\
&\quad \left. - r^2 y_F \int_0^{\bar{r}} f(I) \frac{\partial}{\partial r} (c D_m(I)) dI \right. \\
&\quad \left. + \frac{\partial y_F}{\partial r} \int_0^{\bar{r}} r^2 c D_m(I) f(I) dI \right] \\
&= \frac{\partial}{\partial r} r^2 \left[y_F \frac{\partial (c \bar{D})}{\partial r} + \frac{\partial y_F}{\partial r} c \bar{D} \right. \\
&\quad \left. - y_F \int_0^{\bar{r}} f(I) \frac{\partial}{\partial r} (c D_m(I)) dI \right]
\end{aligned}$$

where an average diffusivity \bar{D} is defined by

$$\bar{D} = \int_0^{\infty} D_m(I) f(I) dI \quad (3-12)$$

A transport equation, in a continuous form, for the vaporizing substance as a whole is then given as:

$$\frac{\partial}{\partial t}(cy_F) + \nabla \cdot (cv \cdot y_F) = \nabla \cdot \left\{ c\bar{D} \nabla y_F + y_F \nabla(c\bar{D}) - y_F \int_0^{\infty} f(I) \nabla(cD_m(I)) dI \right\} \quad (3-13)$$

and $D_m(I)$ is the component diffusivity as a function of I .

Weighting equation (3-8) by I before integrating in the same way equation (3-13) was derived yields a transport equation for the mean θ of the distribution:

$$\frac{\partial}{\partial t}(cy_F \theta) + \nabla \cdot (cv \cdot y_F \theta) = \nabla \cdot \left\{ c\tilde{D} \nabla(y_F \theta) + y_F \theta \nabla(c\tilde{D}) - y_F \int_0^{\infty} f(I) I \nabla(cD_m(I)) dI \right\} \quad (3-14)$$

where a second average diffusivity must be defined as

$$\tilde{D} \theta = \int_0^{\infty} D_m(I) f(I) I dI \quad (3-15)$$

Finally, weighting equation (3-8) with I^2 and integrating in the same manner as previously results in

$$\frac{\partial}{\partial t}(cy_F\Psi) + \nabla \cdot (cv \cdot y_F\Psi) = \nabla \cdot \left\{ c\hat{D}\nabla(y_F\Psi) + y_F\Psi\nabla(c\hat{D}) - y_F \int_0^{\bar{I}} f(I)I^2 \nabla(cD_m(I)) dI \right\} \quad (3-16)$$

where yet another average diffusivity must be defined as

$$\hat{D}\Psi = \int_0^{\bar{I}} D_m(I)f(I)I^2 dI \quad (3-17)$$

The new variable ψ is the second moment about the origin, defined as

$$\psi = \int_0^{\bar{I}} f(I)I^2 dI = \theta^2 + \sigma^2 \quad (3-18)$$

where σ^2 is the variance of the distribution. Further equations can be derived for other moments of the distribution if desired, but these suffice for calculations with a two-parameter distribution.

The equations (3-13), (3-14) and (3-16) describe the variation of vapour phase composition in space and time by means of the "fuel" mol fraction y_f and the distribution parameters θ and ψ (or σ^2). They are general and allow for transport property variation in space and time.

Boundary Conditions for the Droplet Problem:

At the droplet surface, the values of y_F , θ and ψ are considered known; they will be found later from phase equilibrium relations. At a distance far from the droplet surface ($r \rightarrow \infty$), the fuel concentration is zero ($y_F = 0$) because no fuel is present in the ambient gas.

If $y_F = 0$, then $y_F \theta = 0$ and $y_F \psi = 0$, resulting in the following boundary conditions:

$$\begin{aligned} \text{at } r = R: \quad y_F &= y_{FR}; \quad \theta = \theta_R; \quad \sigma^2 = \sigma_R^2 \\ \text{at } r \rightarrow \infty: \quad y_F &= (y_F \theta) = (y_F \psi) = 0 \end{aligned} \quad (3-19)$$

where subscript R refers to the surface. The initial condition is

$$\text{at } t = 0 \quad y_F = 0 \text{ for } r > R \quad (3-20)$$

Simplification of the Transport Equations

As an alternative to the three transport equations just derived, it is possible to reduce equations (3-14) and (3-16) to equations for θ and ψ alone by combining them with equation (3-13). However, this results in more terms when the gradient of the diffusion term is taken (right hand side of 3-13, 3-14 and 3-16), and also necessitates imposing arbitrary finite values of θ and ψ as boundary conditions at $r \rightarrow \infty$. Hence the present equations are easier to work with. One could also, in theory, derive an equation for σ^2 instead of ψ by using $(I - \theta)^2$ as a weighting function rather than I^2 , but since θ itself varies in space and time, the resulting equations would be much more complex than those for ψ , because the variation of θ would have to be accounted for when integrating. The transport equations have been written with density c and diffusion coefficient D grouped together to reduce the effects of

property variations, since for a perfect gas the product (cD) is independent of pressure and varies less rapidly with temperature than D itself does (Bird, Stewart and Lightfoot, 1960). In looking for ways to simplify these equations, it was noted that in each of equations (3-13), (3-14) and (3-16) the last two terms are identical or nearly identical in finite difference approximation, and hence together make very little contribution to the equations. This is shown in more detail in Appendix A for the last two terms of equation (3-13). The same demonstration applies to the other two equations (3-14) and (3-16). This reduces the equations to

$$\frac{\partial}{\partial t}(cy_F) + \nabla \cdot (cv \cdot y_F) = \nabla \cdot (c\bar{D} \nabla y_F) \quad (3-21)$$

$$\frac{\partial}{\partial t}(cy_F \theta) + \nabla \cdot (cv \cdot y_F \theta) = \nabla \cdot (c\bar{D} \nabla (y_F \theta)) \quad (3-22)$$

$$\frac{\partial}{\partial t}(cy_F \Psi) + \nabla \cdot (cv \cdot y_F \Psi) = \nabla \cdot (c\bar{D} \nabla (y_F \Psi)) \quad (3-23)$$

One could further simplify the diffusion terms to the form $(c\bar{D} \nabla \cdot \nabla y_F)$ by assuming that the diffusivities are constant in space, eliminating terms like $(\nabla(c\bar{D}) \cdot \nabla y_F)$. Trial calculations, made after the model was completed, showed that $(\nabla(c\bar{D}) \cdot \nabla y_F)$ could amount to nearly 20% of $(c\bar{D} \nabla \cdot \nabla y_F)$ near the droplet surface; neglecting it had some effect on the vapour phase profiles of y_F and θ , but no significant effect on the development of liquid properties (Appendix B). However, the saving in computational effort in simplifying these terms is slight, and therefore the terms were kept in the form given by eqs. (3-21)-(3-23), with the diffusivities varying in space, for the present work.

3.2.3 Energy Equation in Continuous Form

The energy equation, required for the heat transfer to the droplet and for the temperature field, must also be cast in a continuous thermodynamics formulation. For a mixture with discrete components, the energy equation is given by equation (3-3), where the mixture specific heat \bar{C}_p is

$$\bar{C}_p = \sum y_i C_{p_i} + (1 - \sum y_i) C_{p_A} \quad (3-24)$$

where C_{p_i} is the specific heat for component i , y_i is the mol fraction and C_{p_A} is the air specific heat. The last term in eq. (3-3), $\sum J_i^* \nabla \bar{h}_i$, represents energy transport due to interdiffusion of species. Although often neglected, it is significant whenever the specific heat of the vapour evolved differs appreciably from that of the ambient gas. With the exception of the interdiffusion term, the energy equation is the same for a discrete mixture and a continuous mixture. Assuming a perfect gas

$$\nabla \bar{h}_i = C_{p_i} \nabla T \quad (3-25)$$

while the component diffusion flux is

$$J_i^* = -c D_{im} \nabla y_i \quad (3-26)$$

Introducing the distribution function and integrating gives the interdiffusion term:

$$-\sum_{i=1}^n J_i^* \cdot \nabla \bar{h}_i = \left\{ \int_0^{\infty} C_p(I) c D_m(I) \nabla [y_F f(I)] dI - J_A^* C_{p_A} \right\} \cdot \nabla T \quad (3-27)$$

where $C_p(I)$ is the component specific heat as a continuous function of I .

Continuity requires that

$$\sum_{i=1}^n J_i^* = 0 \quad (3-28)$$

so that the diffusion flux of ambient gas (air, in this case) is

$$J_A^* = - \sum_{i=1}^n J_{i,F}^* = \int_0^{\infty} c D_m(I) \nabla(y_F f(I)) dI \quad (3-29)$$

Hence the interdiffusion term simplifies to

$$-\sum J_i^* \nabla \bar{h}_i = \left\{ \int_0^{\infty} (C_p(I) - C_{pA}) c D_m(I) \nabla(y_F f(I)) dI \right\} \cdot \nabla T \quad (3-30)$$

Integration requires an expression for $C_p(I)$; the correlation of Chou and Prausnitz (1986), discussed later, was used, which gives a linear variation with I :

$$C_p(I) = a_c + b_c I \quad (3-31)$$

where a_c and b_c both include the effect of temperature. Integration of eq. (3-30) then yields

$$\begin{aligned} -\sum J_i^* \nabla \bar{h}_i = & \left\{ \left[(a_c - C_{pA}) c \bar{D} + b_c \theta c \bar{D} \right] \nabla y_F \right. \\ & + y_F \left[(a_c - C_{pA}) \nabla(c \bar{D}) + b_c \theta \nabla(c \bar{D}) + b_c c \bar{D} \nabla \theta \right] \\ & \left. - y_F \int_0^{\infty} (a_c + b_c I - C_{pA}) f(I) \nabla(c D(I)) dI \right\} \cdot \nabla T \end{aligned} \quad (3-32)$$

As was the case with the diffusion equations (3-13, 3-14 and 3-16), the second square bracketed term and the final integral cancel out in finite difference approximation, giving the final form of the energy equation:

$$\bar{C}_p \frac{\partial}{\partial t}(cT) + \bar{C}_p \nabla \cdot (c\mathbf{v} \cdot T) = \left[(a_c - C_{PA})c\bar{D}\nabla y_F + b_c \theta c\bar{D}\nabla y_F \right] \nabla T + \nabla \cdot \lambda \nabla T \quad (3-33)$$

The boundary conditions are:

- * at the surface ($r = R$): $T = T_R$
- * at $r \rightarrow \infty$: $T = T_\infty$

and the initial conditions are:

$$\begin{array}{lll} \text{At } t = 0: & T = T_\infty & r > R \\ & T = T_{LO} & r < R \end{array}$$

3.3 Liquid Phase Balance Equations

Liquid and vapour phases are coupled by molar and heat fluxes at the liquid surface. The variations in droplet temperature and composition as the droplet heats and vaporizes have a great effect on the molar and heat fluxes in the vapour phase and hence on the droplet lifetime.

As discussed in chapter 2, section 2.2.2, the most used simple theories in modelling the liquid phase behaviour in vaporizing droplets are the diffusion-limited model and the

well-mixed model. These two models represent the limiting cases for the liquid phase since the assumptions are either no liquid motion for the diffusion-limited model, or a well-mixed liquid phase for the well-mixed model. In real life, there will be some mixing, and reality will lie somewhere between these two cases. More accurate models of the droplet internal transport, based on vortex flow or on enhanced radial diffusion, have been developed by Talley and Yao (1986) and Tong and Sirignano (1986). Since in real life, droplets present some degree of internal motion, the distillation or well-mixed model was chosen to describe the droplet liquid phase. The difference between the more elaborate models and the well-mixed model seems to be large only when the mixture components have widely differing boiling points. For extreme cases, disruptive boiling can occur, in which bubbles of the most volatile component expand and burst in the droplet. In a study by Randolph, Makino and Law (1986), two component mixtures with closely spaced boiling points were shown to behave in a nearly steady state manner with both components vaporizing at nearly the same rate (see Fig. 3.1, results for the $C_{16}H_{34} / C_{14}H_{30} / C_{12}H_{26}$ system), while in two component mixtures with more widely differing volatilities, the most volatile component vaporizes first and the vapour composition changes a good deal during the droplet lifetime. The solid lines in Fig. 3.1 represent calculations made with internal mixing represented by an enhanced radial diffusivity, the degree of enhancement being shown by the effective Lewis number ($Le = D_{im}(c C_p)/\lambda$). Mixtures with more closely spaced component boiling points require a higher Le to fit the experimental data, indicating a closer approach to a well-mixed state.

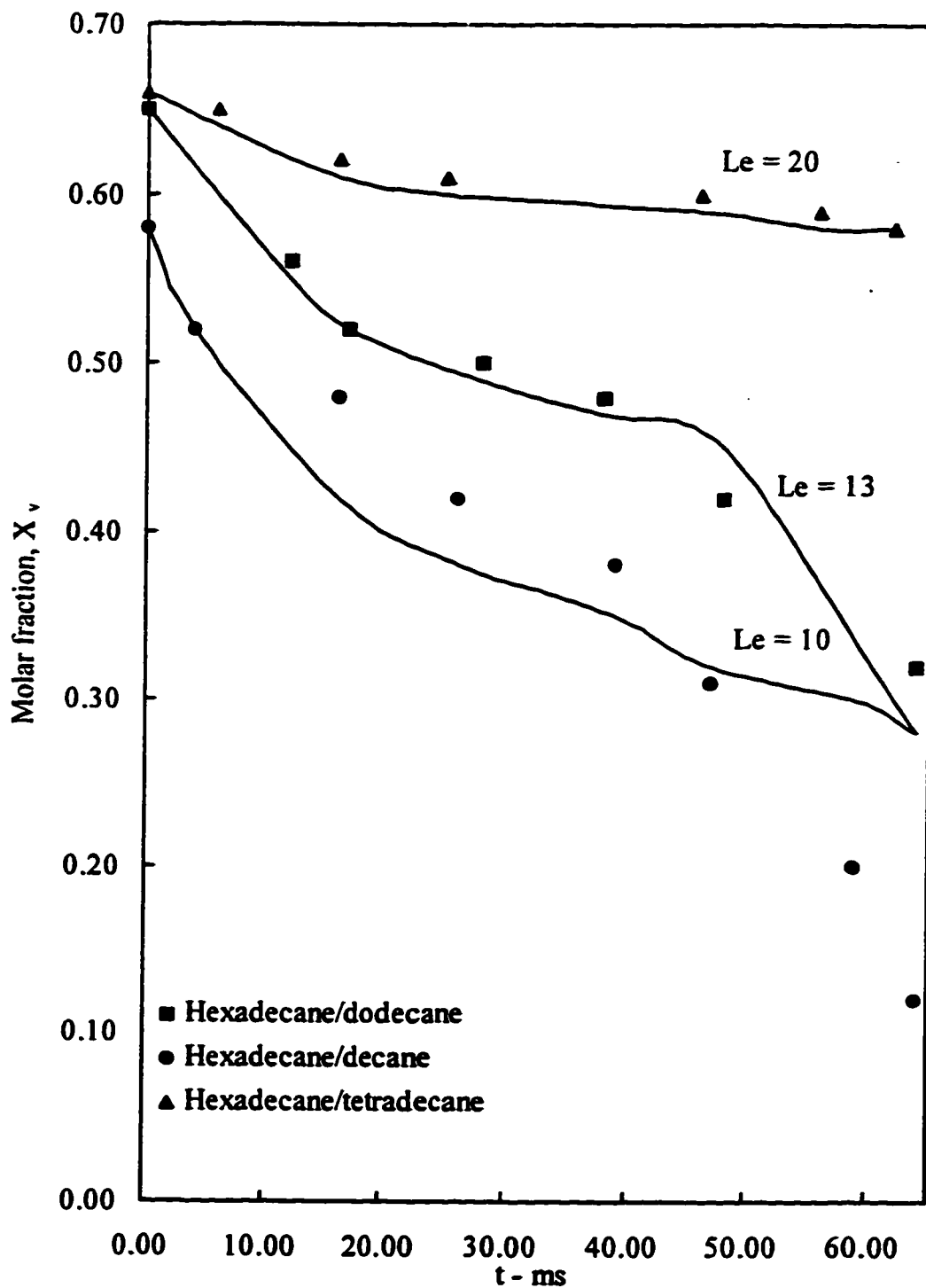


Figure 3.1: Temporal variation of the average volatile molar fractions for mixtures of hexadecane with tetradecane, dodecane, and decane undergoing combustion at about 1300 K. Initial droplet diameter is 0.255 mm; data points are experimental; solid lines are calculations from theory. After Randolph *et al.* (1986).

Since in a continuous mixture there are hundreds of components, the component boiling points are very closely spaced, and the well-mixed model should be much more accurate than it is for a two-component mixture.

The assumption of a well-mixed model for the liquid phase means that the composition and temperature within the droplet are considered to be spatially uniform but vary with time. A mole balance on the droplet gives the total molar flux from the droplet surface as

$$N = -\frac{1}{A} \frac{d}{dt}(c_L V) \quad (3-34)$$

where A and V are the droplet surface area and volume respectively and subscript L indicates liquid. This may be expanded and solved for the rate of recession of the surface:

$$\frac{dR}{dt} = -\frac{1}{c_L} \left(N + \frac{R}{3} \frac{dc_L}{dt} \right) \quad (3-35)$$

The vaporizing molar flux N is obtained by matching component fluxes at the surface. For a discrete component i in the liquid phase the rate of vaporization can be found from a mol balance on the droplet:

$$N_i = -\frac{1}{A} \frac{d}{dt}(x_i c_L V) \quad (3-36)$$

Substituting A and V, the droplet surface area and volume respectively, in terms of the radius, expanding the derivative and then using equation (3-35), the following expression

for the molar flux of i is obtained:

$$N_i = x_i N - c_L \frac{R}{3} \frac{dx_i}{dt} \quad (3-37)$$

In the vapour phase this flux is given by the sum of convection and diffusion from the surface:

$$N_i = N y_{iR} - c D_{im} \left. \frac{\partial y_i}{\partial r} \right|_R \quad (3-38)$$

Equating (3-37) and (3-38) gives

$$N(x_i - y_{iR}) = -c D_{im} \left. \frac{\partial y_i}{\partial r} \right|_R + \frac{c_L R}{3} \frac{dx_i}{dt} \quad (3-39)$$

Introducing the distribution functions in the liquid and vapour phases and integrating gives an equation for the total flux N :

$$N(1 - y_{FR}) = \left[-c \bar{D} \frac{\partial y_F}{\partial r} - y_F \frac{\partial}{\partial r} (c \bar{D}) + y_F \int_0^{\infty} f(I) \frac{\partial}{\partial r} (c D(I)) dI \right]_R \quad (3-40)$$

where the final term in equation (3-39) has been eliminated by the fact that the integral of $f_L(I)$ is 1. Weighting equation (3-39) with I and I^2 respectively and integrating yields equations for the liquid phase distribution parameters:

$$\frac{d\theta_L}{dt} = \frac{3}{c_L R} \left[N(\theta_L - y_F \theta) + c\bar{D} \frac{\partial}{\partial r} (y_F \theta) + y_F \theta \frac{\partial}{\partial r} (c\bar{D}) - y_F \int_0^{\infty} f(I) I \frac{\partial}{\partial r} (cD(I)) dI \right]_R \quad (3-41)$$

$$\frac{d\Psi_L}{dt} = \frac{3}{c_L R} \left[N(\Psi_L - y_F \Psi) + c\bar{D} \frac{\partial}{\partial r} (y_F \Psi) + y_F \Psi \frac{\partial}{\partial r} (c\bar{D}) - y_F \int_0^{\infty} f(I) I^2 \frac{\partial}{\partial r} (cD(I)) dI \right]_R \quad (3-42)$$

Consistent with the treatment of the transport equations (3-13, 3-14, and 3-16), the last two terms in each of these equations will be neglected, simplifying them to

$$N(1 - y_{FR}) = -c\bar{D} \frac{\partial y_F}{\partial r} \Big|_R \quad (3-43)$$

$$\frac{d\theta_L}{dt} = \frac{3}{c_L R} \left[N(\theta_L - y_F \theta) + c\bar{D} \frac{\partial}{\partial r} (y_F \theta) \right]_R \quad (3-44)$$

$$\frac{d\Psi_L}{dt} = \frac{3}{c_L R} \left[N(\Psi_L - y_F \Psi) + c\bar{D} \frac{\partial}{\partial r} (y_F \Psi) \right]_R \quad (3-45)$$

The density c_L required in these equations is calculated from the liquid mass density ρ_L

$$c_L = \rho_L / \theta_L \quad (3-46)$$

As the mass densities of members of homologous groups of hydrocarbons show little variation within the group, ρ_L was assumed constant.

An energy balance is required to describe the transient heating of the droplet:

$$\frac{dT_L}{dt} = \frac{3}{C_{pL} c_L R} (q - N h_{fg}) \quad (3-47)$$

where q is the heat flux to the droplet surface by conduction and , if present, by radiation, and C_{pL} is the specific heat of the liquid.

$$q = -\lambda \left. \frac{\partial T}{\partial r} \right|_R + q_{rad} \quad (3-48)$$

The radiation flux q_{rad} was computed using the correlation of Hottel et al. (1955) as described by Bergeron and Hallett (1989) and is given as

$$\alpha_d = 0.89 (1 - e^{-5.4 R}) \quad (3-49)$$

where α_d is the absorptivity of droplet which is about 0.8 for large droplets, so that radiation makes a significant contribution to droplet heating (Faeth and Olson, 1968).

3.4 Enthalpy of vaporization

The effective enthalpy of vaporization of an evaporating mixture h_{fg} is the sum of those for the pure components weighted by their molar fluxes (not by their concentration).

For discrete components this is given by

$$Nh_{fg} = \sum_{i=1}^n N_i h_{fgi} \quad (3-50)$$

Combining this with the vapour phase flux expression from eq. (3-38) for N_i and introducing the distribution function for a continuous mixture gives the general expression for the effective enthalpy of vaporization,

$$\begin{aligned} Nh_{fg} = & - \int_0^{\bar{r}} cD_m(I)h_{fg}(I) \frac{\partial}{\partial r} (y_F f(I)) \Big|_R dI \\ & + \int_0^{\bar{r}} y_F f(I) \Big|_R Nh_{fg}(I) dI \end{aligned} \quad (3-51)$$

3.5 Vapour Liquid Equilibrium

Most of the literature on continuous thermodynamics deals with the derivation of vapour-liquid expressions in terms of the distribution function, relations such as Gibbs free energy, fugacity, activity coefficient, chemical potentials, etc.

Phase equilibrium calculations for continuous mixtures are performed either using an equation of state or by assuming that the mixture behaviour is ideal and using Raoult's law and the Clausius-Clapeyron equation to find the vapour pressures. The most frequently used equation of state in continuous thermodynamics is the Soave-Redlich-Kwong one (Chou and Prausnitz, 1986; Shibata, Sandler et al., 1987). But in most of the work done, Raoult's law together with the Clausius-Clapeyron equation is used with good results (Rätzsch, Kehlen et al., 1980, 1983, 1985, 1988, 1989). For mathematical simplicity and to be able to perform integrations in closed forms with the distribution function, Raoult's law and the Clausius-Clapeyron equation were chosen in this work to describe the vapour-liquid equilibrium.

For a mixture of discrete components, Raoult's law is

$$y_i = x_i(P_{vi}/P) \quad (3-52)$$

Generalizing this to a continuous distribution yields the total vapour phase mole fraction at the liquid surface

$$y_{FR} = \int_0^{\infty} f_L(I) \frac{P_v(I)}{P} dI \quad (3-53)$$

while integration with I and $(I - \theta)^2$ respectively as weighting functions gives the vapour phase mean and variance:

$$y_{FR} \theta_R = \int_0^{\infty} f_L(I) \frac{P_v(I)}{P} I dI \quad (3-54)$$

$$y_{FR} \sigma_R^2 = \int_0^{\infty} f_L(I) \frac{P_v(I)}{P} (I - \theta)^2 dI \quad (3-55)$$

The component vapour pressure is given by the Clausius-Clapeyron equation:

$$P_v(I) = P_{ATM} \exp \left[\frac{S_{fg}}{R} \left(1 - \frac{T_B(I)}{T} \right) \right] \quad (3-56)$$

A number of studies have used the boiling point as the distribution variable, but in view of the need to devise correlations for transport properties molecular mass was selected instead. For a homologous family of compounds, the boiling point can be approximated as a linear function of molecular mass (fig. 3.2)

$$T_B(I) = a_B + b_B I \quad (3-57)$$

where for n-paraffins values of $a_B = 241.4$ and, $b_B = 1.46$ were chosen to reproduce actual boiling points in the range 100 - 300°C, roughly the range of interest for commercial fuels.

Using Trouton's rule, stating that

$$S_{fg} \approx \text{const} \approx 87.9 \text{ kJ/kmol}\cdot\text{K} \quad (3-58)$$

the vapour pressure can be written in the form

$$P_v(I) = P_{ATM} \exp[A(1 - BI)] \quad (3-59)$$

where

$$\begin{aligned} A &= (S_{fg}/R)(1 - a_B/T) \\ B &= b_B/(T - a_B) \end{aligned} \quad (3-60)$$

Further reduction of the vapour-liquid equilibrium relations requires the introduction of the distribution function.

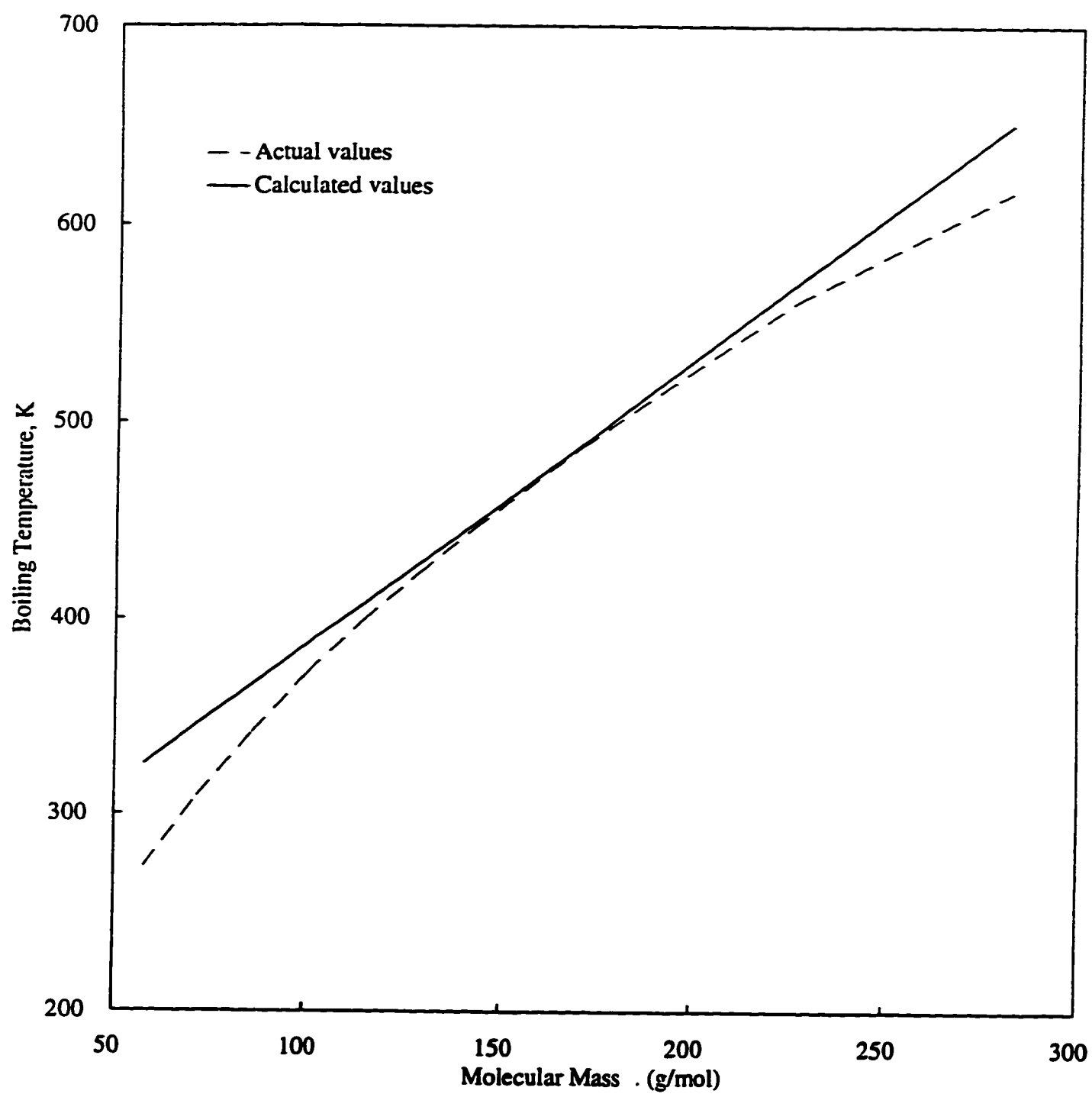


Figure 3.2: Normal boiling points of n-alkanes in terms of molecular mass

3.6 Distribution Function

The distribution function to be used should be versatile and easy to use and should not contain too many unknowns or difficult to find parameters. For petroleum fractions, the Γ distribution (also known as the Schultz or the Pearson Type III) is the most used and was found to best describe the composition of the mixtures considered (Whitson, 1983; Cotterman *et al.*, 1985; Willman and Teja, 1987; Shibata *et al.*, 1987). Rätzsch, Kehlen *et al.* (1980,1983, 1985, 1988, 1989) have used the Gaussian distribution in their works.

The function selected for both liquid and gas phases in this work is the Γ distribution, given as

$$f(I) = \frac{(I - \gamma)^{\alpha - 1}}{\beta^\alpha \Gamma(\alpha)} \exp \left[- \left(\frac{I - \gamma}{\beta} \right) \right] \quad (3-61)$$

where $I = \gamma$ is the origin, α and β are parameters controlling the shape, and $\Gamma(\alpha)$ is the gamma function. The mean and the variance are

$$\begin{aligned} \theta &= \alpha\beta + \gamma \\ \sigma^2 &= \alpha\beta^2 \end{aligned} \quad (3-62)$$

Substitution of this and equation (3-59) into (3-53 to 3-55) gives simple relationships between the distribution parameters in the liquid and vapour phases (Cotterman *et al.*, 1985):

$$\theta - \gamma = \frac{(\theta_L - \gamma)}{1 + AB\sigma_L^2 / (\theta_L - \gamma)} \quad (3-63)$$

$$\sigma^2 = \sigma_L^2 \left[\frac{\theta - \gamma}{\theta_L - \gamma} \right]^2 \quad (3-64)$$

The origin γ is assumed to be the same in both phases, reflecting the idea that the lowest molecular mass component will be present in both phases. It can easily be shown that if one phase is represented by a Γ distribution, the other automatically becomes a Γ distribution if Raoult's law and the Clausius-Clapeyron equation are used to describe the liquid-vapour equilibrium.

The total vapour pressure of fuel vapour in terms of the distribution is obtained by combining (3-53) and (3-55) with the distribution:

$$P_v = y_F P = P_{ATM} \frac{\exp[A(1 - \gamma B)]}{(1 + AB\beta_L)^{\alpha_L}} \quad (3-65)$$

If P_v is set equal to the total pressure P and A and B are substituted for from (3-60) the mixture bubble point T_B can be solved for.

4. NUMERICAL MODEL

4.1 Numerical Solution

The transport equations just derived will be applied to the evaporation of a liquid droplet; the physical problem is that of a droplet which is suddenly exposed to hot surroundings and begins to heat up and vaporize. The solution is based on some assumptions: spherical symmetry, so that the problem is one-dimensional with radius as the only space co-ordinate; transport properties are uniform in space, but may vary in time, with the exception of the diffusivities, which may vary in space as well; a well-mixed liquid phase model, with spatially uniform but time-varying temperature and concentration. The model uses finite difference techniques to solve the governing equations as in the earlier model of Bergeron & Hallett (1989b) and Ruzsalo & Hallett (1991). A full transient solution of the governing equations is done and transport property correlations for the mixture are developed in terms of the distribution variable.

4.1.1 Finite Volume Solution

As in previous work by Bergeron and Hallett (1989b) and Ruzsalo and Hallett (1991), the governing equations together with the boundary and initial conditions were developed into finite volume form and solved numerically. Before setting up the numerical

equations a coordinate transformation is applied. This is needed to keep the first grid point on the surface of the droplet, otherwise the droplet surface would recede with respect to the first grid point as the droplet vaporizes. This is achieved by transforming the coordinates as follows

$$\xi = \frac{r}{R} \quad (4-1)$$

A new velocity has to be defined relative to the new coordinates as

$$w = v - \xi \dot{R} \quad (4-2)$$

where

$$\dot{R} = \frac{dR}{dt} \quad (4-3)$$

The transformed governing equations relative to the new coordinate system are

Continuity Equation:

$$\xi^2 \frac{dc}{dt} + \frac{1}{R} \frac{\partial}{\partial \xi} (\xi^2 c w) + \frac{\dot{R}}{R} c \frac{\partial}{\partial \xi} (\xi^3) = 0 \quad (4-4)$$

Diffusion Equations:

* Equation for y_F (from 3-21):

$$\xi^2 \frac{\partial}{\partial t}(cy_F) + cy_F \frac{\dot{R}}{R} \frac{\partial \xi^3}{\partial \xi} + \frac{1}{R} \frac{\partial}{\partial \xi}(\xi^2 cy_F w) = \frac{1}{R^2} \frac{\partial}{\partial \xi} \left(\xi^2 c \bar{D} \frac{\partial y_F}{\partial \xi} \right) \quad (4-5)$$

* Equation for θ (from 3-22):

$$\begin{aligned} \xi^2 \frac{\partial}{\partial t}(cy_F \theta) + cy_F \theta \frac{\dot{R}}{R} \frac{\partial \xi^3}{\partial \xi} + \frac{1}{R} \frac{\partial}{\partial \xi}(\xi^2 cy_F \theta w) \\ = \frac{1}{R^2} \frac{\partial}{\partial \xi} \left(\xi^2 c \bar{D} \frac{\partial}{\partial \xi}(y_F \theta) \right) \end{aligned} \quad (4-6)$$

* Equation for Ψ (from 3-23):

$$\begin{aligned} \xi^2 \frac{\partial}{\partial t}(cy_F \Psi) + cy_F \Psi \frac{\dot{R}}{R} \frac{\partial \xi^3}{\partial \xi} + \frac{1}{R} \frac{\partial}{\partial \xi}(\xi^2 cy_F \Psi w) \\ = \frac{1}{R^2} \frac{\partial}{\partial \xi} \left(\xi^2 c \hat{D} \frac{\partial}{\partial \xi}(y_F \Psi) \right) \end{aligned} \quad (4-7)$$

Energy equation:

$$\begin{aligned} \xi^2 \bar{C}_p \frac{\partial}{\partial t}(cT) + \bar{C}_p cT \frac{\dot{R}}{R} \frac{\partial \xi^3}{\partial \xi} + \frac{\bar{C}_p}{R} \frac{\partial}{\partial \xi}(\xi^2 T w c) \\ = \frac{1}{R^2} \frac{\partial}{\partial \xi} \left(\xi^2 \lambda \frac{\partial T}{\partial \xi} \right) \\ + \frac{\xi^2}{R} \left[(a_c + C_{pA}) c \bar{D} + b_c \theta c \bar{D} \right] \frac{\partial y_F}{\partial \xi} \end{aligned} \quad (4-8)$$

These equations were integrated over a radial control volume using the finite volume techniques described by Patankar (1980). The general form of the discretization equation is, for the fuel mole fraction for example:

$$ay_{FP} = by_{FE} + cy_{FW} + a^{\circ}y_{FP}^{\circ} \quad (4-9)$$

where P denotes the point solved for, E and W are its east and west neighbours respectively (fig. 4.1), and the coefficients a, b, c and a° are obtained from the integration of each term over the control volume and over the time interval $t+\Delta t$ (Patankar, 1980; Bergeron and Hallett, 1989b; Ruzalo and Hallett, 1991). Superscript $^{\circ}$ (= "old") denotes values at the previous time step. Details of these equations are in Appendix D.

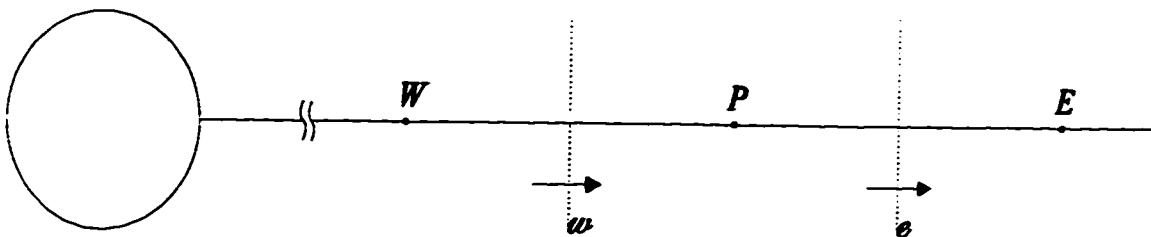


Figure 4.1: Diagram of cell around droplet.

As in previous work (Bergeron and Hallett, 1989b; Ruzalo and Hallett, 1991), an implicit solution was used. The implicit scheme postulates that at time t , the values of T° and y_F° from the previous time step suddenly change to T and y_F and these new values prevail through the whole time step while T° and y_F° are the values from the previous step (Patankar, 1980).

The equations developed in chapter 3 must be solved by iteration at each time step. Fig.4.2 shows the sequence of calculation used. The structure of the algorithm used is the same as that used by Bergeron and Hallett (1989b) with modifications implemented where required. For trial values of temperature and liquid distribution parameters, the energy

equation and the vapour-liquid equilibrium equations at the surface are solved, which gives a new gas phase temperature field and new surface vapour pressure. The diffusion equations are then solved as well as the continuity equation which yield the new vapour and liquid phase compositions and the mol flux from the surface. The surface temperature and mol flux are checked for convergence.

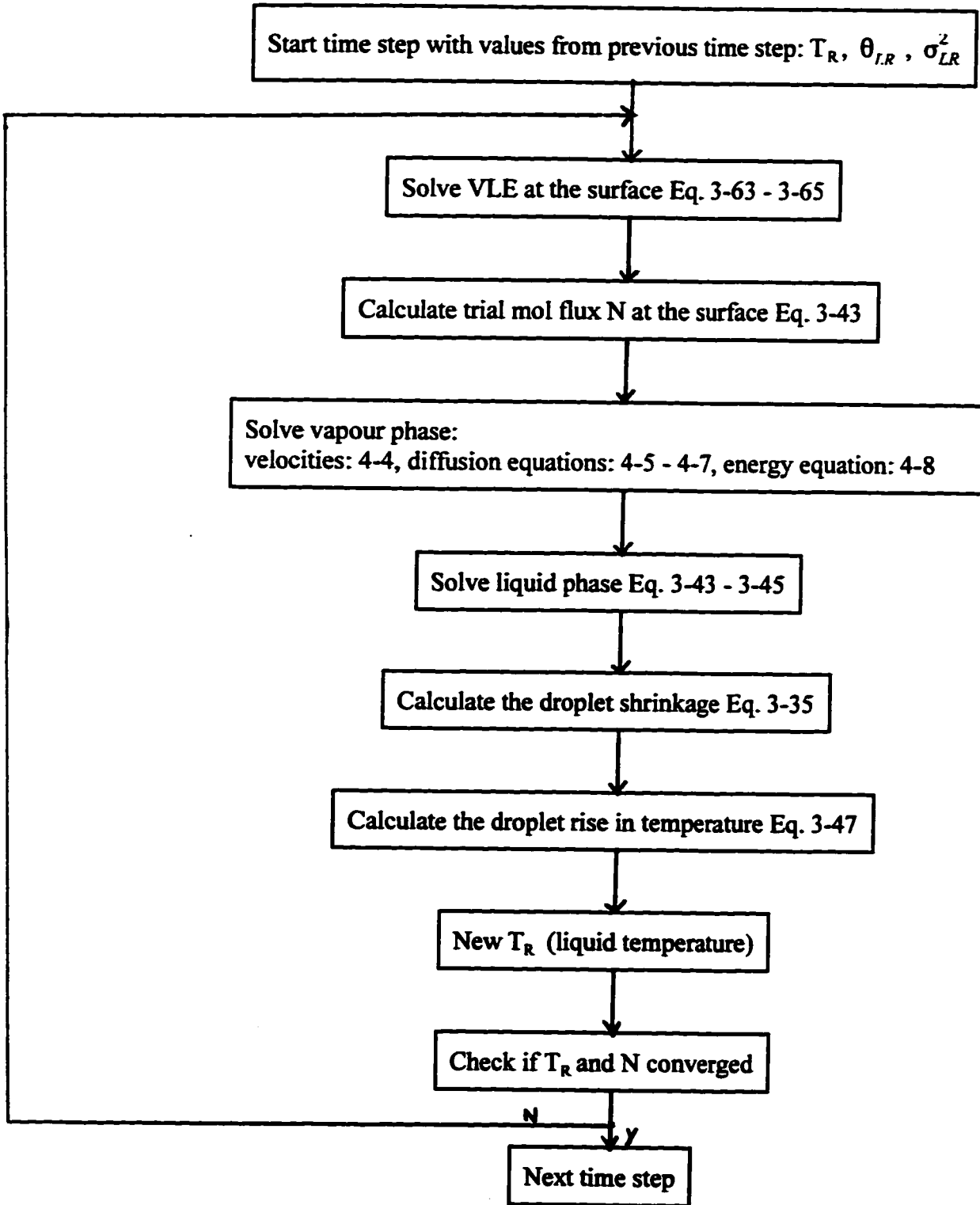


Figure 4.2: Flow chart of computer program

4.1.2 Computational Grid and Time Step

Grid Spacing:

The grid spacing was kept the same as previously used (Bergeron and Hallett, 1989b; Ruszalo and Hallett, 1991). All the important changes happen at the droplet surface initially, then diffuse through the vapour phase away from the droplet, and the steepest gradients are near the surface. The grid spacing used gives more points near the droplet surface to adequately describe the changes and fewer points far from the droplet surface.

The equation describing the vapour phase grid division is given by:

$$\xi(i) = \exp \left[\frac{\ln \xi(N)}{N - 1} (i - 1) \right] \quad (4-10)$$

where i is the grid point index and N the total number of grid points (fig. 4.3). In this case a 20 point grid was used with an outer boundary situated at a distance equal to 500 times the droplet radii.

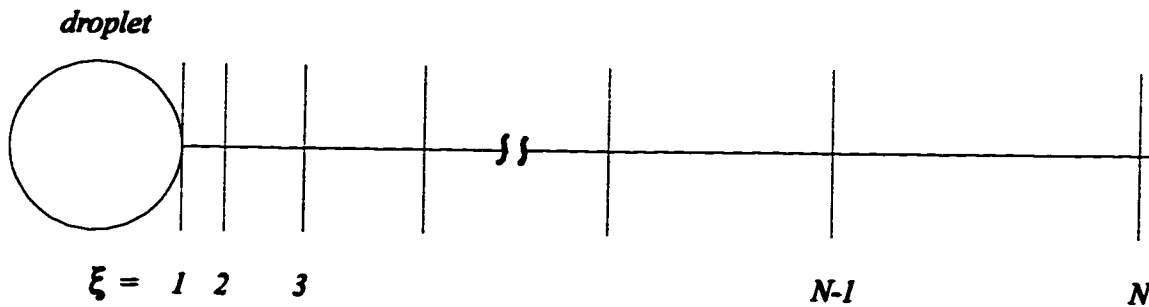


Figure 4.3: Exponentially spaced grid.

Time Step:

Earlier work with ignition (Bergeron & Hallett, 1989b) showed that a time step of about 1% of the ignition time of a droplet gave a sufficiently accurate representation of the transient processes taking place. This led to a selection of a time step of 0.01 sec for a 1.5 mm droplet - this turned out to be about 0.2% of the lifetime of an evaporating (non-igniting) droplet. Smaller droplets evaporate more quickly and have more rapid transients. The classical theory of droplet vaporization, as mentioned earlier in section 2.1.1, shows that droplet lifetime varies as the square of droplet diameter, and this should therefore be the factor used to scale the time step for smaller droplets.

Convergence problems were sometimes encountered when the droplet had been reduced to 1 - 2% of its original mass. To avoid this problem, the time step was reduced to 1/5 of its original value when the droplet mass dropped below 10% of the initial value.

4.2 Transport Property Correlations

An important part in developing the continuous thermodynamics model was to find property correlations which would be easy to integrate with the distribution function. Although some of the correlations found in the literature and commonly used to calculate physical properties are more accurate, they are too complex to integrate in closed form with the distribution. The correlations presented here were developed for the n-paraffin group of compounds. Attention was focused particularly on the species in the Diesel fuel -

kerosene boiling range, from about $100^{\circ}C$ to $300^{\circ}C$ (roughly n-heptane to n-octadecane). These correlations were found to give an adequate estimate of this group's physical properties. These correlations were developed for the purpose of this work only and are not considered as general rules. The goal was to find a relationship relating the physical properties to the molecular mass, since it was the variable chosen for the distribution.

The equations used to calculate the air properties were the Eucken equation for the thermal conductivity of air and the third degree polynomial for the heat capacity (Reid *et al.*, 1987).

4.2.1 Reference State

Transport properties are usually a function of temperature and mixture composition. In this work, all properties (except diffusivity and density) are assumed uniform in space. For an accurate solution, these properties must be evaluated at a suitable average temperature and concentration. As in previous work (Bergeron & Hallett, 1989b; Ruzsalo and Hallett, 1991), the recommendations of Hubbard *et al.* (1975) were used to define the properties at an average temperature and composition at each time step

$$\begin{aligned} T &= \frac{2}{3} T_R + \frac{1}{3} T_{\infty} \\ Y_i &= \frac{2}{3} Y_{iR} + \frac{1}{3} Y_{\infty} \end{aligned} \quad (4-11)$$

where R denotes the droplet surface, ∞ a distance far from the droplet, and Y_i the mass fraction of i at time t .

4.2.2 Enthalpy of vaporization

In section 3.3, a general expression for the effective enthalpy of vaporization was developed as

$$\begin{aligned}Nh_{fg} = & - \int_0^{\infty} cD_m(I)h_{fg}(I) \frac{\partial}{\partial r} (y_F f(I)) \Big|_R dI \\ & + \int_0^{\infty} y_F f(I) \Big|_R Nh_{fg}(I) dI\end{aligned}\tag{4-12}$$

Since h_{fg} per unit mass at the normal boiling point is nearly constant among members of a homologous chemical group (fig. 4.4), a linear variation of the molar h_{fg} with I is a very good approximation.

$$h_{fg}(I) = [a_H + b_H I] \Phi_H\tag{4-13}$$

where factor Φ_H represents the temperature dependence (see later). The polynomial coefficients were found by fitting this equation to data for n-alkanes from Reid *et al.* (1987):

$$a_H = 2.07E07$$

$$b_H = 1.35E05$$

These fit the published values to within a rms error of 1.25 for the paraffin group chosen (fig. 4.5).

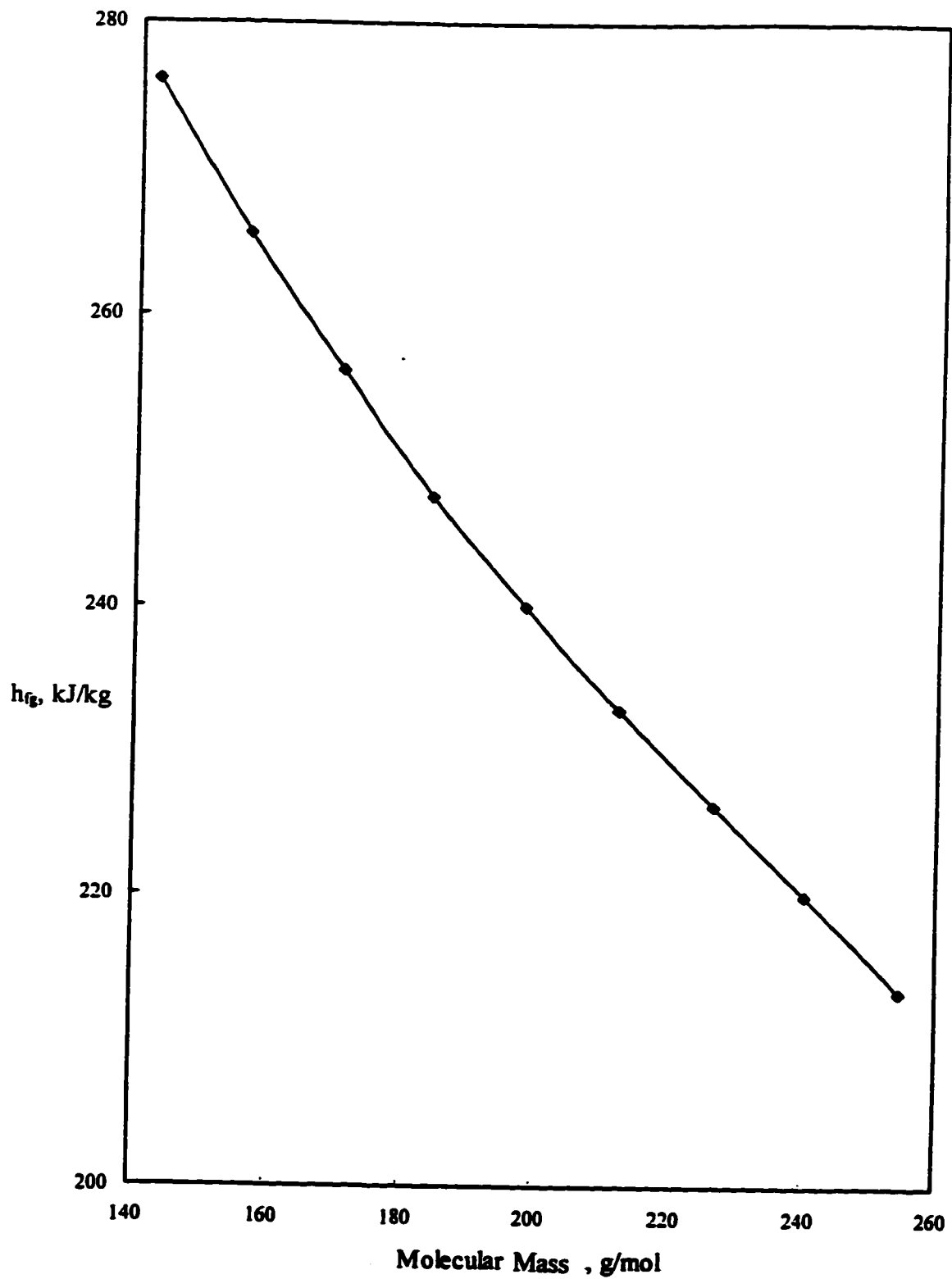


Figure 4.4: Heat of vaporization at normal boiling point as a function of mol. mass , for a series of n-alkanes. Data from Reid *et al.* (1987).

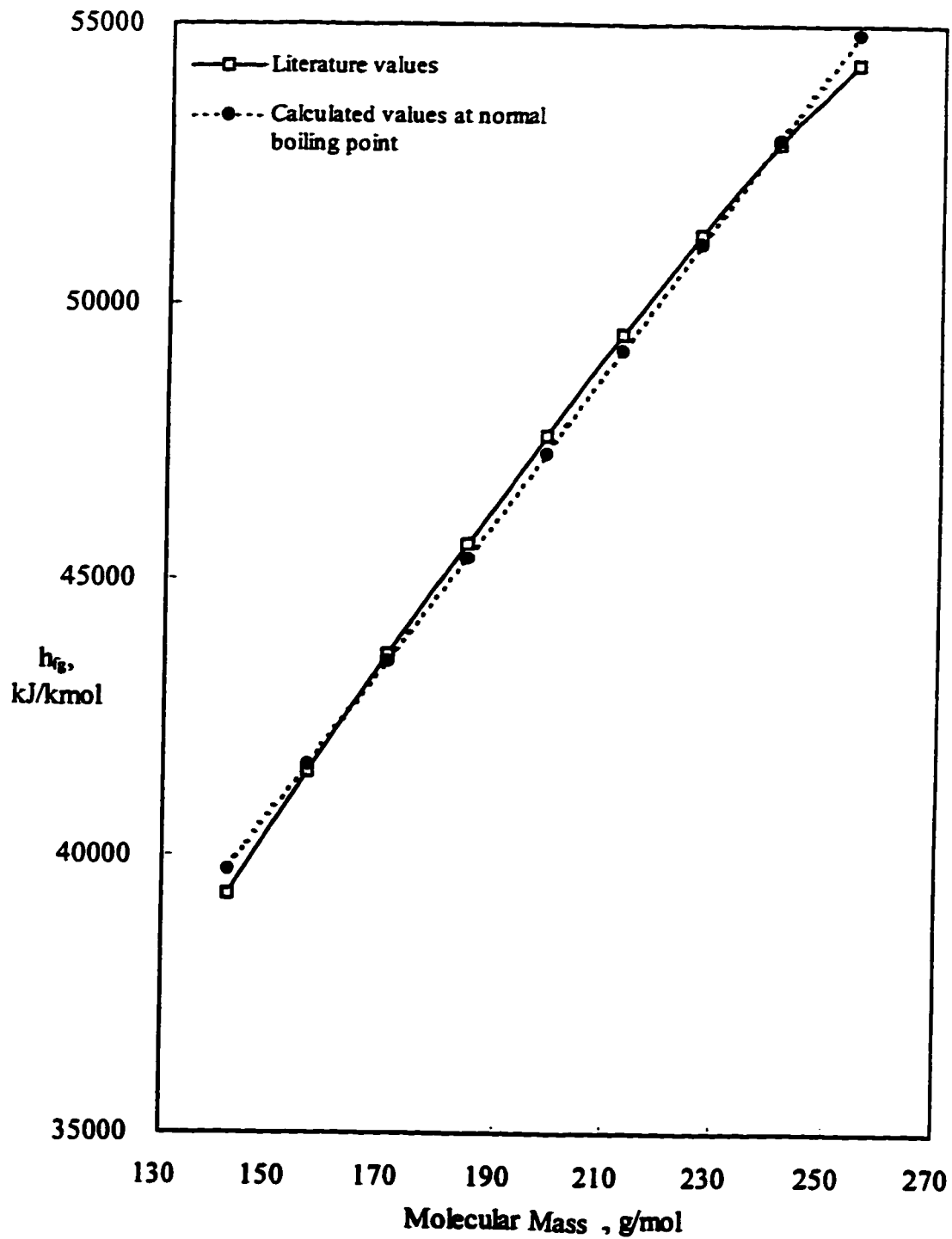


Figure 4.5: Correlated and actual molar heat of vaporization at normal boiling point with respect to molecular mass for n-alkanes.

Introducing (4-13) into the previous equation (4-12),

$$\begin{aligned}
 Nh_{fg} = & -a_H \Phi_H \left[c\bar{D} \frac{\partial y_F}{\partial r} + y_F \frac{\partial}{\partial r}(c\bar{D}) - y_F \int_0^{\bar{r}} f(I) \frac{\partial}{\partial r}(cD_m(I)) dI \right] \\
 & - b_H \theta \Phi_H \left[c\bar{D} \frac{\partial y_F}{\partial r} + y_F \frac{\partial}{\partial r}(c\bar{D}) - y_F \int_0^{\bar{r}} f(I) I \frac{\partial}{\partial r}(cD_m(I)) dI \right] \\
 & - y_F b_H \Phi_H c\bar{D} \frac{\partial \theta}{\partial r} + y_F \Phi_H N(a + b\theta)
 \end{aligned} \quad (4-14)$$

Substituting (3-40) for the first square bracketed expression in (4-14) will give

$$\begin{aligned}
 Nh_{fg} = & \Phi_H \left\{ Na_H + (y_F \theta)_R Nb_H - b_H c\bar{D} \frac{\partial}{\partial r}(y_F \theta) \Big|_R \right. \\
 & \left. - b_H (y_F \theta)_R \left[\frac{\partial}{\partial r}(c\bar{D}) - \int_0^{\bar{r}} f(I) I \frac{\partial}{\partial r}(cD_m(I)) dI \right] \Big|_R \right\}
 \end{aligned} \quad (4-15)$$

Consistent with the treatment of the transport equations, the last two terms in finite difference formulation can be cancelled, resulting in:

$$h_{fg} = \Phi_H \left[a_H + b_H (y_F \theta) \Big|_R - \frac{b_H c\bar{D}}{N} \frac{\partial}{\partial r}(y_F \theta) \Big|_R \right] \quad (4-16)$$

The temperature dependence is based on the often-used Watson equation (Reid *et al.*, 1987)

$$\Phi_H = \frac{h_{fg}}{h_{fgB}} = \left[\frac{T_{cr} - T}{T_{cr} - T_B} \right]^{0.38} \quad (4-17)$$

where subscript B refers to the normal boiling point. The term $(T_{cr} - T_B)^{0.38}$ is approximated as a constant for members of a homologous group of compounds (Table 4.1), while the critical temperature is taken as the pseudo-critical temperature calculated using Kay's rule.

Table 4.1: Values of parameters for enthalpy of vaporization correlation. Values were taken from Reid *et al.* (1987).

Paraffin	Formula	MW (g/mol)	Boiling Temp. (K)	Critical Temp. (K)	$(T_{cr} - T_B)^{0.38}$ (K)
N-HEXANE	C6H14	86.18	341.90	507.40	6.97
N-OCTANE	C8H18	114.23	398.80	568.80	7.04
N-NONANE	C9H20	126.24	425.00	592.00	6.99
N-DECANE	C10H22	142.29	447.30	617.60	7.04
N-UNDECANE	C11H24	156.31	469.10	638.80	7.04
N-DODECANE	C12H26	170.34	489.50	658.30	7.02
N-TRIDECANE	C13H28	184.37	508.60	675.80	7.00
N-TETRADECANE	C14H30	198.40	526.70	694.00	7.00
N-PENTADECANE	C15H32	212.42	543.80	707.00	6.93
N-HEXADECANE	C16H34	226.45	560.00	717.00	6.83
N-HEPTADECANE	C17H36	240.47	575.20	733.00	6.84
N-OCTADECANE	C18H38	254.50	589.50	745.00	6.81
					Avg= 6.959

If component critical temperatures are correlated as (fig. 4.6)

$$T_{cr}(I) = a_{cr} + b_{cr}I \quad (4-18)$$

then for the mixture, the pseudo-critical temperature is

$$T_{cr} = a_{cr} + b_{cr}\theta \quad (4-19)$$

Fitting data for n-alkanes to eq. (4-18) gave

$$a_{cr} = 440.8$$

$$b_{cr} = 1.21$$

with an rms error of 6.1.

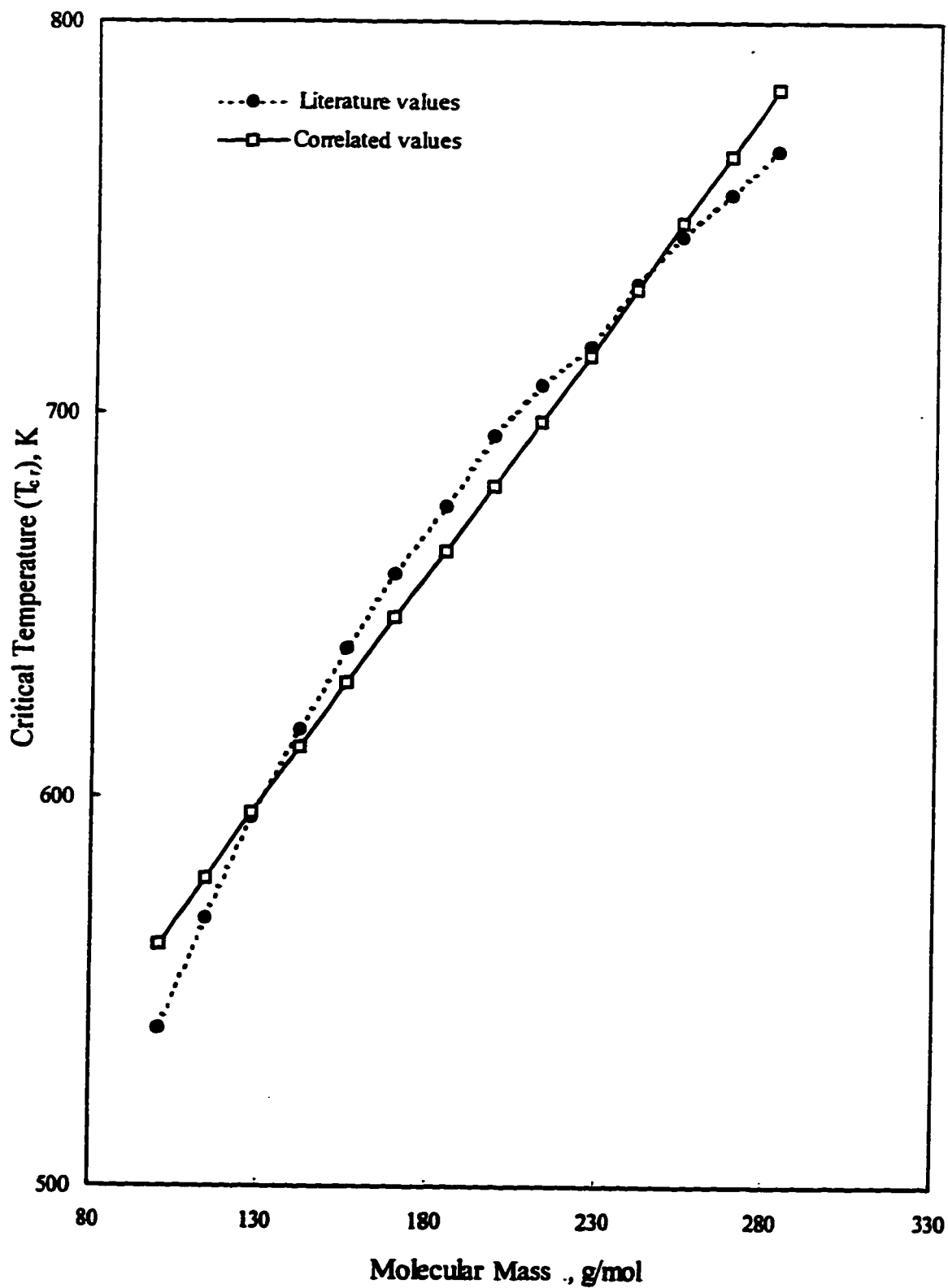


Figure 4.6: Variation of the critical temperature with molecular mass for n-alkanes.

4.2.3 Heat Capacity for Vapour Phase:

The correlation for the gas heat capacity was taken from the paper by Chou and Prausnitz (1986), who found that for hydrocarbon families, the ideal-gas heat capacities are linear functions of molecular mass I at a given temperature. For each family,

$$\frac{C_p}{R} = a_C(T) + b_C(T) * I \quad (4-20)$$

where R is the universal gas constant and $a_C(T)$ and $b_C(T)$ are cubic polynomials in T :

$$\begin{aligned} a_C(T) &= a_0 + a_1 T + a_2 T^2 + a_3 T^3 \\ b_C(T) &= b_0 + b_1 T + b_2 T^2 + b_3 T^3 \end{aligned} \quad (4-21)$$

For n-alkanes the constants given by Chou & Prausnitz are:

$a_0 = 2.465$	$b_0 = -3.561E-2$
$a_1 = -1.144E-2$	$b_1 = 9.367E-4$
$a_2 = 1.759E-5$	$b_2 = -6.030E-7$
$a_3 = -5.972E-9$	$b_3 = 1.324E-10$

4.2.4 Heat Capacity for Liquid Phase

The observed data for the liquid heat capacity was taken from a paper by Luria and Benson (1977) who gathered data for n-alkane liquid heat capacities at different temperatures from various sources (Witt and Kemp, 1937; Kemp and Egan, 1938; Aston and Messerly, 1940; Messerly and Guthrie, 1967). These experimental data gathered by Luria and Benson were compared to two correlations found in the literature: the Hadden correlation for alkanes (1970) was based on the carbon number and the reduced temperature of the liquid component, while Yaws (1991) used a second degree polynomial in

temperature to fit the data. The comparison between these two correlations and the experimental data is plotted in fig. 4.7. The Yaws correlation seems to give better results at 250 K with an average absolute error of 1%, while the Hadden correlation gives more accurate results at 300 K with an error of 0.2% average absolute error. Although the two correlations found in the literature give good approximations of liquid heat capacity data, they are based on some parameters that would not be easily incorporated in the correlation with the distribution function. Fig.4.7 also shows that liquid heat capacity per unit mass does not change much with molecular mass for alkanes. Hence, the molecular mass dependence was ignored and a simple second degree polynomial was used to describe the temperature dependence. A good approximation is obtained especially at high temperatures. Multiplying by $\bar{\theta}$ converts this to molar heat capacity:

$$C_{PL}(T) = \bar{\theta}_L [a_L + b_L T + c_L T^2] \quad (4-22)$$

where $\bar{\theta}_L$ is the liquid mean molecular mass (kg/kmol). The polynomial constants found by fitting this equation to n-alkane data are

$$a_L = 5.41\text{E-}1$$

$$b_L = 7.03\text{E-}4$$

$$c_L = 2.26\text{E-}6$$

which fit Luria and Benson's gathered observed data with an rms error of 0.3 (fig.4.8).

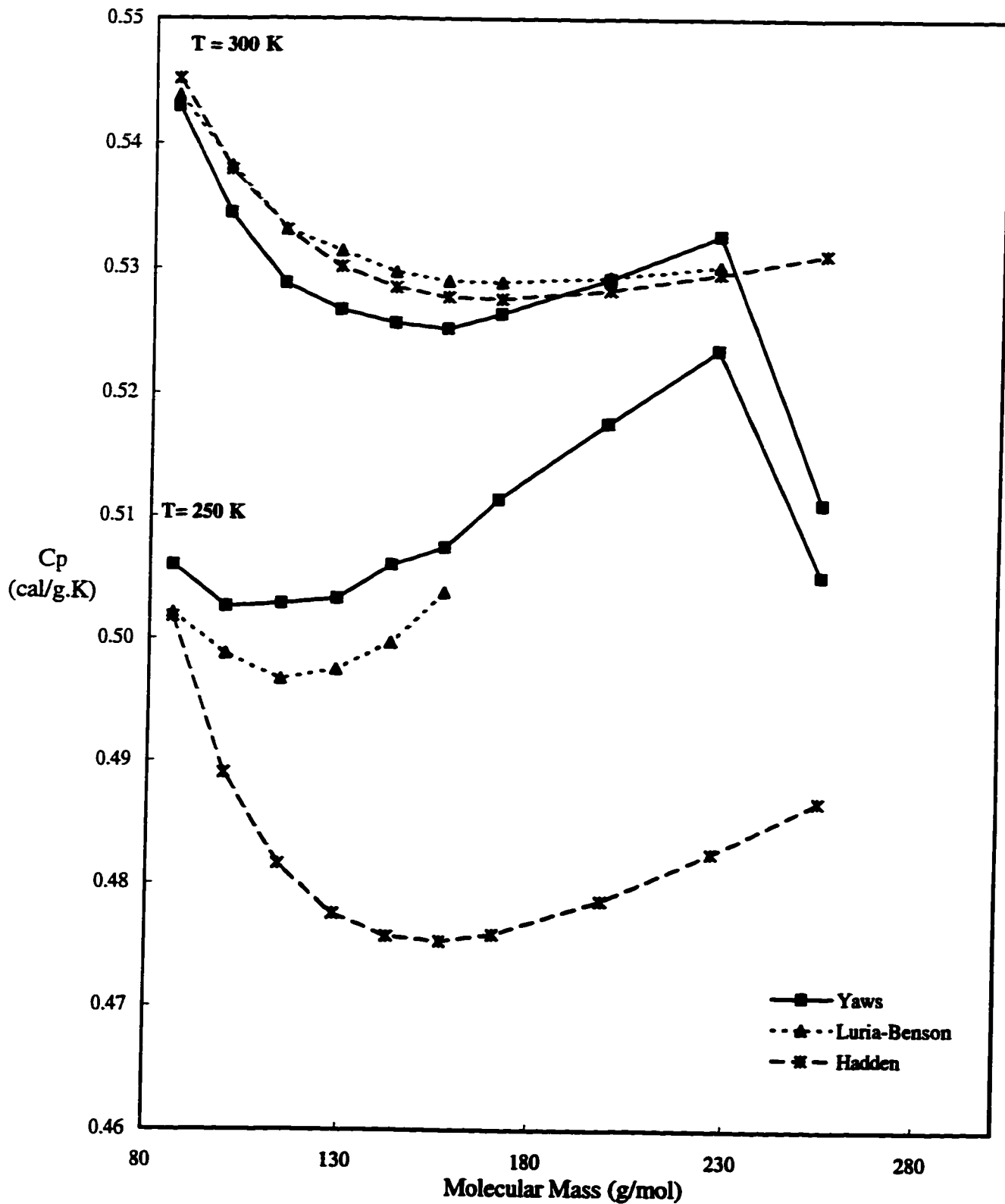


Figure 4.7: Variations of n-alkane liquid heat capacity with molecular mass at two different temperatures: 250 and 300 K.

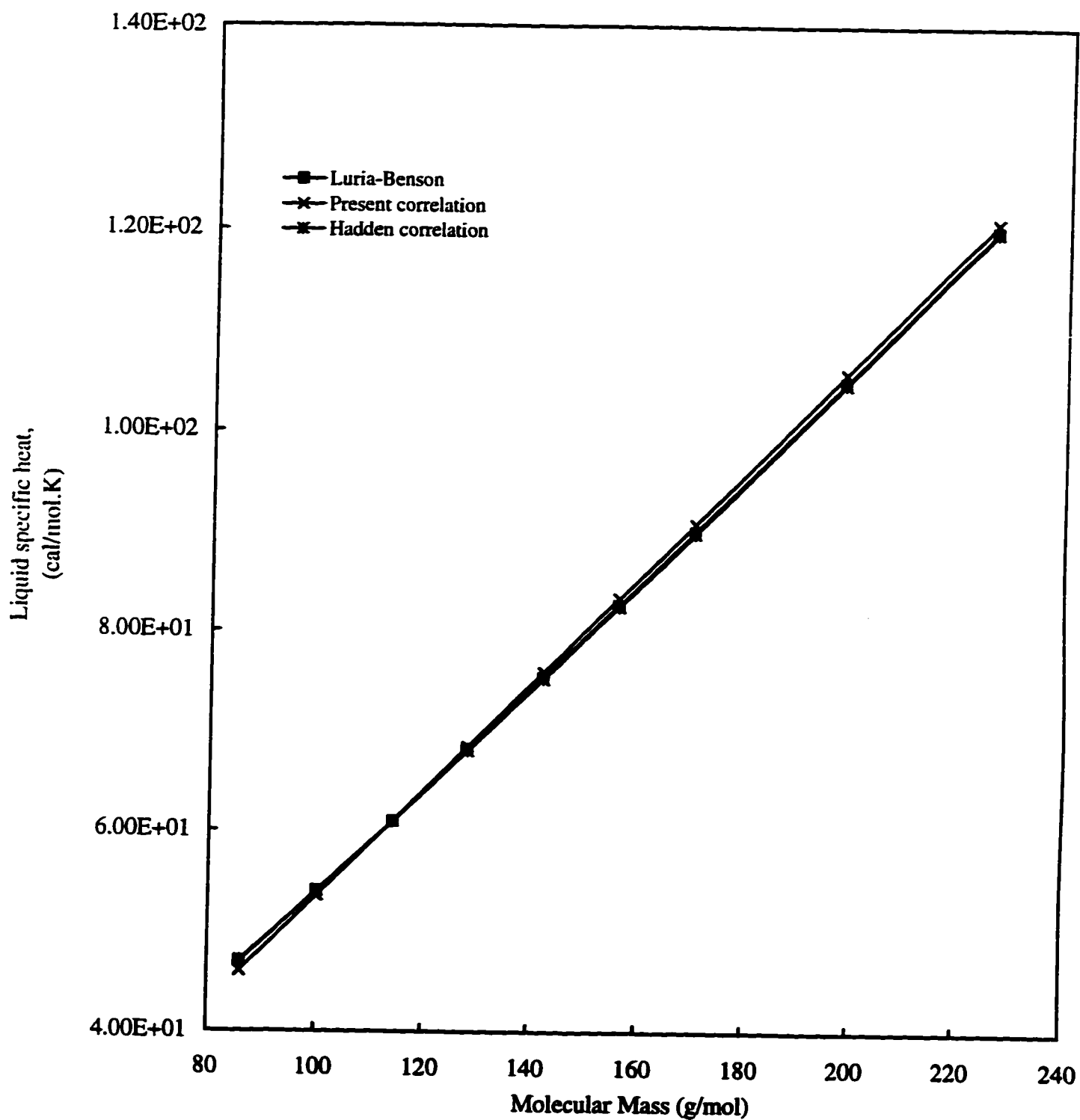


Figure 4.8: Comparison of Luria-Benson, Hadden and the present liquid heat capacity correlation at 300 K for n-alkanes.

4.2.5 Thermal Conductivity of Vapour Phase:

Combining rules for thermal conductivities are complex, especially for multicomponent mixtures, and cannot easily be adapted to a form which can be integrated with the distribution function. In most parts of the vapour field, during most of the vaporization history of the droplet, the vapour concentration is fairly low, and the conductivity of the mixture will approach that of air. The vapour conductivity therefore need not be calculated too accurately. The conductivity of individual components was correlated as a linear function of molecular mass:

$$\lambda(I) = a_K(T) + b_K(T)I \quad (4-23)$$

where $a_K(T)$ and $b_K(T)$ in turn are linear functions of temperature, which were fitted to the temperature behaviour of n-alkanes as

$$\begin{aligned} a_K(T) &= 2.6008E-05 T - 5.6496E-03 \\ b_K(T) &= -4.5511E-08 T + 8.2873E-06 \end{aligned} \quad (4-24)$$

with an rms error of about $1.24E-4$ (fig. 4.9). The literature values were obtained from Hallett (1994), these data were calculated using the Eucken equation.

The overall fuel vapour thermal conductivity was then calculated as that of the component with molecular mass equal to the mean:

$$\lambda_F = a_K(T) + b_K(T)\theta_F \quad (4-25)$$

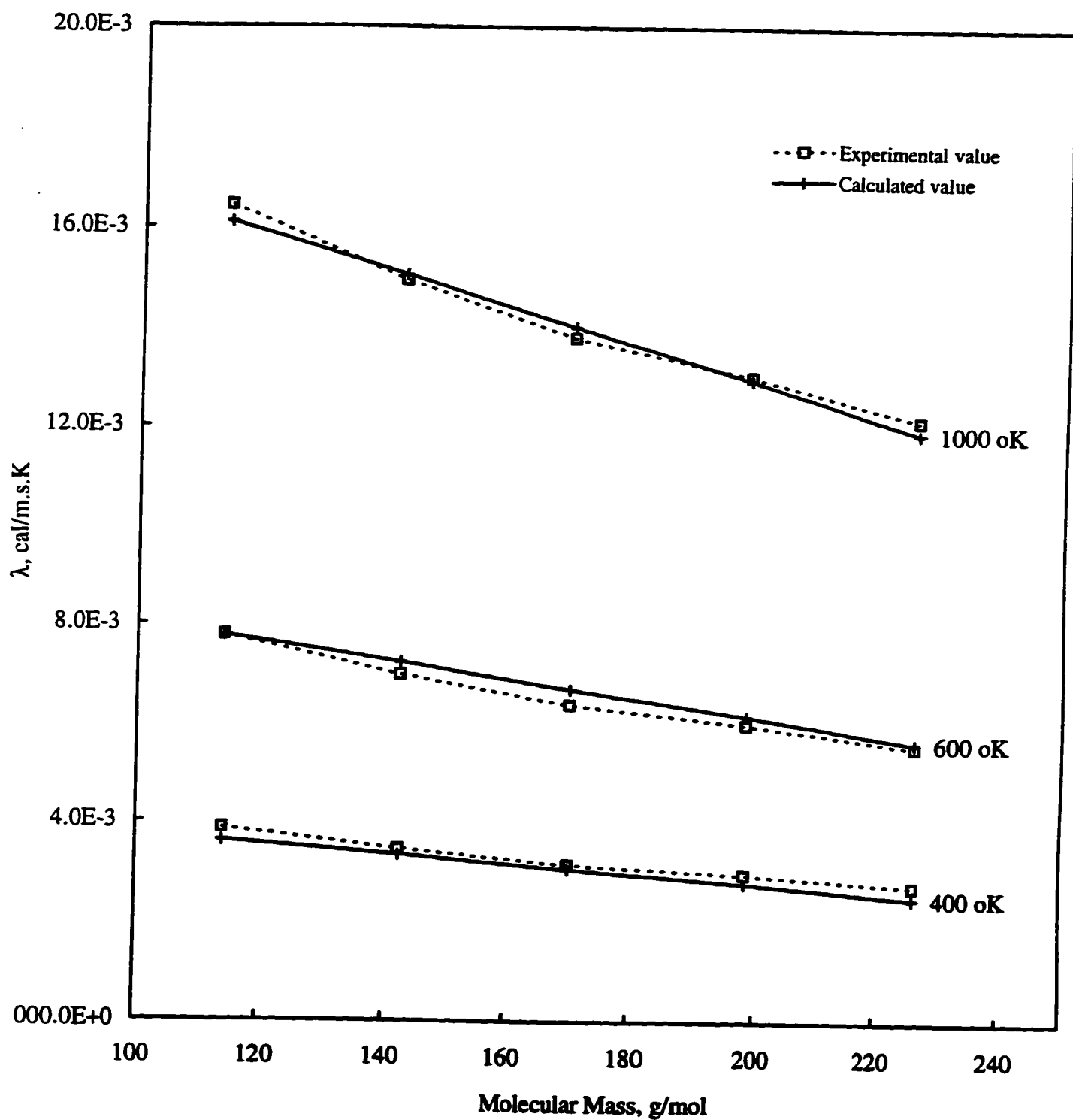


Figure 4.9: Present correlation for vapour phase thermal conductivity compared to literature values.

The thermal conductivity of the air-fuel mixture was then calculated by combining fuel and air values with the Mason-Saxena equation (Reid *et al.*, 1987):

$$\lambda_{mix} = \sum_{i=1}^n \frac{y_i \lambda_i}{\sum_{j=1}^n y_j A_{ij}} \quad (4-26)$$

$$A_{ij} = \frac{[1 + (\lambda_{tri} / \lambda_{trj})^{1/2} (M_i / M_j)^{1/4}]^2}{[8 (1 + M_i / M_j)]^{1/2}} \quad (4-27)$$

$$\frac{\lambda_{tri}}{\lambda_{trj}} = \frac{\Gamma_j \exp(0.0464 T_{ri}) - \exp(-0.2412 T_{ri})}{\Gamma_i \exp(0.0464 T_{rj}) - \exp(-0.2412 T_{rj})} \quad (4-28)$$

where

$$\Gamma_i = \frac{T_{cri}^{1/6} M^{1/2}}{P_{cri}^{2/3}} \quad (4-29)$$

and T_{cr} , P_{cr} and T_r are the critical temperature, critical pressure and reduced temperature ($T_r = T/T_c$) respectively, λ_i is the pure component thermal conductivity, λ_{ir} is the monoatomic thermal conductivity and y_i is the mole fraction.

4.2.6 Vapour Phase Diffusivity

As has already been mentioned, the component diffusivities required for these calculations are those of the components in the mixture, and because of the low

concentration of each component, it has been assumed that Fick's law holds for each species. A further simplification is made here: in most of the vapour field, and during most of a droplet's vaporization history, the overall fuel concentration is low, and air is the predominant species. The diffusivities in the mixture will therefore be approximated as diffusivities in air. The air itself is treated as nitrogen: air is 79% N₂ by mol, and diffusivities in N₂ and O₂ are almost identical because the molecular masses of N₂ and O₂ are so close to one another. The vapour phase diffusivity coefficient was calculated using a linear equation with respect to molecular mass, while the temperature variation was accounted for in the coefficient Φ_D . For the component diffusion coefficient $D_m(I)$

$$D_m(I) = (a_D + b_D I) \Phi_D \quad (4-30)$$

This equation was fitted to values of the diffusivities of various n-alkanes in nitrogen, giving

$$a_D = 2.89E-09$$

$$b_D = -6.60E-12$$

The literature values were taken from Hallett (1992) and were calculated using the Chapman-Enskog theory (Reid *et al.*, 1987).

The three average diffusivities required, \bar{D} , \tilde{D} , \hat{D} , are found from eq. (3-12), (3-15) and (3-17) as

$$\bar{D} = \left(a_D + b_D \frac{\Psi}{\theta} \right) \Phi_D \quad (4-31)$$

$$\tilde{D} = \left(a_D + b_D \left[\frac{\sigma^2}{\theta} + \theta \right] \right) \Phi_D \quad (4-32)$$

$$\hat{D} = \left(a_D + \frac{b_D}{\psi} \left[\gamma_S \sigma^3 + 3 \theta \sigma^2 + \theta^3 \right] \right) \Phi_D \quad (4-33)$$

where θ is the vapour mean molecular mass and ψ the second moment of the distribution, σ is the variance, and γ_S is the skewness coefficient of the distribution, which for a gamma distribution is given by (Abramovitz and Stegun, 1970)

$$\gamma_S = \frac{2}{\sqrt{\alpha}} \quad (4-34)$$

α being one of the distribution parameters.

The temperature dependence was fitted with a Sutherland-type equation, giving the coefficient Φ_D as

$$\Phi_D = \frac{T^{5/2}}{b_\phi + T} \quad (4-35)$$

b_ϕ was found constant and equal to 250 for the n-alkanes fitted.

Fig. 4.10 shows a comparison of the diffusivity coefficient calculated values to theoretical values at different temperature. The calculated values are within 5.56E-7 range of error.

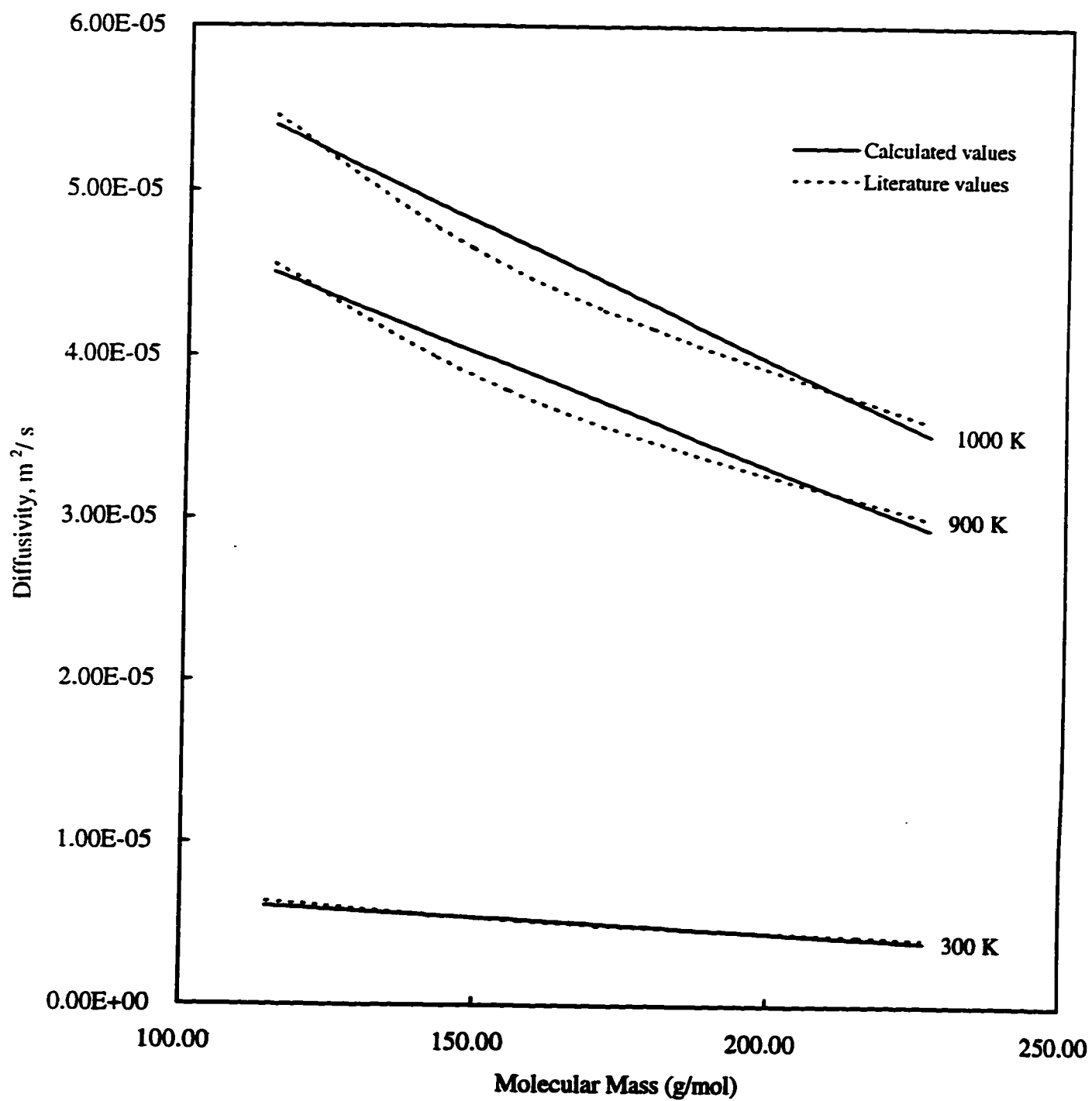


Figure 4.10: Literature and calculated values for vapour phase diffusivities.

5. RESULTS AND DISCUSSION

In this chapter, sample calculations for vaporizing droplets (no chemical reaction) will be presented in order to demonstrate the capabilities of the theory just developed and to show how the distribution function for the liquid was chosen using the ASTM distillation curve.

5.1 Simulation of a single-component fuel

To verify the program, a narrow distribution was chosen to simulate pure n-dodecane. The mean of the distribution θ_L , molecular mass, was set equal to the molecular mass of n-dodecane (170 g/mol) with a very narrow variance ($\sigma^2 = 1$). The minimum of the distribution was chosen to be a little less than the mean: $\gamma = 160$. The distribution parameters α and β were then solved for using eq. (3-61), which gave $\alpha_L = 100$ and $\beta_L = 0.1$ for n-dodecane. The predictions from the current model were compared to the ones obtained from the single component model of Bergeron and Hallett (1989b) for a vaporizing n-dodecane droplet. The results are plotted on fig.5.1 for a 1.5 mm diameter droplet with an initial temperature of 25°C evaporating at an ambient temperature of 700°C. Both models used the same grid with 20 grid points (see section 4.1.2) and the same time step of 0.01 sec.

As the liquid temperature T_L at the surface increases, the mass fraction of fuel

evaporated increases and vapour diffuses outwards. Fig. 5.1 also shows that the single component droplet vaporizes at an almost constant temperature, very close to the boiling temperature, for most of the droplet lifetime. The two models are in good agreement; the discrepancy between the liquid temperatures is largely due to the fact that the single component model uses the more accurate Antoine equation for VLE. To demonstrate this, Fig. 5.2 shows the single component model with the vapour pressure taken as the Clausius-Clapeyron equation used in this work (eq. 3-56). The Clausius-Clapeyron equation (as in the continuous model) predicts lower liquid temperatures than the Antoine equation, which supports the fact that the discrepancies between the continuous model and the single component model are mainly due to the relation chosen to describe the vapour-liquid equilibrium.

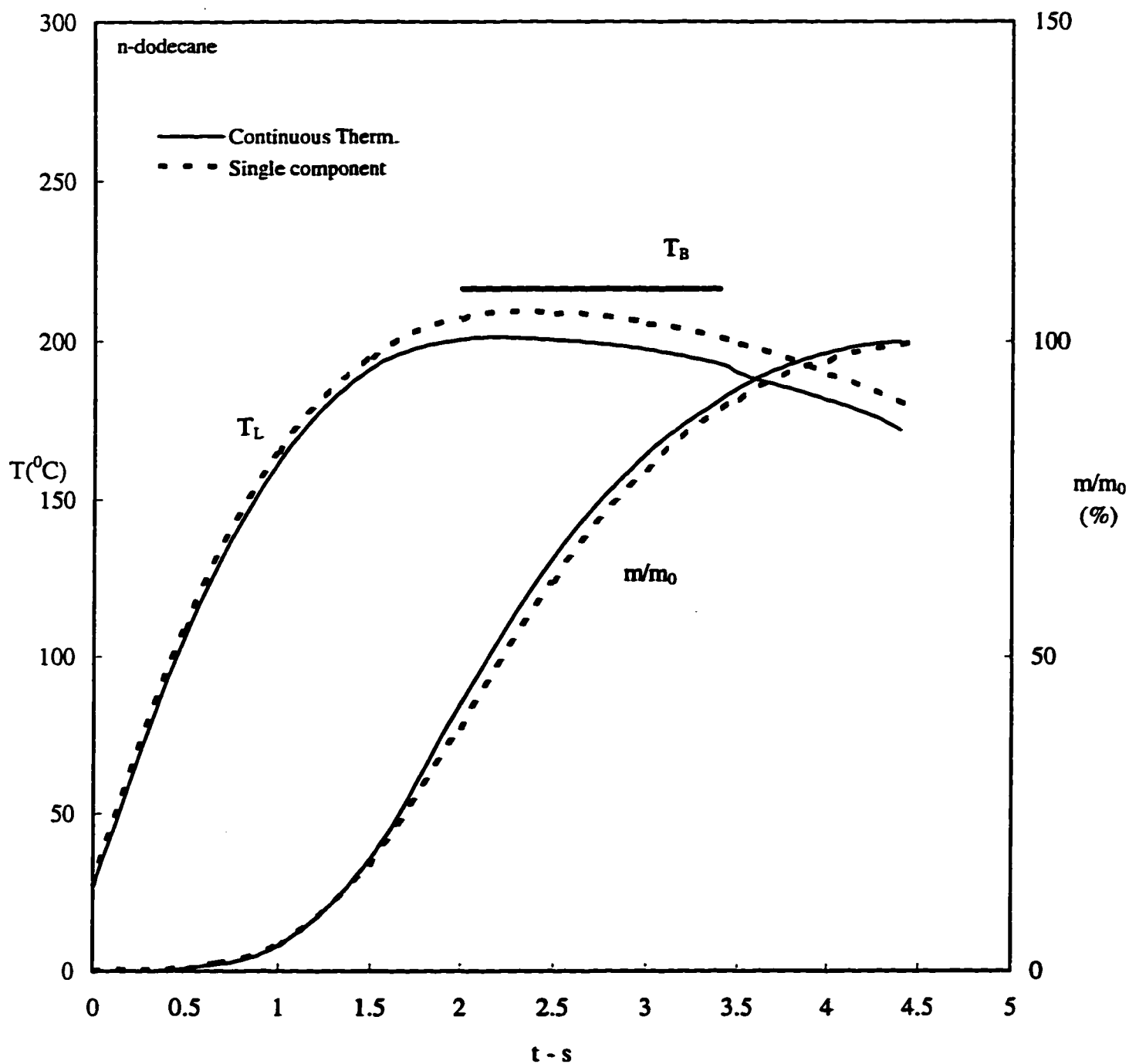


Figure 5.1: Liquid Temperature T_L and mass fraction evaporated m/m_0 versus time for 1.5 diameter n-dodecane droplet evaporating at $T_{\infty} = 700^{\circ}\text{C}$, initial liquid temperature 25°C . Comparison of predictions from the continuous thermodynamics model with single pure component calculations. The T_B line gives the boiling point of n-dodecane.

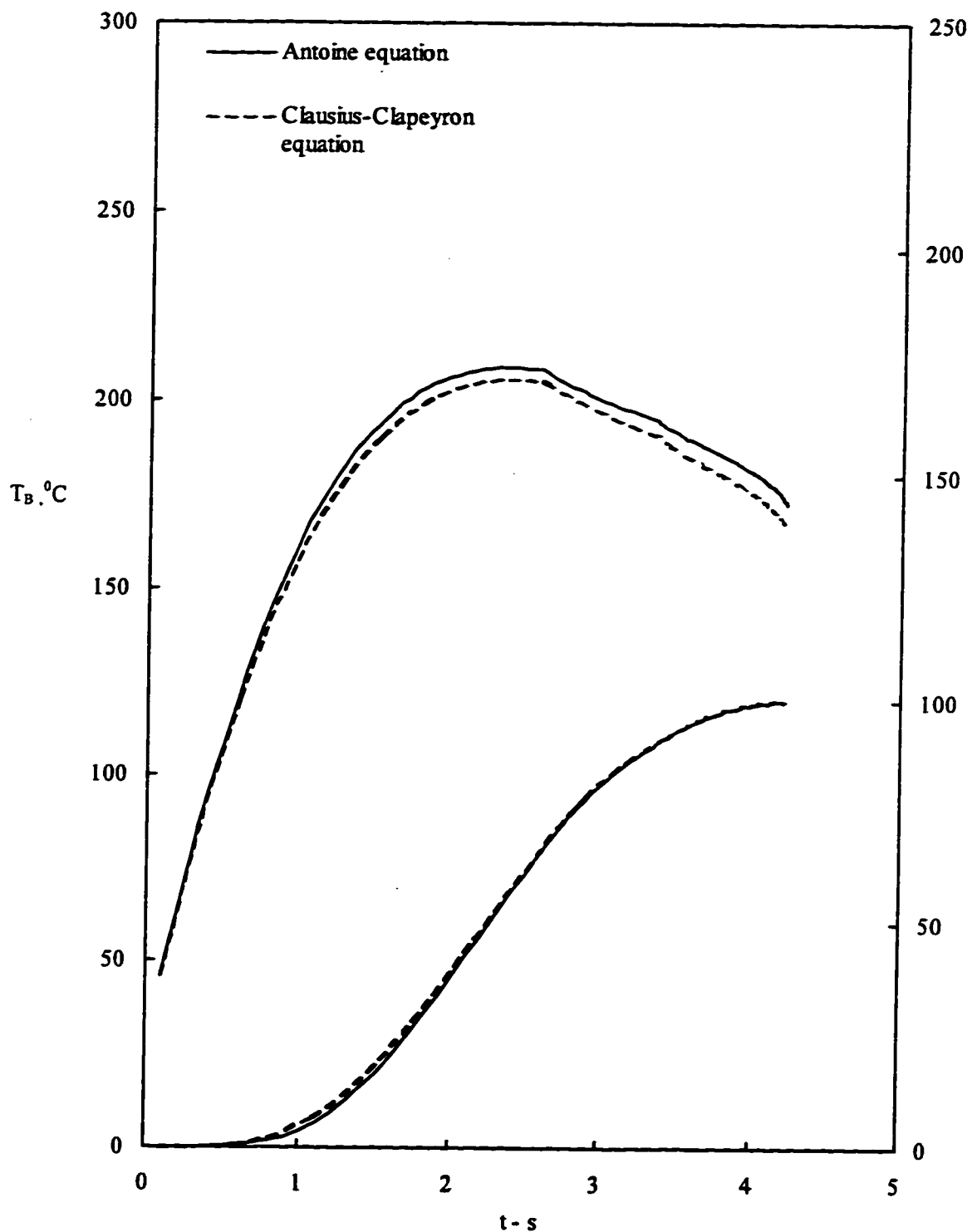


Figure 5.2: Comparison of the results obtained from single pure component calculations using the Antoine equation and the Clausius-Clapeyron relation for vapour-liquid equilibrium for a 1.5 mm n-dodecane droplet evaporating at $T_\infty = 700$ °C, initial temperature 25°C.

5.2 Selection of distribution functions for commercial fuels

To illustrate the capabilities of the model, distribution functions have to be selected that simulate the two commercial fuels chosen: Diesel and gasoline.

The distribution parameters for each fuel were calculated by continuous thermodynamics simulation of the ASTM D86 distillation test described in section 1.1. The number of moles of i in the sample volume V can be written, as:

$$n_i = x_i c_L V \quad (5-1)$$

As a quantity dV of liquid evaporates from the sample, this changes as

$$dn_i = x_i d(c_L V) + c_L V dx_i \quad (5-2)$$

The total moles of vapour created is $d(c_L V)$ of which y_i is i , so that

$$dn_i = y_i d(c_L V) \quad (5-3)$$

Equating these gives the change in liquid composition as

$$dx_i = (y_i - x_i) \frac{d(c_L V)}{c_L V} \quad (5-4)$$

Introducing the distribution, integrating and using eq. (3-46), a relationship between the distribution parameters and the volume fraction evaporated can be obtained:

$$d\theta_L = (\theta - \theta_L) \left[\frac{dV}{V} - \frac{d\theta_L}{\theta_L} \right] \quad (5-5)$$

$$d\psi_L = (\psi - \psi_L) \frac{dV}{V} \frac{\theta_L}{\theta}$$

These equations were numerically integrated to get θ_L , σ_L and the boiling point as functions of the volume evaporated using the equations developed previously (3-59, 3-61, 3-64). The distribution parameters were then chosen to match the 10% and 90% volume evaporated points of the ASTM D86 curve predicted using continuous thermodynamics with those for real fuels. The “Diesel” parameters were chosen to best represent the data from a commercial fuel given by Kallio *et al.* (1985) shown in Table 5.1:

Table 5.1: ASTM Distillation Test for Diesel Fuel (Kallio *et al.*, 1985)

% Volume evaporated	IBP	10%	50%	90%	EP
Boiling Temperature (°C)	173	203	257	323	351
Fitted Boiling Points (°C)	191	205	258	322	375

where IBP is the initial boiling point and EP is the end point.

Fitting the 10% and 90% points gives the distribution parameters as follows

$$\alpha = 18.5$$

$$\beta = 10$$

$$\gamma = 0$$

For gasoline, values were chosen which lie roughly in the mid range of the ASTM D439

specification for gasoline as shown in the following table:

Table 5.2: ASTM Distillation Test for gasoline

% Volume evaporated	IBP	10%	50%	90%	EP
Boiling Temperature (°C)	30	55	110	170	200
Fitted Boiling Points (°C)	44	56	107	170	218

Again fitting the 10% and 90% points gives the distribution parameters as follows

$$\alpha = 5.7$$

$$\beta = 15$$

$$\gamma = 0$$

Fig. 5.3 shows the ASTM curves predicted using eq. (5-4) and these parameters, while fig. 5.4 shows the corresponding distribution functions using these values for both Diesel and gasoline. Although Peng *et al.* (1986) have questioned the use of an unbounded distribution for crude petroleum, these ASTM curves show that it can give very reasonable approximation of distillate fuels. The only discrepancy due to the unbounded distribution is the higher end point in the predictions (Fig. 5.3).

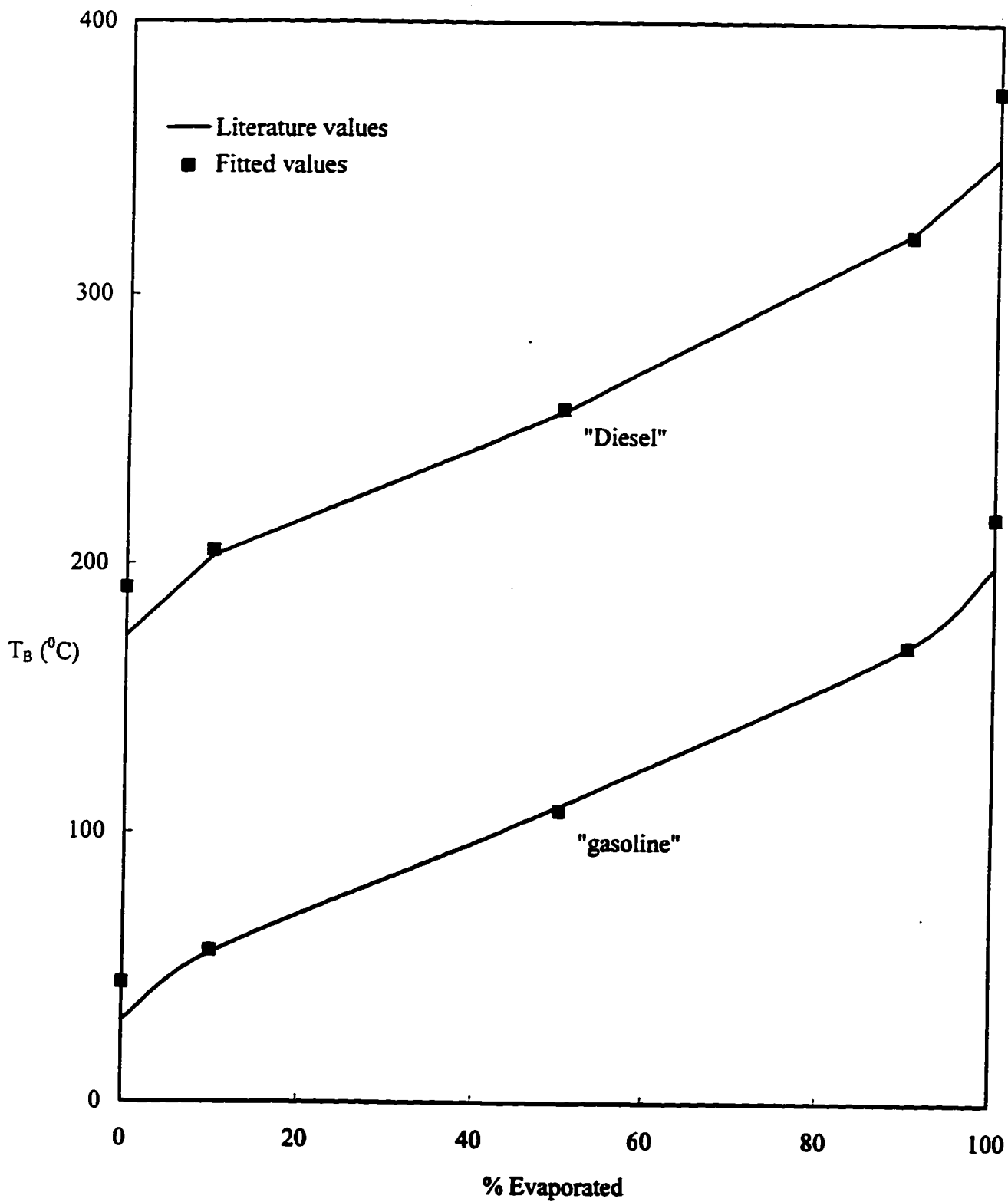


Figure 5.3: ASTM D86 curves predicted using continuous thermodynamics for gasoline and Diesel, compared to actual values (Kallio et al., 1985).

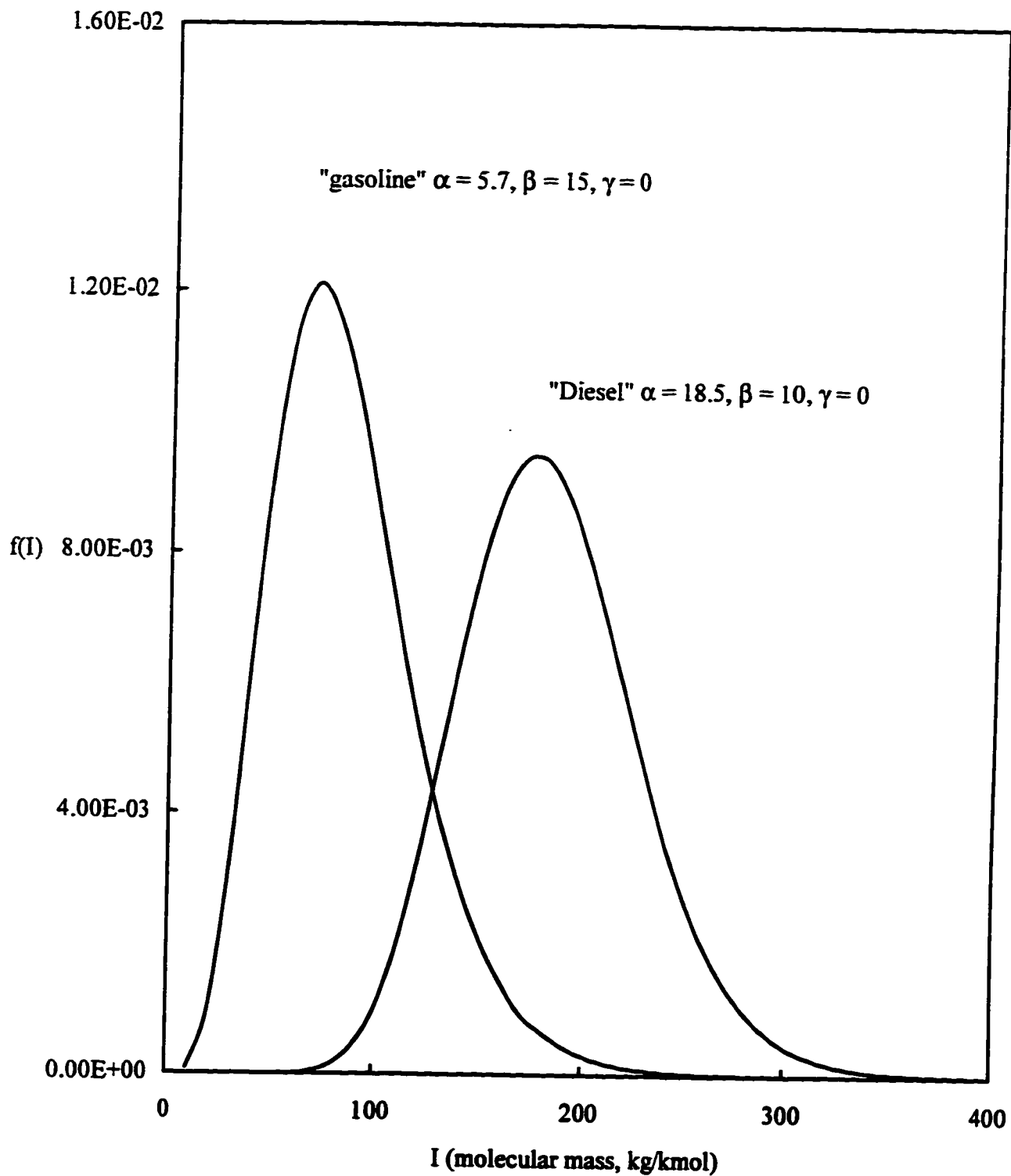


Figure 5.4: Distribution curves for both gasoline and Diesel using the parameter values fitted to the ASTM curve.

5.3 Simulation of a gasoline fuel

Two droplet radii were chosen to represent the droplet vaporization of a small and a large droplet. A large droplet radius is about 1.5 mm and is typical of those used in laboratory experiments. The small radius is about 0.1 mm and is considered to be a typical radius of the larger droplet sizes found in a fuel spray.

For both fuels, gasoline and Diesel, the initial droplet temperature assumed was 25°C and the ambient temperature was assumed to be 700°C, which is typical for Diesel engines during ignition.

Fig. 5.5 illustrates the distribution functions in the liquid phase and at the surface of the droplet in the vapour phase for a 1.5 diameter gasoline droplet at the beginning of the evaporation time. Fig. 5.6 and 5.7 show the time histories of liquid phase properties as well as of the bubble point T_b of the liquid for a 0.1 and a 1.5 diameter droplet, respectively. Comparing the liquid temperatures to those for the single component fuel (Fig. 5.1), it can be seen that in the case of the continuous models, the liquid temperatures remain below the bubble point, so that vapour mole fractions at the surface are fairly low; this is quite different from the single component model in which the liquid temperature approaches the boiling point very closely. The bubble point T_b shown in the graphs is found from eq. (3-65) by setting $y_F = 1$. The reason for this is the continuous transient heating of the mixture droplet which absorbs some of the heat as distillation proceeds. For the larger droplet (Fig. 5.7), the mass flux from the surface is roughly proportional to $1/R$ so that the

evaporating liquid has less cooling effect; the liquid temperature approaches the bubble point more closely than for the smaller diameter but not as closely as it does for the single-component model.

Fig. 5.6 and 5.7 show that both gasoline droplets rapidly reach a sort of quasi-steady state, during which the liquid temperature T_L and the liquid molecular mass increase nearly linearly as light components are distilled out. As the mean molecular mass increases the boiling temperature of the new mixture resulting also increases. The heat flux to the multicomponent droplet is divided in two: one fraction is used to heat up the droplet, the other fraction is used for evaporation. This is very different from a single component droplet, which reaches a more or less steady equilibrium temperature, so that once the droplet is heated, all the heat is used for evaporation. Near the end of the multicomponent droplet lifetime, only heavy components remain in the liquid, causing the liquid temperature and molecular mass to increase sharply. Some of this behaviour may be due to the use of an unbounded distribution function. The width of the distribution, as characterized by the standard deviation, decreases slowly during the process, indicating that as light components are distilled out, only heavy components are left.

The 1.5 mm droplet has a consistently higher liquid temperature because its evaporation rate is proportionally less. The simple classical theory of droplet evaporation shows that the mass flux ($\text{kg/m}^2\text{s}$) evaporated depends on droplet size as $(1/R)$, so that the larger droplet has a lower mass flux and more heat is available for liquid heating. This causes the droplet to follow a vaporization history with a somewhat greater yield of light fraction, reflected in a slightly lower value of θ_L for a given fraction evaporated; because of

this, the sharp upturn in θ_L evident for the smaller droplet is less obvious.

Fig. 5.8 and Fig. 5.9 give a sample of the information provided by the model in the vapour phase, Fig. 5.8 being for a small droplet about halfway through its lifetime and Fig. 5.9 for a large droplet near the end. The vapour mean molecular mass θ drops with increasing radius away from the droplet, reflecting the increase in θ_L with time and the time needed for this change to diffuse outwards. The fuel mole fraction decreases while the vapour temperature increases with increasing radius. A curious feature is the slight “hump” in the profile of σ^2 , which rises to values greater than any recorded at the surface. Physically this corresponds to a broadening of the distribution as it diffuses outwards from the surface, which occurs because distributions at different radii can mix with each other by means of diffusion. This is a phenomenon similar to dispersion in chemical reactors. This effect disappears far from the droplet, where fuel concentrations drop to negligible levels. It is of interest to note that this “hump” remained even in predictions made with all three average diffusivities set equal (Fig. 5.10). It is evident that the vapour composition varies significantly in space, a fact which may have interesting consequences for ignition or combustion.

Fig. 5.11 shows results for the vaporization of gasoline droplet with a 1.5 mm diameter using a time step cut in half, 0.005 s. The boiling point and the liquid temperature show that there is hardly any difference between the two time steps, the maximum error on the boiling temperature being about 0.09% at the end of the droplet lifetime. Fig. 5.12 shows the effect of increasing the number of grid points. Results obtained with a 20 and 40 points grid agree within a 1.3% error. It can be concluded that the grid and time step used

for these calculations are sufficiently fine for accuracy.

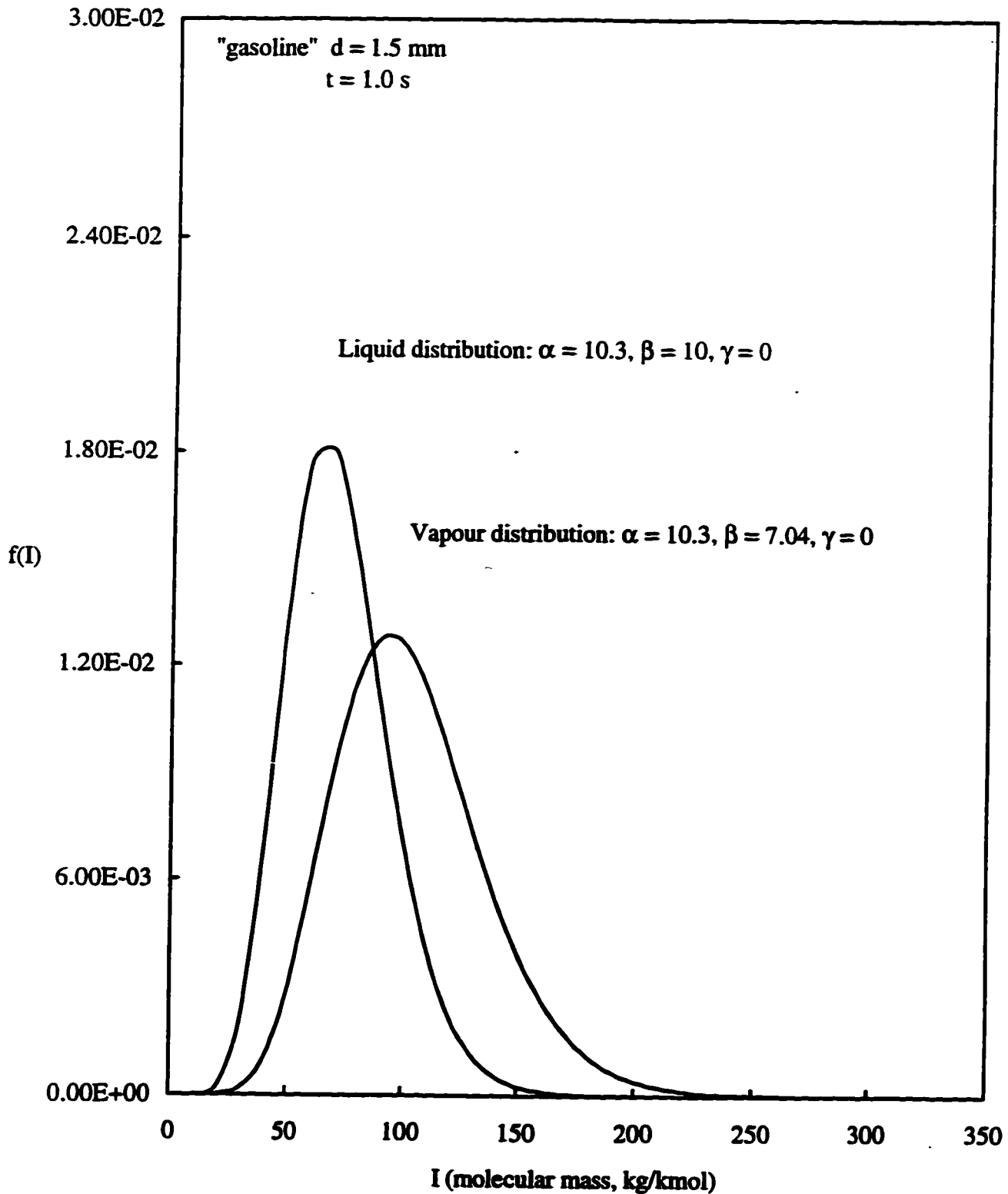


Figure 5.5: Distribution functions of the liquid phase and the vapour phase at the droplet surface for a 1.5 mm gasoline droplet evaporating at $T = 700$ °C, initial temperature 25 °C. The distributions are a representation of the composition of the liquid and the vapour phase at the beginning of the droplet lifetime (1.0 s).

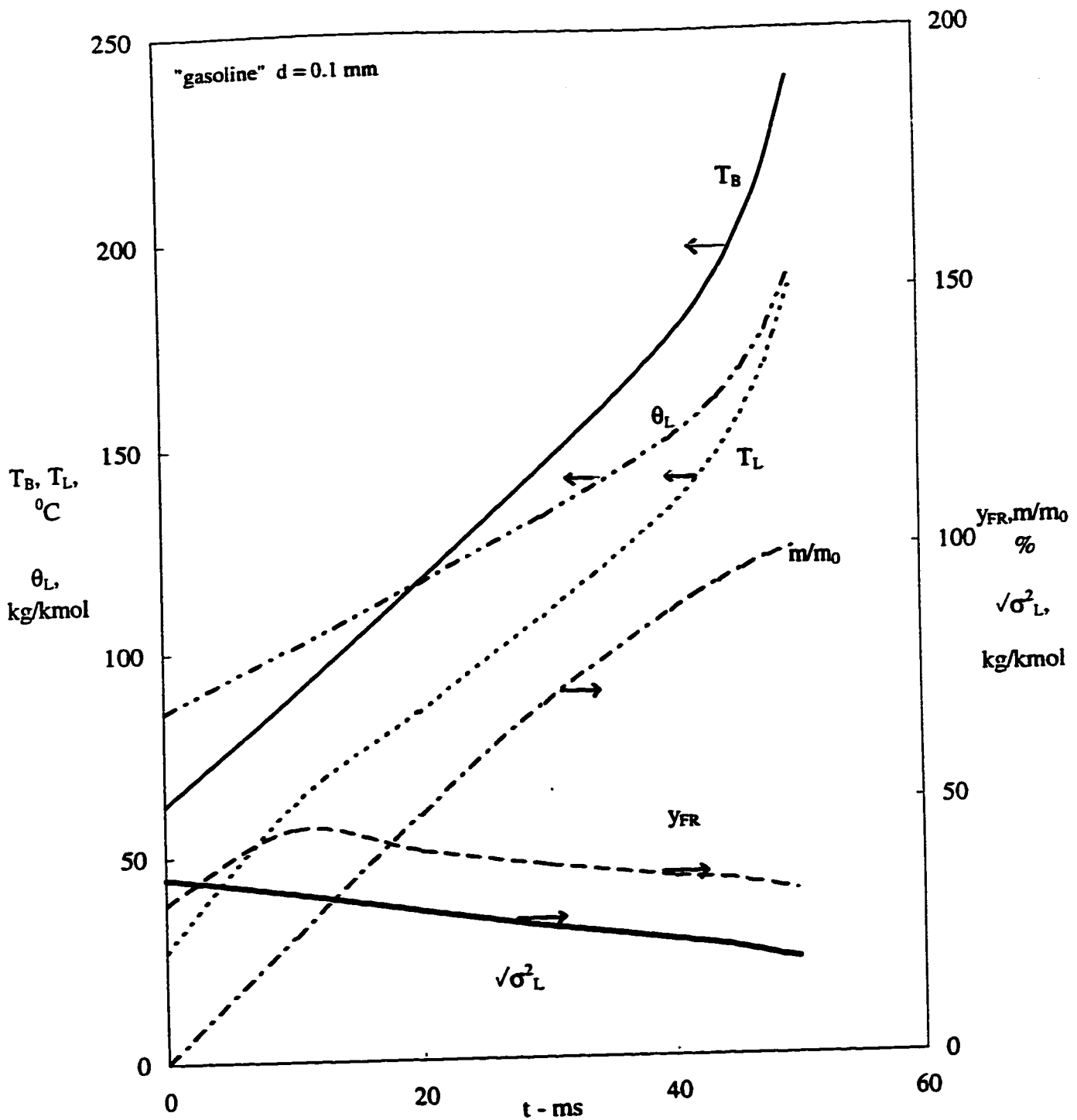


Figure 5.6: Time histories of liquid phase properties and of vapour phase mol. fraction at the surface y_{FR} for a 0.1 mm gasoline droplet evaporating at $T_{\infty} = 700^{\circ}\text{C}$, initial temperature 25°C .

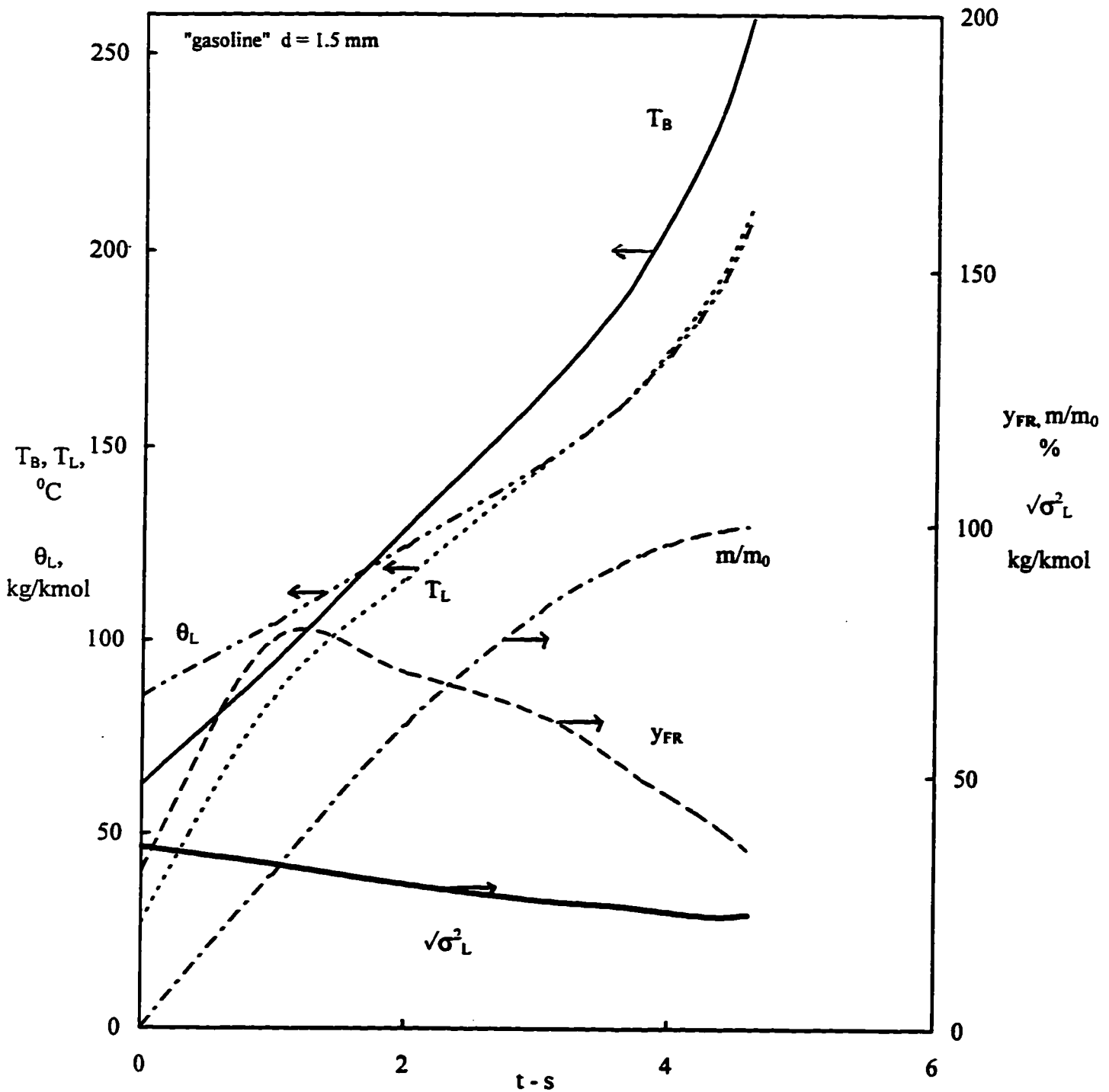


Figure 5.7: Time histories of liquid phase properties and of vapour phase mol fraction at the surface y_{FR} for a 1.5 mm gasoline droplet evaporating at $T_{\infty} = 700^{\circ}\text{C}$, initial temperature 25°C .

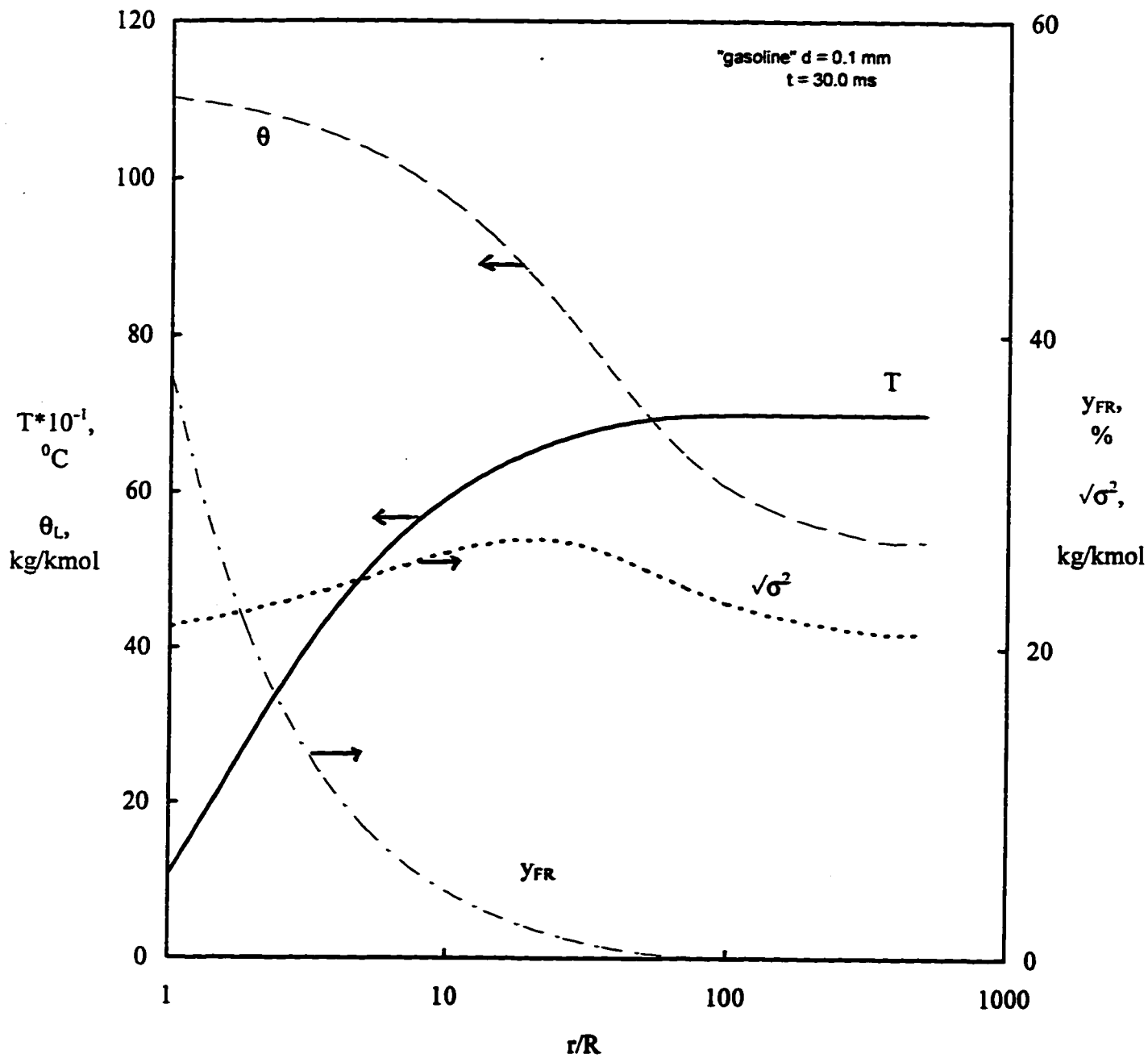


Figure 5.8: Vapour phase properties as a function of dimensionless radius (r/R) for a 0.1 mm "gasoline" droplet evaporating at $T_\infty = 700^\circ\text{C}$, initial temperature 25°C and shown at time $t = 30$ ms. The calculation domain extends to $(r/R) = 500$.

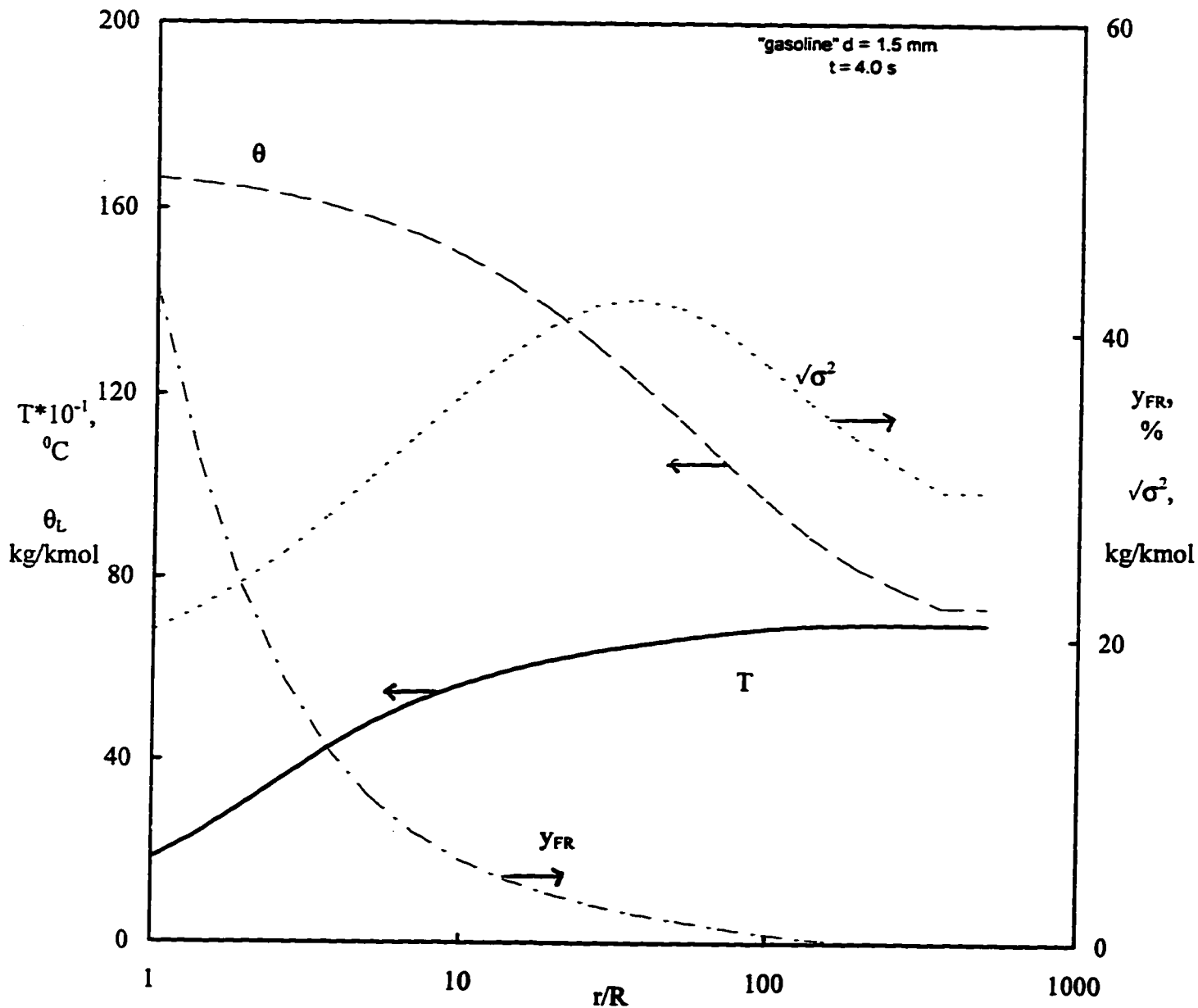


Figure 5.9: Vapour phase properties as a function of dimensionless radius (r/R) for a 1.5 mm "gasoline" droplet evaporating at $T_{\infty} = 700^{\circ}\text{C}$, initial temperature 25°C and shown at time $t = 4.0$ s. The calculation domain extends to $(r/R) = 500$.

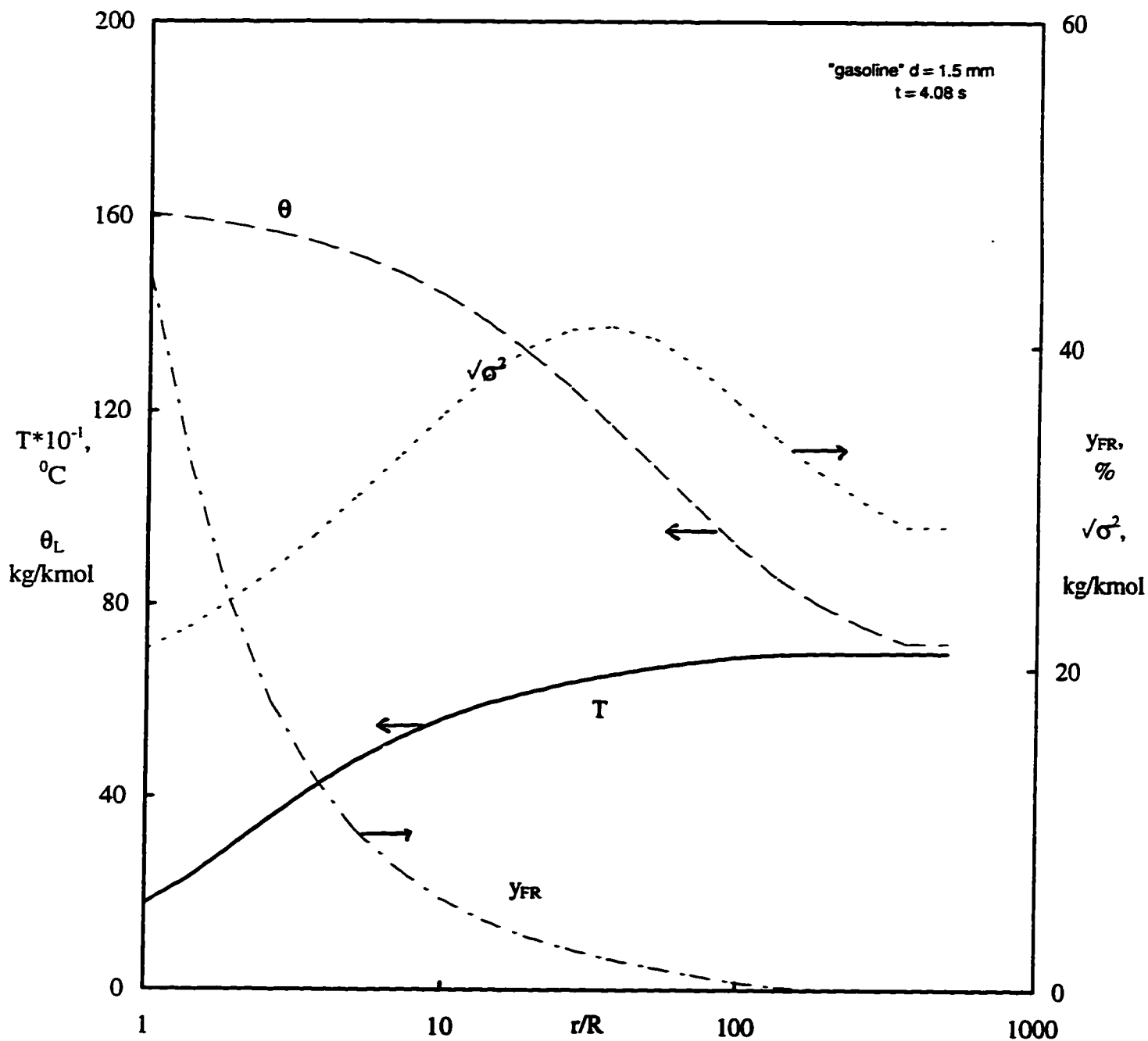


Figure 5.10: Vapour phase properties as a function of dimensionless radius (r/R) for a 1.5 mm “gasoline” droplet evaporating at $T_{\infty} = 700^{\circ}\text{C}$, initial temperature 25°C . Model run with all three average diffusivities set equal.

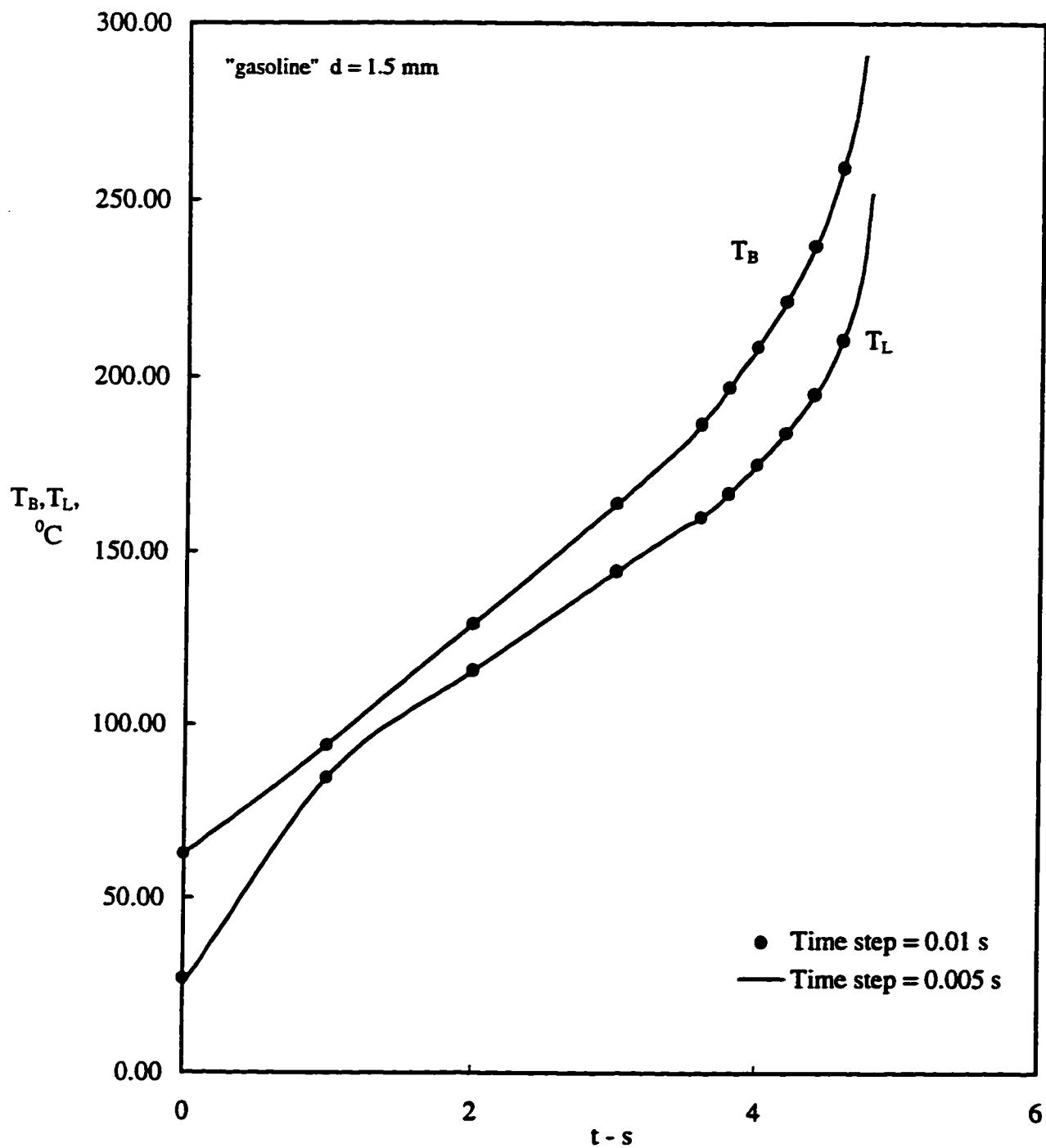


Figure 5.11: Liquid temperature and boiling point temperature for a 1.5 mm "gasoline" droplet evaporating at $T_{\infty} = 700^{\circ}C$, initial temperature $25^{\circ}C$. Comparison of results obtained with a time step of 0.01 s with results obtained with a time step half time smaller.

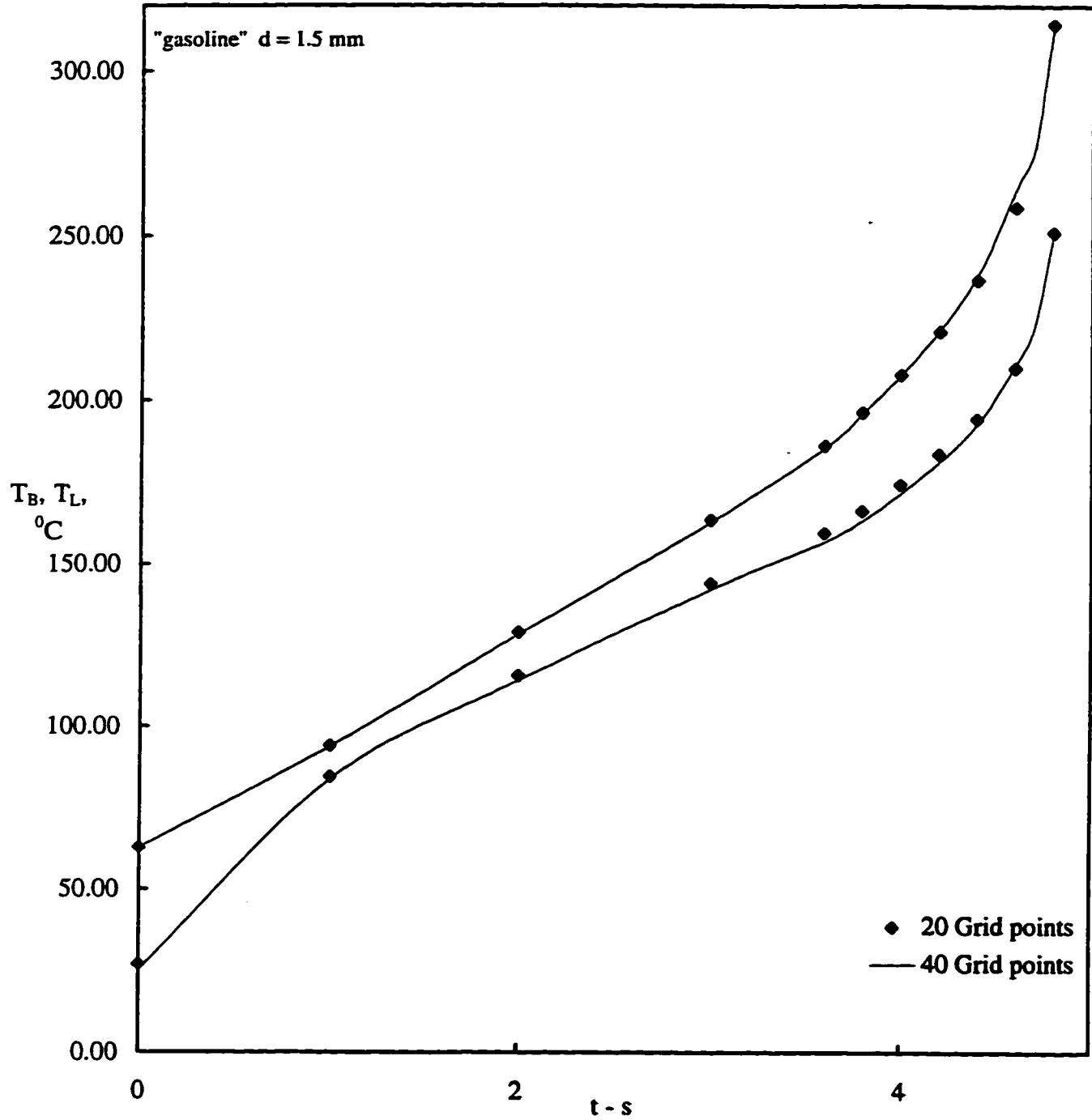


Figure 5.12: Liquid and boiling point temperatures for a 1.5 mm “gasoline” droplet evaporating at $T_{\infty} = 700^{\circ}\text{C}$, initial temperature 25°C . Comparison of the results obtained with a 20 and a 40 grid point model.

5.4 Simulation of a Diesel fuel

The exact same phenomena as for gasoline are observed for the Diesel droplets. Fig. 5.13 and Fig. 5.14 show that the transient heating of the droplet is much more pronounced since Diesel is a “heavier” (less volatile) fuel. At the beginning of the droplet lifetime, most of the heat is used to heat up the liquid and hardly any fuel is vaporized. Once the liquid temperature reaches the boiling point of the lightest components, the mass fraction evaporated starts increasing. The fuel mole fraction increases up to a maximum at the beginning of the droplet lifetime, then, as the droplet radius decreases, the mass flux from the droplet surface increases, causing a slight cooling of the droplet so that the surface mole fraction decreases slightly. Diesel being a heavier fuel than gasoline, the droplets have longer lifetimes than gasoline droplets. Fig. 5.15 and 5.16 show the vapour phase changes for Diesel.

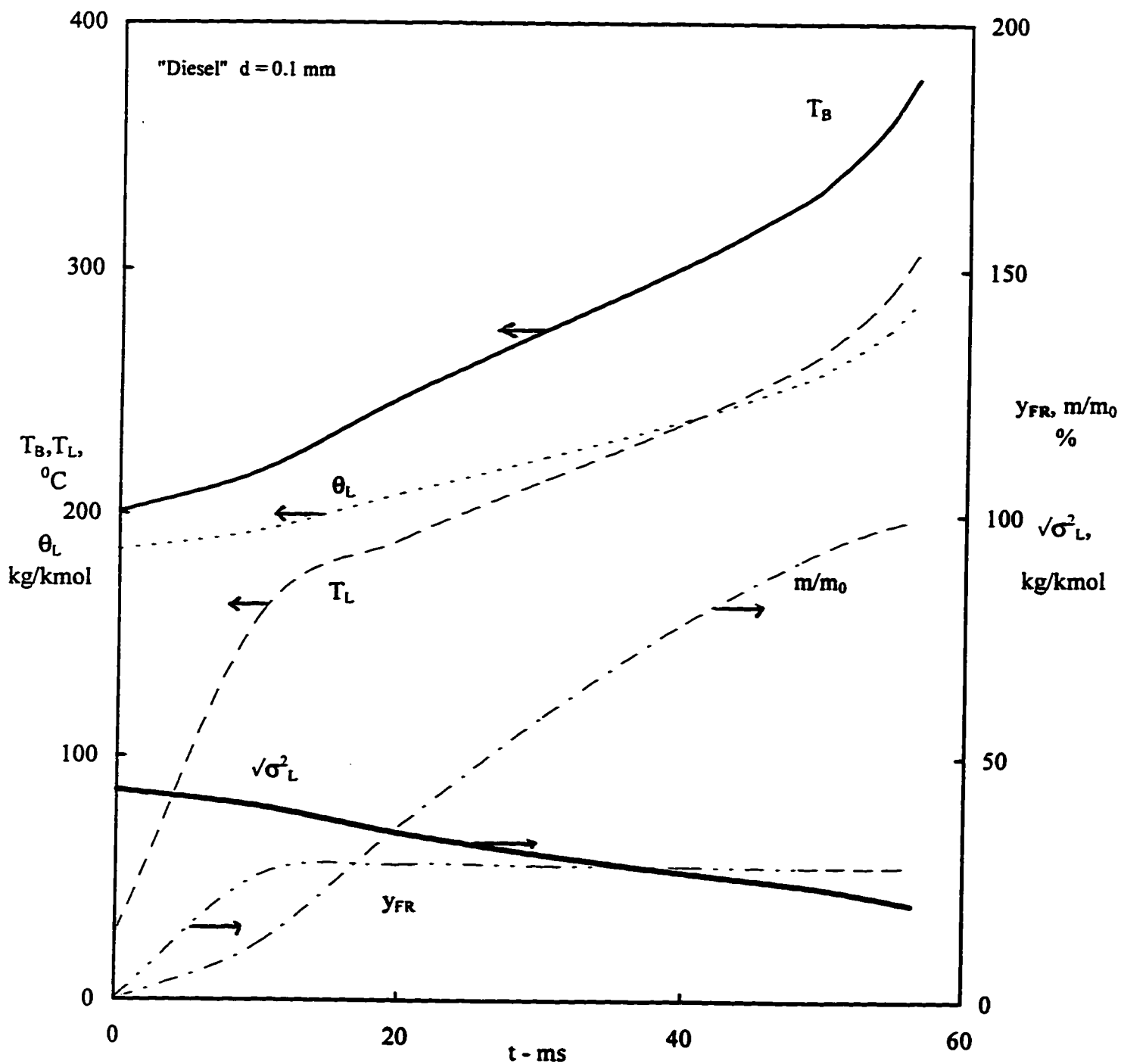


Figure 5.13: Time histories of liquid phase properties and of vapour phase mol fraction at the surface y_{FR} for a 0.1 mm Diesel droplet evaporating at $T_\infty = 700$ °C, initial temperature 25 °C.

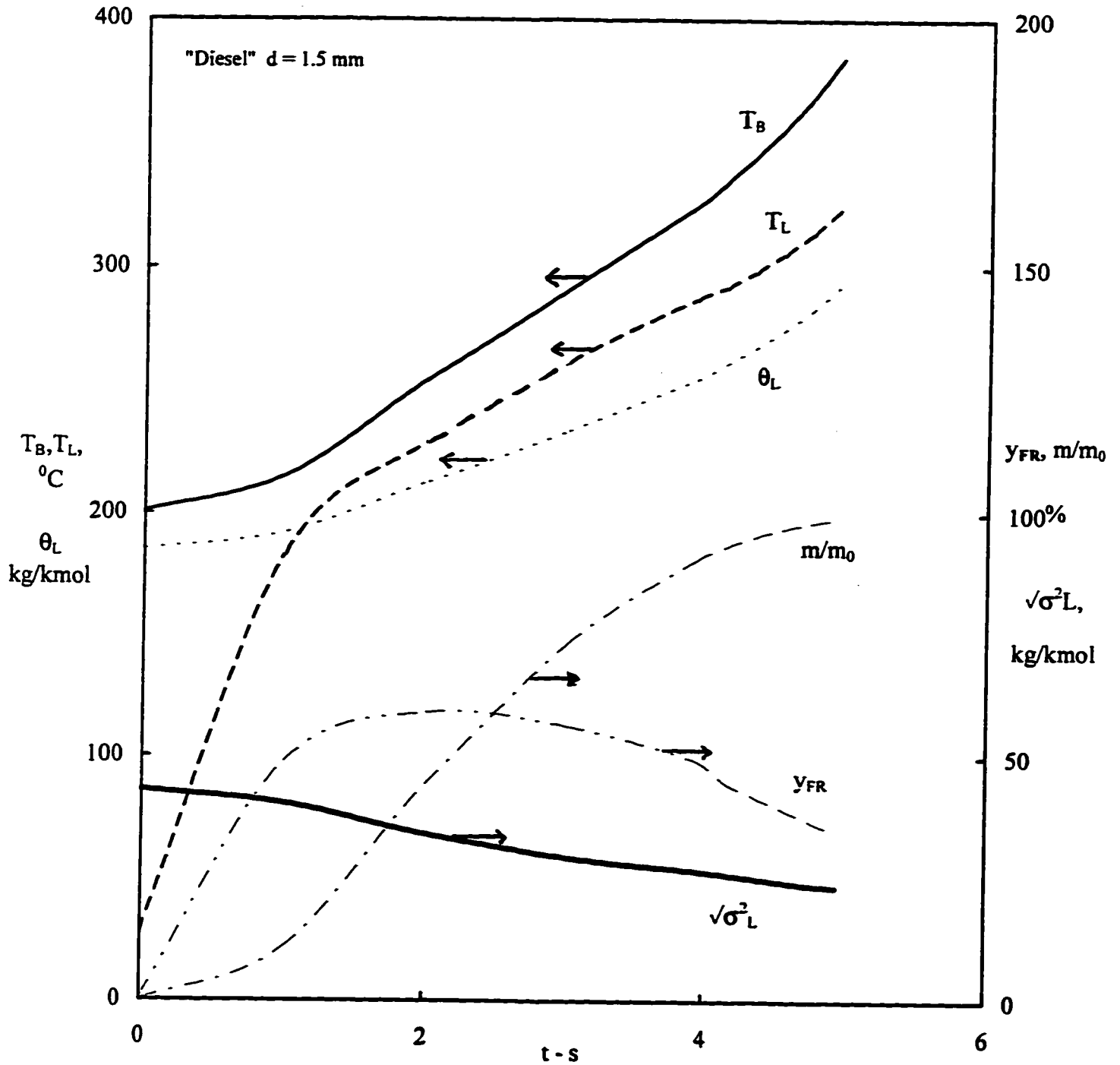


Figure 5.14: Time histories of liquid phase properties and of vapour phase mol fraction at the surface y_{FR} for a 1.5 mm Diesel droplet evaporating at $T_{\infty} = 700^{\circ}\text{C}$, initial temperature 25°C .

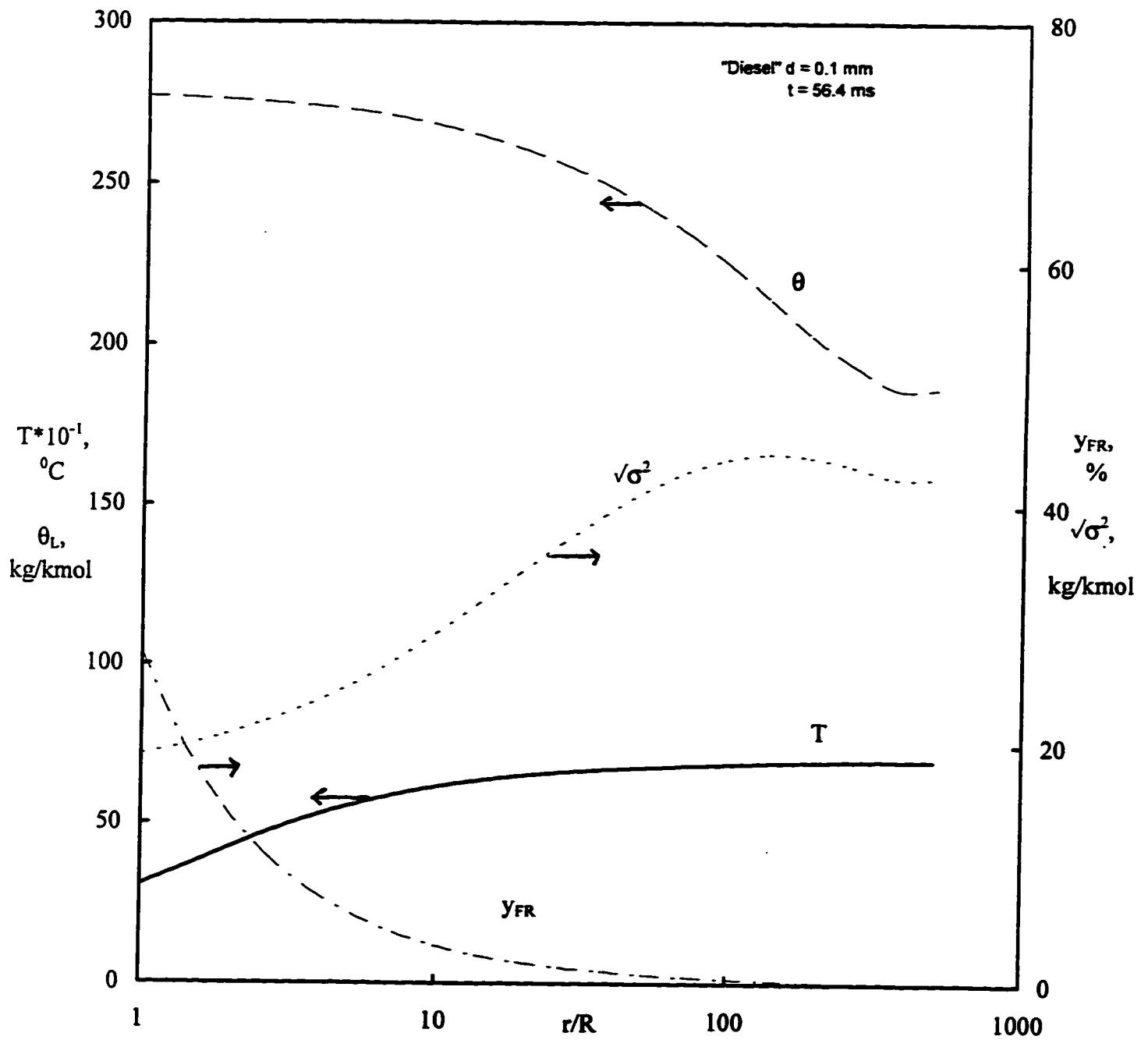


Figure 5.15: Vapour phase properties as a function of dimensionless radius (r/R) for a 0.1 mm Diesel droplet evaporating at $T_{\infty} = 700^{\circ}\text{C}$, initial temperature 25°C and shown at time $t = 56.4$ ms (end of lifetime). The calculation domain extends to $(r/R) = 500$.

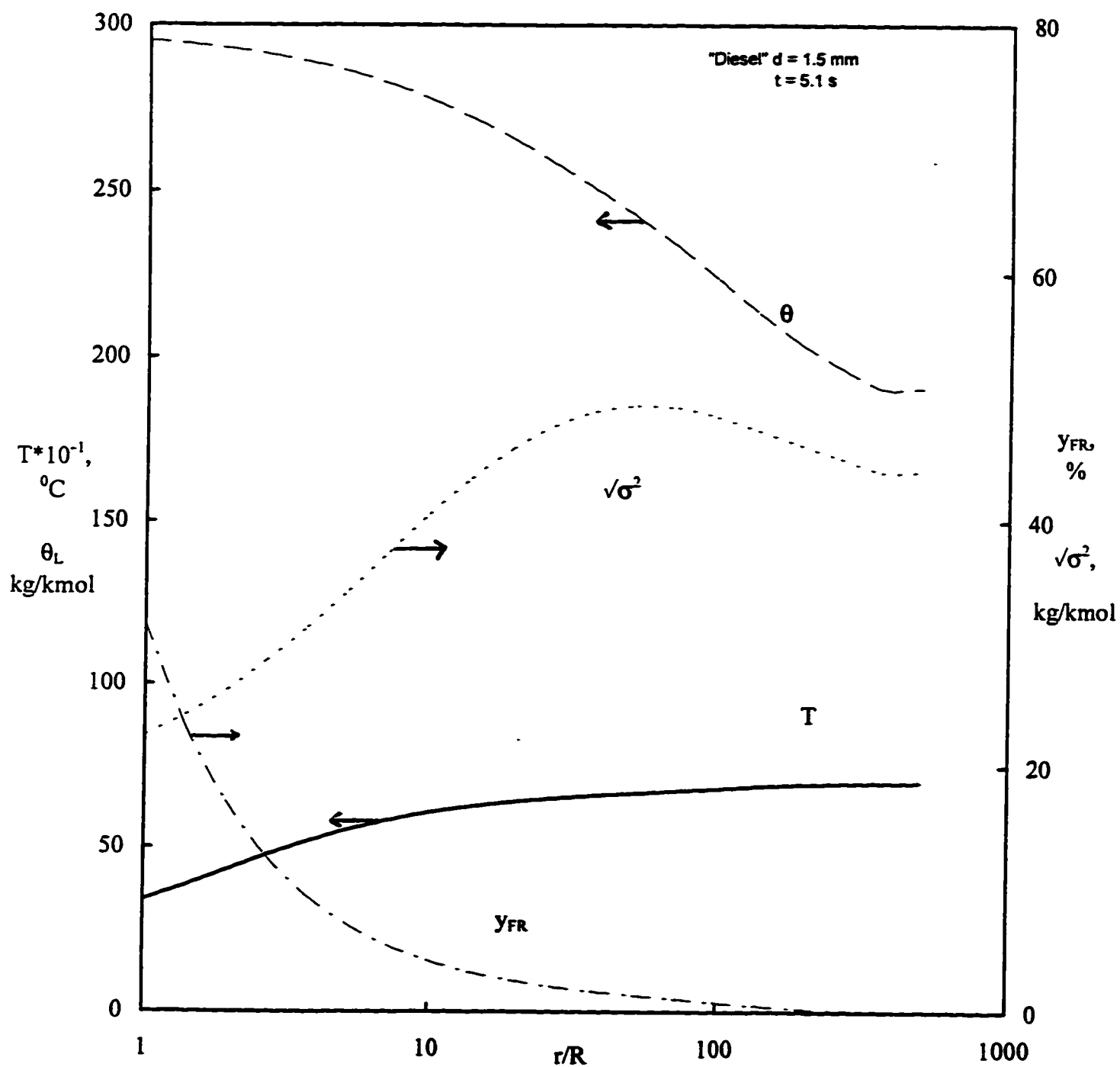


Figure 5.16: Vapour phase properties as a function of dimensionless radius (r/R) for a 1.5 mm Diesel droplet evaporating at $T_{\infty} = 700^{\circ}\text{C}$, initial temperature 25°C and shown at $t = 5.1$ s.

6. CONCLUSIONS AND RECOMMENDATIONS

6.1 Conclusions

Continuous thermodynamics principles were applied to develop the transport equations necessary to model the vaporization of a multicomponent fuel droplet. The Gamma distribution was chosen to represent the fuel mixture with molecular weight as the characterizing variable and correlations for the necessary transport properties were developed in terms of the distribution variable.

The model developed was applied to two fuel mixtures, Diesel and gasoline, and the calculations were made for two droplet sizes: 0.1 mm and 1.5 mm diameter droplets. The following conclusions were reached:

- Continuous thermodynamics provide a useful procedure for representing the composition of mixtures of many components. Instead of solving for hundreds of equations, one for each component, only the continuity, three diffusion equations and the energy equation are solved for, saving a lot of computational effort.
- This work demonstrates the potential of this method in engineering applications.
- The transport equations can be simplified with very little loss of accuracy to equations which are only slightly more complex than the diffusion equation for a single component.
- The physical behaviour of the droplet predicted by the model shows that:

- the droplet temperature rises continuously as the droplet gets heated but stays well below bubble point,
 - as the droplet evaporates, the liquid distribution becomes narrower,
 - the curves of the vapour mean molecular weight θ and the variance σ^2 versus “r” give a complete picture of vapour phase composition field.
- The Gamma distribution function used provides a very good representation of the ASTM distillation curves of commercial distillate fuels. The distribution parameters can be fitted by matching the 10% and 90% points on an ASTM curve. The only deficiency is that the end point is some 10 - 20°C too high, owing to the unbounded nature of the gamma distribution. This is a minor problem, and only effects results during the last few percent evaporated.

6.2 Recommendations

- An equation of state can be used to represent the vapour-liquid equilibrium which would give more accurate results at the droplet surface than the Clausius-Clapeyron equation.
- A distribution other than the Γ function can be used in trying to avoid the effects of an unbounded distribution.
- To complete the model for ignition or combustion, the chemical reaction has to be modelled with the distribution chosen.
- A rigorous experimental test of the calculations presented here would require the

creation of liquid mixtures whose composition is known in sufficient detail to allow accurate construction of the necessary distribution functions. There are no data available in the literature which meet these requirements, the experiments in the literature on the evaporation or combustion of droplets of mixtures having been performed with fuels of unspecified composition or boiling behaviour (Braide *et al.*, 1979; Chen and El Wakil, 1969).

- For more realistic models of commercial petroleum mixtures it will be necessary to account for the presence of different families of compounds (for example cycloparaffins and aromatics); this can be done using multiple distribution functions for each continuous group and/or by adding discrete components together (Cotterman *et al.*, 1985).

LIST OF REFERENCES

- Abramovitz, M. and I. A. Stegun, *Handbook of Mathematical Functions*, Dover, New York (1970).
- Bardon, M. F., J. E. D. Gauthier and V. K. Rao, "Flame propagation through sprays of multicomponent fuel", *J. Inst. Energy* **63**, 53-60 (1990).
- Bergeron, C.A and W. L. H. Hallett, "Autoignition of single droplets of two-component liquid fuels", *Combust. Sci. Technol.* **65**, 181-194 (1989a).
- Bergeron, C.A and W. L. H. Hallett, "Ignition characteristics of liquid hydrocarbon fuels as single droplets", *Can. J. Chem. Eng.* **67**, 142-149 (1989b).
- Bird, R. B., W. E. Stewart and E. N. Lightfoot, *Transport Phenomena*, John Wiley & Sons, Inc (1960).
- Braide, K. M., G. L. Isles, J. B. Jordan and A. Williams, "The combustion of single droplets of some fuel oils and alternative liquid fuel combinations", *J. Inst. Energy* **52**, 115-124 (1979).
- Briano, J. G. and E. D. Glandt, "Molecular thermodynamics of continuous mixtures", *Fluid Phase Equilibria* **14**, 91-102 (1983).
- Chen, C. S. and M. M. El-Wakil, "Experimental and theoretical studies of burning drops of hydrocarbon mixture", *Proc. Instn. mech. Engrs* **184**, Pt 3J, 95-108 (1969).
- Chou, G. F. and J. M. Prausnitz, "Adiabatic flash calculations for continuous or semicontinuous mixtures using an equation of state", *Fluid Phase Equilibria* **30**, 75-82 (1986).
- Cotterman, R. L., R. Bender and J. M. Prausnitz, "Phase equilibria for mixtures containing very many components. Development and application of continuous thermodynamics for chemical process design", *Ind. Engng Chem. Process Des. Dev.* **24**, 194-203 (1985).
- Du, P. C. and G. A. Mansoori, "Phase equilibrium computational algorithms of continuous mixtures", *Fluid Phase Equilibria* **30**, 57-64 (1986).
- Faeth, G. M., "Current status of droplet and liquid combustion", *Prog. Energy Combust. Sci.* **3**, 191-224 (1977).

- Gal-Or, B., H. T. Cullinan and R. Galli, "New thermodynamic-transport theory for systems with continuous component density distributions", *Chem. Engng Sci.* **30**, 1085-1092 (1975).
- Gualtieri, J. A., J. M. Kincaid and G. Morrison, "Phase equilibria in polydisperse fluids", *J. Chem. Phys.* **77**, 521-531 (1982).
- Hadden, S. T., "Heat Capacity of Hydrocarbons in the Normal Liquid Range", *Journal of Chemical and Engineering Data*, **15**, No. 1, 92-97 (1970).
- Hallett, W. L. H. and M. A. Ricard, "Calculation of the auto-ignition of liquid hydrocarbon mixtures as single droplets", *Fuel* **71**, 225-229 (1992).
- Hallett, W. L. H., Combustion in diffusion systems, Course notes for MCG 5192, Department of Mechanical Engineering, University of Ottawa, (1994).
- Haynes W. H. and A. M. Matthews, "Continuous-mixture vapour-liquid equilibria computations based on true boiling point distillations", *Industrial and Engineering Chemistry Research* **30**, 1911-1915 (1991).
- Hoffman, E. J., "Flash calculations for petroleum fractions", *Chem. Eng. Sci.* **23**, 957-964 (1968).
- Hubbard, G.L., V. E. Denny and A. F. Mills, "Droplet evaporation: effects of transients and variable properties", *Int. J. Heat Mass Transfer* **18**, 1003-1008 (1975).
- Kallio, N. N., B. W. Moyes, G. D. Webster and R. B. Whyte, SAE Technical Paper 850052 (1985).
- Katz, D. L. and G. G. Brown, "Vapour pressure and vaporization of petroleum fractions", *Industrial and Engineering Chemistry* **25**, 1373-1384 (1933).
- Kehlen, H. and M. T. Rätzsch, "Continuous thermodynamics of multicomponent mixtures", *Proceedings Sixth International Conference on Thermodynamics, Mersburg (GDR)*, pp. 41-51 (1980).
- Kehlen, H., M. T. Rätzsch and J. Bergmann, "Continuous thermodynamics of multicomponent systems", *A.I.Ch.E. J.* **31**, 1136-1148 (1985).
- Landis, R. B. and A. F. Mills, "Effect of internal diffusional resistance on the evaporation of binary droplets", *Fifth International Heat Transfer Conference*, pp. 345-349 (1974).

- Law, C. K., "Recent advances in droplet vaporization and combustion", *Prog. Energy Combust. Sci.* **8**, 171-201 (1982).
- Luria, M. and S. W. Benson, "Heat capacities of liquid hydrocarbons. Estimation of heat capacities at constant pressure as a temperature function, using additivity rule", *J. Chem. Eng. Data* **22**, 90-100 (1977).
- Newbold, F. R. and N. R. Amundson, "A model for evaporation of a multicomponent droplet", *A.I.Ch.E. J.* **19**, 22-30 (1973).
- Patankar, S. V., *Numerical Heat Transfer and Fluid Flow*, McGraw-Hill (1980).
- Peng, D.-Y., R. S. Wu and J. P. Batycky, "Application of continuous thermodynamics to oil reservoir fluid systems using an equation of state", *AOSTRA J. Res.* **3**, 113-122 (1987).
- Perry, R. H., ed., *Perry's Chemical Engineering Handbook*, 6th edition, McGraw-Hill (1984).
- Rah, S.-C., A. F. Sarofeim and J. M. Beér, "Ignition and combustion of liquid fuel droplets. Part II. Ignition studies", *Combust. Sci. Technol.* **49**, 169-184 (1986).
- Randolph, A. L., A. Makino and C. K. Law, "Liquid-phase diffusional resistance in multicomponent droplet gasification", *Twenty-first Symposium (International) on Combustion*, The Combustion Institute, pp. 601-608 (1986).
- Rätzsch, M. T., H. Kehlen and J. Schumann, "Flash calculations for a crude oil by continuous thermodynamics", *Chem. Eng. Comm* **71**, 113-125 (1988).
- Rätzsch, M. T., H. Kehlen and J. Schumann, "Computer simulation of complex multicomponent hydrocarbon distillation by continuous thermodynamics", *Fluid Phase Equilibria* **51**, 133-146 (1989).
- Rätzsch, M. T. and H. Kehlen, "Continuous thermodynamics of complex mixtures", *Fluid Phase Equilibria* **14**, 225-234 (1983).
- Reid, R. C., J. M. Prausnitz and B. E. Poling, *The Properties of Gases and Liquids*, 4th Edition, McGraw-Hill (1987).
- Ruszalo, R. and W. L. H. Hallett, "A model for the auto-ignition of single liquid droplets at high pressure", *Combust. Sci. Technol.* **86**, 183-187 (1992).
- Shibata, S. K., S. I. Sandler, and R. A. Behrens, "Phase equilibrium calculations for continuous and semicontinuous mixtures", *Chem. Eng. Sci.* **42**, 1977-1988 (1987).

Talley, D.G. and S. C. Yao, "A semi-empirical approach to thermal and composition transients inside vaporizing fuel droplets", *Twenty-first Symposium (International) on Combustion*, The Combustion Institute, pp. 609-616 (1986).

Tong, A. Y. and W. A. Sirignano, "Multicomponent droplet vaporization in a high temperature gas", *Combust. Flame* **66**, 221-235 (1986).

Whitson, C. H., "Characterizing hydrocarbon plus fractions", *Soc. Pet. Engrs J.* **23**, 683-694 (1983).

Williams, A., "Combustion of droplets of liquid fuels: a review", *Combust. Flame* **21**, 1-31 (1973).

Willman, B. and A. S. Teja, "Prediction of dew points of semicontinuous natural gas and petroleum mixtures. 2. Nonideal solution calculations", *Ind. Eng. Chem. Res.* **26**, 953-957 (1987).

Yaws, C. L., "Calculate liquid heat capacity", *Hydrocarbon Processing*, 73-77 (1991).

Ying, X., R. Ye and Y. Hu, "Phase equilibria for complex mixtures. Continuous thermodynamics method based on spline fit", *Fluid Phase Equilibria* **53**, 407-414 (1989).

APPENDIX A

Elimination of Terms from Transport Equations

This appendix justifies the elimination of two of the terms from equation 3-13. The original equation reads:

$$\frac{\partial}{\partial t}(cy_F) + \nabla \cdot (cv \cdot y_F) = \nabla \cdot \left\{ c\bar{D} \nabla y_F + y_F \nabla (c\bar{D}) - y_F \int_0^{\bar{D}} f(I) \nabla (cD_m(I)) dI \right\}$$

The second term on the right hand side in finite difference formulation gives

$$\begin{aligned} I_1 = \nabla \cdot (y_F \nabla (c\bar{D})) &= \nabla \cdot \left[y_F \frac{(c\bar{D})_{i-1} - (c\bar{D})_i}{R(\xi_{i+1} - \xi_i)} \right] \\ &= \frac{1}{R(\xi_{ei} - \xi_{ei-1})} \left[\frac{y_{F_{i+1}} + y_{F_i}}{2} \left(\frac{(c\bar{D})_{i-1} - (c\bar{D})_i}{R(\xi_{i+1} - \xi_i)} \right) - \frac{y_{F_i} + y_{F_{i-1}}}{2} \left(\frac{(c\bar{D})_i - (c\bar{D})_{i-1}}{R(\xi_i - \xi_{i-1})} \right) \right] \end{aligned} \quad \text{A-1}$$

where subscripts i+1, i etc. refer to the grid nodes, and "ei" refers to the "east" interface between nodes (i+1) and i.

The last term is

$$I_2 = -\nabla \cdot \left[y_F \int_0^{\bar{D}} f(I) \nabla (cD(I)) dI \right] \quad \text{A-2}$$

this can be estimated in finite difference form as follows

$$\nabla(cD(I)) = \frac{[cD(I)]_{i-1} - [cD(I)]_i}{R(\xi_{i-1} - \xi_i)} \quad \text{A-3}$$

integrating:

$$\int_0^{\bar{I}} f(I) \nabla(cD(I)) dI = \frac{(c\bar{D})_{i-1} - (c\bar{D})_i}{R(\xi_{i-1} - \xi_i)} \quad \text{A-4}$$

then

$$I_2 = - \frac{1}{R(\xi_{ei} - \xi_{ei-1})} \left[\frac{y_{F_{i+1}} + y_{F_i}}{2} \left(\frac{(c\bar{D})_{i-1} - (c\bar{D})_i}{R(\xi_{i-1} - \xi_i)} \right) - \frac{y_{F_i} + y_{F_{i-1}}}{2} \left(\frac{(c\bar{D})_i - (c\bar{D})_{i-1}}{R(\xi_i - \xi_{i-1})} \right) \right] \quad \text{A-5}$$

I_1 and I_2 are identical in finite difference form; they cancel each other and can be dropped from the equation. The same calculations apply to equation 3-14 and 3-16.

APPENDIX B

Evaluation of the Neglected Terms in Eq. 3-20

Sample calculation of the diffusion terms in eq. 3-20, calculations done for a 1.5 mm gasoline droplet evaporating in 700°C ambient temperature at $t = 1.0$ s .

Node point	$c\bar{D}\nabla\cdot\nabla y_F$ (1)	$\nabla(c\bar{D})\cdot\nabla y_F$ (2)	% RATIO (1)/(2)
2	8.39E-08	-1.15E-08	13.64
3	4.46E-08	-7.10E-09	15.92
4	2.22E-08	-3.74E-09	16.84
5	1.05E-08	-1.74E-09	16.51
6	4.80E-09	-7.42E-10	15.47
7	2.13E-09	-3.03E-10	14.25
8	9.31E-10	-1.22E-10	13.12
9	4.08E-10	-4.90E-11	12.00
10	1.85E-10	-1.93E-11	10.40
11	8.91E-11	-6.90E-12	7.74
12	4.50E-11	-1.94E-12	4.31
13	1.94E-11	-3.59E-13	1.85
14	5.05E-12	-4.13E-14	0.82
15	7.60E-13	-3.39E-15	0.44
16	7.85E-14	-2.32E-16	0.29
17	6.56E-15	-1.43E-17	0.22
18	4.70E-16	-7.99E-19	0.17
19	2.93E-17	-2.23E-20	0.076

APPENDIX C

Comparison of the Different Averaged Diffusivities:

Average diffusivities calculated with respect to mol fraction, mean of the distribution and the standard deviation of the distribution for a 1.5 mm “gasoline” droplet with an initial temperature of 25°C and evaporating at $T_{\infty} = 700^{\circ}\text{C}$.

Time (s)	\bar{D}	\tilde{D}	\hat{D}
1	2.23E-05	2.19E-05	2.14E-05
2	2.21E-05	2.17E-05	2.14E-05
3	2.16E-05	2.13E-05	2.11E-05
3.6	2.11E-05	2.09E-05	2.06E-05
3.8	2.08E-05	2.06E-05	2.04E-05
4.0	2.05E-05	2.03E-05	2.01E-05
4.2	2.02E-05	2.00E-05	1.98E-05
4.4	1.98E-05	1.96E-05	1.94E-05
4.6	1.92E-05	1.90E-05	1.88E-05
4.8	1.76E-05	1.74E-05	1.72E-05

APPENDIX D

Derivation of Finite Volume Equations by Integration of Differential Equations

1 - Continuity Equation (eq. 4-4)

Integrating eq. (4-4) over a control volume (CV) (Fig. 4-1) from “west” w to “east” e to get $(c w)_e$ in terms of $(c w)_w$:

$$\xi^2 \frac{dc}{dt} + \frac{1}{R} \frac{\partial}{\partial \xi} (\xi^2 c w) + \frac{\dot{R}}{R} c \frac{\partial}{\partial \xi} (\xi^3) = 0 \quad \text{D-1}$$

gives

$$(\xi^2 c w)_e = (\xi^2 c w)_w - \frac{R}{3 \Delta t} (\xi_e^3 - \xi_w^3) (c_p - c_p^0) - \dot{R} c_p (\xi_e^3 - \xi_w^3) \quad \text{D-2}$$

Beginning at the droplet surface ($\xi = 1$), where

$$(c w)_1 = G \quad \text{D-3}$$

where G is the evaporating mol flux ($\text{kmol/m}^2\text{s}$), all other velocities can be found in turn.

Since the first node of the grid lies on the surface (Fig. 4.3), the first cell is actually only a half - cell, so that in calculating $(\xi^2 c w)_e$ the value of c_p is set to

$$c_{p1} = \frac{3}{4} c_1 + \frac{1}{4} c_2 \quad \text{D-4}$$

2 - Transport Equation for y_F (eq. 4-5)

$$\xi^2 \frac{\partial}{\partial t} (cy_F) + cy_F \frac{\dot{R}}{R} \frac{\partial \xi^3}{\partial \xi} + \frac{1}{R} \frac{\partial}{\partial \xi} (\xi^2 cy_F w) = \frac{1}{R^2} \frac{\partial}{\partial \xi} \left(\xi^2 c \bar{D} \frac{\partial y_F}{\partial \xi} \right) \quad \text{D-5}$$

Integrate over CV from w to e and over time t to Δt to get y_{FP} in terms of neighbours W and

P. The first two terms integrate to

$$\frac{1}{3} (\xi_e^3 - \xi_w^3) (c_P y_{PF} - c_P^o y_{FP}^o) + c_P y_{FP} \frac{\dot{R} \Delta t}{R} (\xi_e^3 - \xi_w^3) \quad \text{D-6}$$

The last two terms represent convection and diffusion, and are modelled using the power-law hybrid scheme of Patankar. This gives these terms as

$$a_E y_E + a_P y_P + a_W y_W \quad \text{D-7}$$

where

$$\begin{aligned} a_E &= D_e A(P_e) + \parallel -F_e, 0 \parallel \\ a_W &= D_w A(P_w) + \parallel -F_w, 0 \parallel \\ a_P &= -a_e - a_w - F_e + F_w \end{aligned} \quad \text{D-8}$$

D and F represent diffusion and convection respectively

$$\begin{aligned} D_e &= \frac{c \bar{D} \xi_e^2 \Delta t}{R^2 (\xi_E - \xi_P)} \\ F_e &= \frac{(\xi^2 c w)_e \Delta t}{R} \end{aligned} \quad \text{D-9}$$

and P is the Peclet number

$$P = F / D \quad \text{D-10}$$

and the function A(P) is given by

$$A(P) = \max\{0, (1 - 0.1 |P|)^5\} \quad \text{D-11}$$

where the brackets $\max\{\dots\}$ mean “the greater of”.

3 - Transport equation for θ (eq. 4-6):

$$\frac{\partial}{\partial t} (c y_F \theta) + c y_F \theta \frac{\dot{R}}{R} \frac{\partial \xi^3}{\partial \xi} + \frac{1}{R} \frac{\partial}{\partial \xi} (\xi^2 c y_F \theta w) = \frac{1}{R^2} \frac{\partial}{\partial \xi} \left(\xi^2 c \tilde{D} \frac{\partial}{\partial \xi} (y_F \theta) \right) \quad \text{D-12}$$

The first two terms integrated over the CV from w to e and over time t to Δt give

$$\frac{1}{3} (\xi_e^3 - \xi_w^3) (c_P y_{PF} \theta_P - c_P^o y_{FP}^o \theta_P^o) + c_P y_{FP} \theta_P \Delta t \frac{\dot{R}}{R} (\xi_e^3 - \xi_w^3) \quad \text{D-13}$$

The last two terms represent the convection and diffusion respectively of the mean of the distribution, and are again modelled using the power-law hybrid scheme. The expressions are the same as for the diffusion equation except for the diffusion coefficient, and the equation is solved for $y_F \theta$, the value of θ at each node then being obtained by dividing by y_F :

$$D_e = \frac{c\tilde{D} \xi_e^2 \Delta t}{R^2 (\xi_E - \xi_P)}$$

$$F_e = \frac{(\xi^2 c w)_e \Delta t}{R}$$
D-14

4 - Transport equation for ψ (eq. 3-67):

$$\xi^2 \frac{\partial}{\partial t} (c y_F \psi) + c y_F \psi \frac{\dot{R}}{R} \frac{\partial \xi^3}{\partial \xi} + \frac{1}{R} \frac{\partial}{\partial \xi} (\xi^2 c y_F \psi w) = \frac{1}{R^2} \frac{\partial}{\partial \xi} \left(\xi^2 c \hat{D} \frac{\partial}{\partial \xi} (y_F \psi) \right)$$
D-15

This equation integrates exactly the same way as the θ equation with the first two terms given as

$$\frac{1}{3} (\xi_e^3 - \xi_w^3) (c_P y_{PF} \psi_P - c_P^o y_{FP}^o \psi_P^o) + c_P y_{FP} \psi_P \Delta t \frac{\dot{R}}{R} (\xi_e^3 - \xi_w^3)$$
D-16

The diffusion and convection terms are modelled the same way as previous equations with the exception of the diffusion coefficient,

$$D_e = \frac{c\hat{D} \xi_e^2 \Delta t}{R^2 (\xi_E - \xi_P)}$$

$$F_e = \frac{(\xi^2 c w)_e \Delta t}{R}$$
D-17

5 - Energy Equation (eq. 4-8):

$$\begin{aligned} \xi^2 \frac{\partial}{\partial t}(cT) + cT \frac{\dot{R}}{R} \frac{\partial \xi^3}{\partial \xi} = & -\frac{1}{R} \frac{\partial}{\partial \xi} (\xi^2 c_w T) + \frac{1}{R^2 \bar{C}_p} \frac{\partial}{\partial \xi} \left(\xi^2 \lambda \frac{\partial T}{\partial \xi} \right) \\ & + \frac{\xi^2}{R^2 \bar{C}_p} \left[(a_c + C_{PA}) c \bar{D} \frac{\partial y_F}{\partial \xi} \right. \\ & \left. + b_c c \bar{D} \frac{\partial y_F \theta}{\partial \xi} \right] \frac{\partial T}{\partial \xi} \end{aligned} \quad \text{D-18}$$

The left hand side integrates to

$$\frac{1}{3} (\xi_e^3 - \xi_w^3) (c_p T_p - c_p^o T_p^o) + c_p T_p \frac{\dot{R} \Delta t}{R} (\xi_e^3 - \xi_w^3) \quad \text{D-19}$$

For the last term on the right hand side, if the term between the squared brackets is set to

$$Z = \left[(a_c + C_{PA}) c \bar{D} \frac{\partial y_F}{\partial \xi} + b_c c \bar{D} \frac{\partial y_F \theta}{\partial \xi} \right] \quad \text{D-20}$$

the last term on the right hand side can be expanded to

$$\begin{aligned} \frac{\xi^2}{R^2 \bar{C}_p} \left[(a_c + C_{PA}) c \bar{D} \frac{\partial y_F}{\partial \xi} + b_c c \bar{D} \frac{\partial y_F \theta}{\partial \xi} \right] \frac{\partial T}{\partial \xi} = & \frac{1}{R^2 \bar{C}_p} \left[\frac{\partial}{\partial \xi} (\xi^2 Z T) \right. \\ & \left. - T \frac{\partial}{\partial \xi} (\xi^2 Z) \right] \end{aligned} \quad \text{D-21}$$

The first term in the right hand side term is treated as a convection term and is combined with the first term on the right hand side of eq. (D-18). The combined term is then integrated as done previously using a power-law hybrid scheme. The expressions are as for

the diffusion equation, except that now

$$D_e = \frac{\lambda \xi_e^2 \Delta t}{c_p R^2 (\xi_E - \xi_P)} \quad \text{D-22}$$

$$F_e = \frac{(\xi^2 c w)_e \Delta t}{R} \quad \text{D-23}$$

$$- \frac{\xi_e^2 \Delta t}{c_p R^2 (\xi_E - \xi_P)} \left[c \bar{D} \left((y_F)_E - (y_F)_P \right) (a_{CP} - C_{PA}) \right. \\ \left. + b_{CP} c \bar{D} \left((y_F \theta)_E - (y_F \theta)_P \right) \right]$$

The second term on the right hand side can be integrated to

$$- T_P \frac{\xi_e^2 Z_e - \xi_w^2 Z_w}{\xi_e - \xi_w} \quad \text{D-24}$$

and included in the a_p term.


```

531  FORMAT(1X,F5.0,1X,F5.0,1X,E11.5)
      WRITE(90,502)N,ZETAN,W,FUEL
      WRITE(90,513)A,B,SFG
      WRITE(90,*)BH,AH,AD,BD
      WRITE(90,*)AT,BT,AP,BP
      WRITE(91,701)AO,A1,A2,A3
701  FORMAT('AO=',2X,E12.5,2X,'A1=',2X,E12.5,/,
1'A2=',2X,E12.5,2X,'A3=',2X,E12.5)
      WRITE(91,702)BO,B1,B2,B3
702  FORMAT('BO=',2X,E12.5,2X,'B1=',2X,E12.5,/,
1'B2=',2X,E12.5,2X,'B3=',2X,E12.5)
*
*  INPUT INITIAL CONDITIONS:
*
      READ(7,503)TDROP,TFURN1,RDROP,TEND
503  FORMAT(1X,F4.0,1X,F5.0,1X,F8.6,1X,F5.0)
      WRITE(6,519) RDROP
519  FORMAT(10X,'* HFG TERM CALCULATED USING AMEANL',/,10X,
1'* AMEANV AND VARV CALCULATED',/,10X,
1'* RDROP CHANGED TO',1X,F8.6,1X,'M',/,10X,
1'* RHOREL          ',1X,'0.50',/,10X,
1'* DTIME           ',1X,'0.010')
      WRITE(6,504)
c 504  FORMAT(/,/,1X,'GASOLINE: ALPHA = 5.7, BETA = 15, GAMMA = 0')
504  FORMAT(/,/,1X,'DIESEL: ALPHA = 18.5, BETA = 10, GAMMA = 0')
      WRITE(6,505)TDROP
505  FORMAT(/,' INITIAL DROPLET TEMPERATURE: ',F4.0,' K')
      WRITE(6,506)TFURN1
506  FORMAT(1X,'FURNACE TEMPERATURE: ',F5.0,' K')
      WRITE(6,507)TFURN1-20.0
507  FORMAT(1X,'EFFECTIVE RADIATING TEMPERATURE: ',F5.0,' K')
      WRITE(6,508)RDROP
508  FORMAT(1X,'INITIAL RADIUS: ',F8.6,' M')
      WRITE(6,509)EA
509  FORMAT(/,' ACTIVATION ENERGY: ',F5.2,' KCAL/MOL')
      WRITE(6,510)K
510  FORMAT(1X,'PRE-EXPONENTIAL CONSTANT: ',E9.3,' M^3/KMOL.S')
*
*****
*
*  SET CONSTANTS, DEFINE COMPUTATIONAL GRID
*
*****
*
*  DATA REQUIRED (CONSTANTS & PROPERTIES):
      MA=28.97
      MO=32.
      MN=28.
      PATM=1.000
      PAMB=PATM*760.
      PRES=101.3*PATM
      RUGC=8.314
      SFGR=87.9/RUGC
      YOAMB=0.21
      YNAMB=0.79
      SIGMA=5.669E-8
*  SET CONVERGENCE CRITERION FOR MASS
*  FLUX (CRITG, RELATIVE ERROR) AND TEMP
*  (CRITT IN K) AND RELAXATION FACTOR FOR VELOCITY AND TEMP.
      CRITG = 0.00001
      CRITT = 0.00001
      RELAX = 0.5
      WRITE(6,527)CRITG,CRITT
527  FORMAT(1X,'CRITG =',E7.1,/,',CRITT =',E7.1)
      DTIME=0.01
      IFLAGT=0
      NITER=0
      NITER1=0
c      AMEANL = 85.5

```

```

MOD00770
MOD00780
MOD00790
MOD00800
MOD00810
MOD00820
MOD00830
MOD00840
MOD00850
MOD00860
MOD00870
MOD00880
MOD00890
MOD00900
MOD00910
MOD00920
MOD00940
MOD00950
MOD00960
MOD00970
MOD00980
MOD00990
MOD01000
MOD01010
MOD01020
MOD01030
MOD01040
MOD01050
MOD01060
MOD01070
MOD01080
MOD01090
MOD01100
MOD01110
MOD01120
MOD01130
MOD01140
MOD01150
MOD01160
MOD01170
MOD01180
MOD01190
MOD01200
MOD01210
MOD01220
MOD01230
MOD01240
MOD01250
MOD01260
MOD01270
MOD01280
MOD01290
MOD01300
MOD01310
MOD01320
MOD01330
MOD01340
MOD01350
MOD01360
MOD01370
MOD01380
MOD01390
MOD01400
MOD01410
MOD01420
MOD01430
MOD01440
MOD01450
MOD01460

```

```

C      VARL = 1282.5
      AMEANL = 185.0
      VARL = 1850.0
      VARLM2 = VARL + AMEANL**2
      VLGAMA = 0.0
      BETAL = VARL/(AMEANL-VLGAMA)
      ALPHAL = (AMEANL - VLGAMA)/BETAL
*
*
      RHOL = RHOLI/AMEANL
*
* BOILING POINT TEMPERATURE (K):
*
      CALL BOILIN
      WRITE(90,512)TBOIL
512  FORMAT(/,'TBOIL=',F9.2)
*
* GEOMETRY OF GRID:
* N=NUMBER OF GRID POINTS
* ZETA(N)=THE LAST GRID POINT
      ZETA(N)=ZETAN
      DZ=LOG(ZETA(N))/(N-1)
      DO 11 I=1,N
          ZETA(I)=EXP(DZ*(I-1))
          IF (I.EQ.1) GOTO 11
          ZETA(I-1)=(ZETA(I-1)+ZETA(I))/2.
          ZE3(I-1)=ZETA(I-1)**3
C      ZETAD(I-1)=ZETA(I) - ZETA(I-1)
11  CONTINUE
      DO 12 I=1,N-1
          ZE2DT(I)=ZETA(I)**2*DTIME/(ZETA(I+1)-ZETA(I))
12  CONTINUE
      DO 13 I=2,N-1
          ZE3D(I)=ZE3(I)-ZE3(I-1)
13  CONTINUE
*
* MASS OF LIQUID FUEL:
9000 MASS=4./3.*3.1416*RDROP**3*RHOLI
*
      TFURN=TFURN1
      TRAD=TFURN-20.0
*
*****
*
* INITIALIZE QUANTITIES FOR FIRST TIME STEP
*****
*
* LOOP FOR FURNACE TEMPERATURE (IF REQUIRED):
* -----
3000 TIME=0.0
      CNT=0
      IGNITE=0
      TR=TDROP
      TROLD = TR
      R=RDROP
      ROLD = R
      MASSEV=0.0
      MASSP=MASSEV/MASS*100.
      TI=0
*
* INITIAL TEMPERATURE FIELD:
      T(1)=TR
      DO 22 I=2,N
          T(I)=TFURN
22  CONTINUE
      TAVG=2./3.*T(1)+1./3.*T(N)
*

```

```

MOD01470
MOD01480
MOD01490
MOD01500
MOD01510
MOD01520
MOD01530
MOD01540
MOD01550
MOD01560
MOD01570
MOD01580
MOD01590
MOD01600
MOD01610
MOD01620
MOD01630
MOD01640
MOD01650
MOD01660
MOD01670
MOD01680
MOD01690
MOD01700
MOD01710
MOD01720
MOD01730
MOD01740
MOD01750
MOD01760
MOD01770
MOD01780
MOD01790
MOD01800
MOD01810
MOD01820
MOD01830
MOD01840
MOD01850
MOD01860
MOD01870
MOD01880
MOD01890
MOD01900
MOD01910
MOD01920
MOD01930
MOD01940
MOD01950
MOD01960
MOD01970
MOD01980
MOD01990
MOD02000
MOD02010
MOD02020
MOD02030
MOD02040
MOD02050
MOD02060
MOD02070
MOD02080
MOD02090
MOD02100
MOD02110
MOD02120
MOD02130
MOD02140
MOD02150

```

```

* INITIAL ESTIMATES OF SURFACE CONDITIONS AND CONCENTRATION PROFILES MOD02160
* REQUIRED TO CALCULATE PROPERTIES FOR FIRST TIME STEP: MOD02170
  AA = SFGR*(1.- (A/TR)) MOD02180
  BB = B/(TR-A) MOD02190
  YFR =PATM*EXP(AA*(1.-VLGAMA*BB))/((1.+AA*BB*BETAL)**ALPHAL) MOD02200
* ALPHA, BETA, VLGAMA FOR VAPOUR PHASE IN TERMS OF MOLES MOD02210
  ALPHAV = ALPHAL MOD02220
  BETAV = BETAL/(1.+ AA*BB*BETAL) MOD02230
  AMEANV = ALPHAV*BETAV + VLGAMA MOD02240
  VARV = ALPHAV*(BETAV**2) MOD02250
  VARVM2 = VARV + AMEANV**2 MOD02260
  MF = AMEANV MOD02270
* MOD02280
* MOD02290
  VAR(1)=VARV MOD02300
  VARM2(1) = VARVM2 MOD02310
  DISTY(1) = AMEANV MOD02320
  YO(1)=YOAMB*(1.-YFR) MOD02330
  YN(1)=YNAMB/YOAMB*YO(1) MOD02340
  YF(1)=YFR MOD02350
  YMF(1)=YF(1)*AMEANV/AMEANL MOD02360
  YFTHET(1) = YF(1)*DISTY(1) MOD02370
  YFPSI(1) = YF(1)*VARM2(1) MOD02380
  DO 23 I=2,N MOD02390
  YF(I)=0. MOD02400
  YMF(I)=0. MOD02410
  DISTY(I)=AMEANV MOD02420
  VAR(I) = VAR(1) MOD02430
  VARM2(I) = VARM2(1) MOD02440
  YFTHET(I) = YF(I)*DISTY(I) MOD02450
  YFPSI(I) = YF(I)*VARM2(I) MOD02460
  YO(I)=YOAMB MOD02470
  YN(I)=YNAMB MOD02480
23 CONTINUE MOD02490
* MOD02500
* CALCULATE DENSITIES, TRIAL HEAT AND MASS FLUXES FOR FIRST TIME STEP MOD02510
  CALL DENSIT MOD02520
  DO 24 I=1,N MOD02530
  TOLD(I)=T(I) MOD02540
  RHOOLD(I)=RHO(I) MOD02550
  YFOLD(I)=YF(I) MOD02560
  DISTOL(I) = DISTY(I) MOD02570
  VAROLM(I) = VARM2(I) MOD02580
  YFTOLD(I) = YFTHET(I) MOD02590
  YFSIOL(I) = YFPSI(I) MOD02600
  RHOP(I)=RHO(I) MOD02610
  DISTPR(I) = DISTY(I) MOD02620
24 CONTINUE MOD02630
* MOD02640
  YFAV=2.*YF(1)*DISTY(1)/M(1)/3. + YF(N)*DISTY(N)/3./M(N) MOD02650
  YFAVG = 1./(1. +(MREF/MA)*(1.-YFAV)/YFAV) MOD02660
  CALL PROPS MOD02670
* MOD02680
* CALCULATE THE INITIAL TRIAL MASS FLUX: MOD02690
  BMF=YFR/(1.-YFR) MOD02700
  GAMMA=RHOAVG*DIFFUS MOD02710
  G0=GAMMA/R*LOG(1.+BMF) MOD02720
  RDOT=G0/RHOL MOD02730
  VEL(1)=G0*(1.+RHO(1)/RHOL)+(ZE3(1)-1.)*RDOT*(0.75*RHO(1)+
10.25*RHO(2)) MOD02750
  CALL COEF MOD02760
  DO 60 I=2,N-1 MOD02770
  VEL(I)=VEL(I-1)+ZE3D(I)*RDOT*RHO(I) MOD02780
60 CONTINUE MOD02790
* MOD02800
* CALCULATE QUASI-STEADY HEAT FLUX FOR THE FIRST TIME STEP MOD02810
* MOD02820
* MOD02830
  DTHEDR= (YFTHET(2) - YFTHET(1))/(ZETA(2) - ZETA(1))/R MOD02840
* MOD02850

```

```

*      HFGR AND HFG IN J/KMOL
*
HFGR = AH + BH*YFTHET(1) - BH*GAMMA*DTHEDR/GO
TC = AT + BT*AMEANL
HFG=HFGR*((TC-TR)**0.38)/6.959
QTOT=G0*CPF*(TFURN-TR)/(EXP(G0*CPF*R/CONDK)-1.)
IF(QTOT.LT.G0*HFG)G0=QTOT/HFG
*****
*      BEGIN TIME STEP
*
1000 EMISS=0.89*(1.-EXP(-5.4*R*1000.))
DTHEDR= (YFTHET(2) - YFTHET(1))/(ZETA(2)- ZETA(1))/R
HFGR = AH + BH*YFTHET(1) - BH*GAMMA*DTHEDR/GO
TC = AT + BT*AMEANL
HFG=HFGR*((TC-TR)**0.38)/6.959
GAMMA=RHOAVG*DIFFUS
*
CALL COEF
*
CALCULATE TRIAL VALUE OF TR AT END OF TIME STEP:
*
DTLDT=3./(RHOL*CPL*ROLD)*(QTOT-G0*HFG)
TRP=TROLD + DTLDT*DTIME
G0 = G0*ROLD/R
GSTAR = G0
TR = TRP
DIDR = ((YFTHET(2)-YFTHET(1)) / (ZETA(2) - ZETA(1)))/R
DILDY=3.*(G0*(AMEANL - YFTHET(1))+GAMMA*DIDR)/(RHOL*R)
AMEANP = AMEANL + DILDY * DTIME
*
DVARDR = ((YFPSI(2) - YFPSI(1))/(ZETA(2) - ZETA(1)))/R
DVLDT = 3.*(G0*(VARLM2-YFPSI(1))+ GAMMA*DVARDR)/(RHOL*R)
VARLPM = VARLM2 + DVLDT * DTIME
VARLP = VARLPM - AMEANP**2
*
IF(TRP.GE.TBOIL)TRP=TBOIL-0.25
CNTTEM=0
*****
*      LOOP FOR TEMPERATURE CONVERGENCE ITERATIONS:
*
7000 T(1)=TRP
BETAL = VARLP/(AMEANP -VLGAMA)
ALPHAL = (AMEANP -VLGAMA)/BETAL
*
CALCULATE FUEL FRACTION AT THE SURFACE:
*
AA = SFGR*(1 - A/TRP)
BB = B/(TRP-A)
YFR =PATM*EXP(AA*(1.-VLGAMA*BB))/((1.+AA*BB*BETAL)**ALPHAL)
*
ALPHA, BETA, VLGAMA FOR VAPOUR PHASE IN TERMS OF MOLES
*
ALPHAV = ALPHAL
BETAV = BETAL/(1.+AA*BB*BETAL)
AMEANV = ALPHAV*BETAV + VLGAMA
VARV = ALPHAV*BETAV**2
VARVM2 = VARV + AMEANV**2
*
DISTY(1) = AMEANV
VAR(1)=VARV

```

```

MOD02860
MOD02870
MOD02880
MOD02890
MOD02900
MOD02910
MOD02920
MOD02930
MOD02940
MOD02950
MOD02960
MOD02970
MOD02980
MOD02990
MOD03000
MOD03010
MOD03030
MOD03040
MOD03050
MOD03060
MOD03070
MOD03080
MOD03090
MOD03100
MOD03110
MOD03120
MOD03130
MOD03140
MOD03150
MOD03160
MOD03170
MOD03180
MOD03190
MOD03200
MOD03210
MOD03220
MOD03230
MOD03240
MOD03250
MOD03260
MOD03270
MOD03280
MOD03290
MOD03300
MOD03310
MOD03320
MOD03330
MOD03340
MOD03350
MOD03360
MOD03370
MOD03380
MOD03390
MOD03400
MOD03410
MOD03420
MOD03430
MOD03440
MOD03450
MOD03460
MOD03470
MOD03480
MOD03490
MOD03500
MOD03510
MOD03520
MOD03530
MOD03540
MOD03550

```

```

VARM2(1) = VARVM2
YF(1) = YFR
YO(1)=YOAMB*(1.-YF(1))
YN(1)=YNAMB/YOAMB*YO(1)
YFTHET(1) = YF(1)*DISTY(1)
YFPSI(1) = YF(1)*VARM2(1)
*
*****
*
* LOOP FOR CONCENTRATION AND VELOCITY FIELDS
*
*****
*
CALL TEMP
CALL CONC
CALL CONCI
CALL DENSIT
NITER=NITER+1
NITER1=NITER1+1
DO 65 I=1,N
DISTPR(I) = DISTY(I)
RHOP(I)=RHO(I)
65 CONTINUE
*
* CALCULATE VELOCITY FIELD
*
AG=YF(1)+((1.-YF(2))/(1.-YF(1)))**((ZETA(2)/(1.-ZETA(2)))
IF(AG.LE.YF(1)) THEN
WRITE(6,*)'AG IS LESS OR EQUAL TO YF(1) - ABORT'
WRITE(6,634)TIME,MASSEV,MASSP
GOTO 6000
ENDIF
*
GP =-GAMMA*(YF(2)-YF(1))/(ZETA(2)-ZETA(1))/R/(1.-YF(1))
IF(GP.LT.0.) THEN
WRITE(6,*)'NEGATIVE MASS FLUX - ABORT'
WRITE(6,634)TIME,MASSEV,MASSP
GOTO 6000
ENDIF
*
GO=RELAX*GP+(1.-RELAX)*GO
*
RDT=R/3./DTIME
RDOT=GP/RHOL - R*DILDT/(3.*AMEANL)
VEL(1)=GP*(1.+RHO(1)/RHOL)+
1 (ZE3(1)-1.)*(RDOT/4.*(3.*RHO(1)+
1 RHO(2))-RDT/4.*(3.*RHO(1)+RHO(2)-3.*RHOOLD(1)-RHOOLD(2)))
CALL COEF
DO 61 I=2,N-1
WF=WF0(I)*YF(I)**RCA*YO(I)**RCB*RHO(I)**(RCA+RCB)
VEL(I)=VEL(I-1)+ZE3D(I)*(RDOT*RHO(I)-RDT*(RHO(I)-RHOOLD(I)))
1 +WF*R*CP/DHF/DTIME/MF
61 CONTINUE
*
*****
*
* END OF CONCENTRATION AND VELOCITY LOOP
*
*****
*
DO 17 I=1,N
IF(T(I).GT.2000.) THEN
IGNITE=1
GOTO 15
ENDIF
17 CONTINUE
*
* CALCULATE THE TEMPERATURE GRADIENT AT THE SURFACE:
*

```

```

MOD03560
MOD03570
MOD03580
MOD03590
MOD03600
MOD03610
MOD03620
MOD03630
MOD03640
MOD03650
MOD03660
MOD03670
MOD03680
MOD03690
MOD03700
MOD03710
MOD03720
MOD03730
MOD03740
MOD03750
MOD03760
MOD03770
MOD03780
MOD03790
MOD03800
MOD03810
MOD03820
MOD03830
MOD03840
MOD03850
MOD03860
MOD03870
MOD03880
MOD03900
MOD03910
MOD03920
MOD03930
MOD03940
MOD03950
MOD03960
MOD03970
MOD03980
MOD03990
MOD04000
MOD04020
MOD04030
MOD04040
MOD04050
MOD04060
MOD04070
MOD04080
MOD04090
MOD04100
MOD04110
MOD04120
MOD04130
MOD04140
MOD04150
MOD04160
MOD04170
MOD04180
MOD04190
MOD04200
MOD04210
MOD04220
MOD04230
MOD04240
MOD04250
MOD04260

```

```

      THETA2=(T(2)-T(1))/(TFURN-T(1))
      DTDR=LOG(1.-THETA2)/(R*(1.-ZETA(2)))*(TFURN-T(1))
      DIDR = ((YFTHET(2)-YFTHET(1)) / (ZETA(2) - ZETA(1)))/R
      DVARDR = ((YFPSI(2)-YFPSI(1)) / (ZETA(2) - ZETA(1)))/R
*
* THERMAL RADIATION TRANSFER TO THE DROPLET:
      QRAD=SIGMA*EMISS*(T(1)**4-TRAD**4).
*
* TOTAL HEAT FLUX DURING TIME STEP:
      QTOTP=CONDK*DTDR-QRAD
      QTOT = RELAX*QTOTP + (1.-RELAX)*QTOT
*
* RISE IN DROPLET TEMPERATURE DURING TIME STEP:
      DTLDT=3./(RHOL*CPL*R)*(QTOT-GO*HFG)
      TRP = TROLD + DTLDT*DTIME
      DILDT=3.*(GO*(AMEANP - YFTHET(1)) + RHOAVG*DTUITL*DIDR)/
1      (RHOL*R)
      AMEANL = AMEANP + DILDT*DTIME
      DVLDT=3.*(GO*(VARLPM - YFPSI(1)) + RHOAVG*DCHAT*DVARDR)/
1      (RHOL*R)
      VARLCM = VARLM2 + DVLDT * DTIME
*
*****
* CONVERGENCE TEST - END OF TIME STEP
*
* CHECK IF CONVERGENCE HAS BEEN ACHIEVED:
      CNTTEM=CNTTEM+1
      IF (CNTTEM.GT.25.AND.MASSP.GT.10.0.AND.RELAX.GE.0.05) THEN
        RELAX = RELAX/2.
        WRITE(6,*) '*****RELAXATION FACTOR HALVED'
        CNTTEM = 0
      ENDIF
      IF (CNTTEM.GT.100) THEN
        WRITE(6,632)
632      FORMAT(' ITERATIONS FOR TEMP AND VELOCITY EXCEED 100 - ABORT ')
        WRITE(6,634) TIME,MASSEV,MASSP
634      FORMAT(/,' MASS EVOLVED AFTER ',F8.5,' SECONDS: ',E10.4,' KG',
1      5X,F6.2,' %')
        GOTO 6000
      ENDIF
      TESTT=ABS(TRP-TR)/TR
      TESTG = ABS(GO-GSTAR)/GO
      GSTAR = GO
      TR = TRP
      AMEANP = RELAX*AMEANL + (1.-RELAX)*AMEANP
      VARLPM = RELAX*VARLCM + (1.-RELAX)* VARLPM
      VARLP=VARLPM-AMEANP**2
      IF (TESTT.GT.CRITT.OR.TESTG.GT.CRITG) GOTO 7000
*
15      TIME=TIME+DTIME
      NITER=0
      TR=TRP
      AMEANL = AMEANP
      VARLM2 = VARLPM
      VARL = VARLM2 - AMEANL**2
      MF = AMEANV
      RHOL = RHOLI/AMEANL
      CALL BOILIN
630      FORMAT('TIME=',F6.2,' SEC, DROP TEMP.=',F7.2)
*
* AVERAGE TEMPERATURE FOR PROPERTIES ACCORDING TO HUBBARD ET AL.:
*
      TAVG=2./3.*T(1)+1./3.*T(N)
      YMFAVG=2./3.*YMF(1)+1./3.*YMF(N)
      YFAVG=2.*YF(1)*DISTY(1)/M(1)/3. + YF(N)*DISTY(N)/3./M(N)

```

```

      YFAVG = 1./(1. +(MREF/MA)*(1.-YFAV)/YFAV)
      CALL PROPS
*
* NEW DROPLET RADIUS
*
      ROLD=R
      R=ROLD-RDOT*DTIME
      TROLD = TR
*
      DO 16 I=1,N
        TOLD(I)=T(I)
        RHOOLD(I)=RHO(I)
        YFOLD(I)=YF(I)
        YFTOLD(I) = YFTHET(I)
        YFSIOL(I) = YFPSI(I)
16    CONTINUE
*
* MASS OF FUEL THAT EVAPORATED:
      MASSEV=MASSEV+4./3.*3.1416*(ROLD**3-R**3)*RHOLI
* PERCENTAGE OF FUEL EVAPORATED:
      MASSP=MASSEV/MASS*100.
      IF(MASSP.GT.90.0.AND.IFLAGT.NE.1)THEN
        DTIME=DTIME/5.
        IFLAGT=1
        WRITE(6,654)TIME
654    FORMAT('*****TIME STEP DIVIDED BY 5 AT ',F8.5,' SEC *****')
      ENDIF
*
      CNT=CNT+1
      IF(TIME.GT.6.0)GOTO 6000
      IF(IGNITE.EQ.1)CNT=100
6001 IF(CNT.GE.200)THEN
* PRINT TEMPERATURE PROFILE AT END OF TIME STEP:
      WRITE(6,603)
603    FORMAT(/,' TEMPERATURE PROFILE AT END OF TIME STEP')
      WRITE(6,613)
613    FORMAT(1X,39('-'))
      BMF=YF(1)/(1.-YF(1))
      WRITE(6,602)TIME,g0*mref,MASSP,TBOIL
602    FORMAT(/,' MASS EVOLVED AFTER ',F8.5,' SECONDS: ',E10.4,
*      ' KG',1X,F6.2,'% ', TBOIL =',F7.1)
      WRITE(6,619)TAVG,YFAVG*MF/AVGM
619    FORMAT(' PROPERTIES EVALUATED AT T=',F6.2,'K, YF=',F6.4)
      WRITE(6,615)AMEANL,VARL,ALPHAL,BETAL
615    FORMAT('LIQUID PROPERTIES ',/, 'AMEANL=',E10.4,2X, 'VARL=',
1    E10.4,2X, 'alpha',e10.4,2X, 'BETAL=',E10.4)
      WRITE(91,215)time,ameanl,varl,tboil,massp
215    FORMAT('time',f8.4'AMEANL=',E10.4,2X, 'VARL=',
1    E10.4,2X, 'tboil',f7.1,2X, 'massp',f6.2)
      WRITE(6,617)RHOAVG*AVGM,DIFFUS
617    FORMAT(' MOLAR AVERAGE DENSITY=',F6.3,' KMOL/M3',2X, 'DIFFUS=',
1E12.6)
      WRITE(6,612)RDROP*1000.0,R*1000.0
612    FORMAT(' INITIAL RADIUS:',F6.3,' DROPLET RADIUS:',F6.3,' MM')
      WRITE(6,901)DBAR,DTUITL,DHAT
901    FORMAT(1X,'DIFFUSIVITIES: BAR, TWIDDLE, HAT: ',3(E12.5))
      WRITE(6,605)
605    FORMAT(/,' I',4X, 'ZETA(I)',3X, 'T(I)',3X, 'YF(I)',3X, 'DISTY(I)',
12X, 'YO(I)',3X, 'VAR(I)',3X, 'varm2(I)',4X, 'YFPSI(I)')
      WRITE(6,621)
621    FORMAT(1X,'---',3X,'-----',6X,'----',5X,'-----',5X,'-----',
14X,'-----',4X,'-----')
      DO 14 I=1,N
        WRITE(6,606)I,ZETA(I),T(I),YF(I),DISTY(I),YO(I),var(i),VARM2(I)
1, YFPSI(I)
606    FORMAT(I2,1X,F8.3,1X,F9.3,1X,F6.4,1X,F9.4,1X,F6.4,1X,E10.4
1,1X,E10.4,1X,E12.5)
*

```

```

14      CONTINUE
*
C651    CONTINUE
      CNT=0
      ENDIF
*
*
      TI=TI+1
      IF (IGNITE.EQ.1) TI=100
*
      IF (IGNITE.EQ.1) THEN
        WRITE(6,623) RDROP*2000.
623     FORMAT(/, ' DROPLET DIAMETER =', F5.3, ' MM')
        WRITE(1,622) TIME, TFURN
        WRITE(6,622) TIME, TFURN
622     FORMAT(1X, ' IGNITION OCCURRED AFTER ', F8.5, ' SECONDS IN A FURNACE
*E AT ', F5.0, ' KELVIN. ')
        GOTO 2000
      ENDIF
      IF (R.GT.0.) GOTO 1000
      WRITE(6,610) TFURN
610     FORMAT(1X, ' DROPLET VAPORIZED WITHOUT IGNITION IN A FURNACE AT ',
*F5.0, ' KELVIN. ')
2000    TFURN=TFURN-50.0
      TRAD=TFURN-20.0
      IF (TFURN.GE.TEND) GOTO 3000
6000    STOP
      END
*
*****
*
      SUBROUTINE PROPS
*
*****
*
      REAL KTRAA, KTRAF, KTRFA, KTRFF, CONDAK, CONDFK
      REAL M(40), MF, MA, MO, MN, CONDK, MREF
      COMMON/AREA1/TC, PC, W, R, TAVG, CP, CPL,
1CPF, CPAIR, RHOAVG, AL, BL, CL, DL, TR, DIFFUS, CONDK, DTIME, GO, RHOL, K, RCA,
2RCB, EA, DHF, PATM, YOAMB, YNAMB, GAMMA, ZETA(40), ZETA(40), ZE2DT(40),
3ZE3(40), ZE3D(40), VEL(40), RHOOLD(40), YFOLD(40), TOLD(40), VISCM, PCF
      COMMON/AREA2/N, MA, MF, MN, MO, MREF, PRES, RUGC, M, RHO(40), RHOE(40),
1T(40), YF(40), YN(40), YO(40), TIME, DISTY(40), DISTOL(40), VAR(40),
1VARM2(40), VAROLD(40), DISTPR(40), VARPR(40), YMF(40), YMO(40),
1AVGM, YFAVG, VAROLM(40), VARPRM(40), ADT, BDT, VARVM2
      COMMON/AREA3/RDOT, AMEANL, AMEANV, DTLDT, VARV
      COMMON/AREA4/A, B, SFG, ALPHAL, BETAL, VLGAMA, YFR, TBOIL, DT, TSTART,
1ALPHAV, BETAV
      COMMON/AREA5/VISCA, VISCF, CONDAK, CONDFK, CVA, CVF, YAMOLE, YFMOLE,
1AAF, AFA, RAVG, CPN, CPO, AO, A1, A2, A3, A4, BO, B1, B2, B3, B4, AT, BT, CT, AP, BP,
1DP, DBAR, DTUITL, DHAT
*
*
      TCF = AT + BT*MF
      IF (MF.LT.270.0) THEN
        PCF = AP + BP * MF
      ELSE
        PCF = 11.0
      ENDIF
*
SIGMA FOR AIR AND FUEL:
      SA=3.711
      SF=(TCF/PCF)**(1./3.)*(2.3551-0.087*W)
*
E/K FOR AIR AND FUEL:
      EKA=78.6
      EKF=TCF*(0.7915+0.1693*W)
*
SIGMA AND E/K FOR AIR-FUEL MIXTURE:
      SAF=(SA+SF)/2.

```

```

*          EKAF=(EKA*EKF)**(1./2.)
*
*  CONSTANTS REQUIRED FOR ESTIMATING THE VISCOSITY:
*  AV=1.16145
*  BV=0.14874
*  CV=0.52487
*  DV=0.77320
*  EV=2.16178
*  FV=2.43787
*
*  CALCULATE SPECIFIC HEAT FOR FUEL AND AIR (J/KMOL.K):
*  ACP = AO + A1*TAVG + A2*TAVG**2 + A3*TAVG**3
*  BCP = BO + B1*TAVG + B2*TAVG**2 + B3*TAVG**3
*  CPF = RUGC*1000*(ACP + BCP*MF)
*
*  CPO=(6.713-0.879E-6*TAVG+4.170E-6*TAVG**2-2.544E-9*TAVG**3)
*  **4186.
*  CPN=(7.440-0.324E-2*TAVG+6.400E-6*TAVG**2-2.790E-9*TAVG**3)
*  **4186.
*  CPAIR=YOAMB*CPO+YNAMB*CPN
*  CALCULATE SPECIFIC HEAT OF MIXTURE:
*  YOAVG=YOAMB*(1.-YFAVG)
*
*  CP=YFAVG*CPF+(1.-YFAVG)*CPAIR
*  RHOAVG=PRES/RUGC/TAVG
*
*  VARIABLE LIQUID SPECIFIC HEAT (CAL/KMOL.K)
*  CPL = (0.541 -0.703E-3*TR+0.226E-5*TR**2)*MF*4186.
*
*  *****
*
*  *** ESTIMATION METHOD FOR THE DIFFUSION COEFFICIENT ***
*  *** LENNARD-JONES 12-6 POTENTIAL ***
*
*  DIMENSIONLESS TEMPERATURE (T*):
*  TAST=TAVG/EKAF
*
*  DIFFUSION COEFFICIENT (M^2/S):
*
*  AD = 2.402E-8
*  BD = -5.49E-11
*  DIFFUS=(AD + BD*MF)*TAVG**(5./2.)/(RUGC*PATM*(250.+TAVG))
*
*  ADT=AD*TAVG**(5./2.)/(RUGC*PATM*(250.+TAVG))
*  BDT=BD*TAVG**(5./2.)/(RUGC*PATM*(250.+TAVG))
*  DBAR= ADT +BDT*MF
*  DTUITL = ADT+ BDT*VARVM2/MF
*  DHAT= ADT + BDT*(2*VARV*(BETAV+MF)+VARVM2*MF)/VARVM2
*
*
*  *** ESTIMATION OF LOW PRESSURE THERMAL CONDUCTIVITY FOR MIXTURE ***
*
*  ESTIMATE VISCOSITY USING THE LENNARD-JONES 12-6 POTENTIAL:
*
*  SIGMA AND E/K FOR AIR AND FUEL ARE THE SAME AS THOSE USED FOR
*  ESTIMATING THE DIFFUSION COEFFICIENT.
*
*  DIMENSIONLESS TEMPERATURES:
*  TASTA=TAVG/EKA
*  TASTF=TAVG/EKF
*
*  OMEGA FOR THE VISCOSITY FOR AIR AND FUEL:
*  OMGVA=AV/TASTA**BV+CV/EXP(DV*TASTA)+EV/EXP(FV*TASTA)
*  OMGVF=AV/TASTF**BV+CV/EXP(DV*TASTF)+EV/EXP(FV*TASTF)

```

```

MOD06810
MOD06820
MOD06830
MOD06840
MOD06850
MOD06860
MOD06870
MOD06880
MOD06890
MOD06900
MOD06910
MOD06920
MOD06930
MOD06940
MOD06950
MOD06960
MOD06970
MOD06980
MOD06990
MOD07000
MOD07010
MOD07020
MOD07030
MOD07040
MOD07050
MOD07060
MOD07070
MOD07080
MOD07090
MOD07100
MOD07110
MOD07120
MOD07130
MOD07140
MOD07150
MOD07160
MOD07170
MOD07180
MOD07190
MOD07200
MOD07210
MOD07220
MOD07230
MOD07240
MOD07250
MOD07260
MOD07270
MOD07280
MOD07290
MOD07300
MOD07310
MOD07320
MOD07330
MOD07340
MOD07350
MOD07360
MOD07370
MOD07380
MOD07390
MOD07400
MOD07410
MOD07420
MOD07430
MOD07440
MOD07450
MOD07460
MOD07470
MOD07480
MOD07490

```

```

* VISCOSITY OF AIR AND FUEL (MICROPOISE):
  VISCA=26.69*(MA*TAVG)**(1./2.)/(SA**2.*OMGVA)
  VISCF=26.69*(MF*TAVG)**(1./2.)/(SF**2.*OMGVF)
*
* MONATOMIC VALUES OF THERMAL CONDUCTIVITY (KTR(I)/KTR(J)):
*
  TCA = 126.2
  PCA = 33.5
  TRF = TAVG/TCF
  TRA = TAVG/TCA
  GAMA = TCA**(1./6.)*MA**0.5/PCA**(2./3.)
  GAMF = TCF**(1./6.)*MF**0.5/PCF**(2./3.)
  KTRAF = (GAMF/GAMA)*((EXP(0.0464*TRA) - EXP(-0.2412*TRA))/
1 (EXP(0.0464*TRF) - EXP(-0.2412*TRF)))
  KTRFA = GAMA*(EXP(0.0464*TRF) - EXP(-0.2412*TRF))/
1 (GAMF*(EXP(0.0464*TRA) - EXP(-0.2412*TRA)))
  KTRAA =1.0
  KTRFF =1.0
*
* FUNCTION (A(I,J)):
*
  AAA =1.0
  AFF =1.0
  AAF = (1.+KTRAF ** (1./2.)*(MA/MF)**(1./4.))**2./(8.*(1.+MA/MF)
*** (1./2.))
  AFA = (1.+KTRFA ** (1./2.)*(MF/MA)**(1./4.))**2./(8.*(1.+MF/MA)
*** (1./2.))
*
* ESTIMATE INDIVIDUAL THERMAL CONDUCTIVITIES USING THE EUCKEN EQUATION
*
* ESTIMATE CV AS CV=CP-R (CAL/GMOL.K):
  CVA=CPAIR*0.239/1000.-1.99
  CVP=CPF/4186.-1.99
*
  AK = 2.6008E-5*TAVG - 5.6496E-3
  BK = -4.5511E-8*TAVG + 8.2873E-6
  CONDAK=(CVA+4.47)*VISCA*1.E-6/MA
  CONDFK = (AK + BK*MF)*1.E-2
*
* CONVERT MASS FRACTIONS TO MOLE FRACTIONS:
  YAMOLE= 1.-YFAVG
  YFMOLE= YFAVG
*
* THERMAL CONDUCTIVITY OF AIR-FUEL MIXTURE:
  CONDK=(YAMOLE*CONDAK/(YAMOLE*AAA+YFMOLE*AAF)
*+YFMOLE*CONDFK/(YAMOLE*AFA+YFMOLE*AFF))*418.6
*
* VISCOSITY OF AIR-FUEL MIXTURE(KG/M-S)
  VISCM=(YAMOLE*VISCA/(YAMOLE*AAA+YFMOLE*AAF)+YFMOLE*VISCF/
1(YAMOLE*AFA+YFMOLE*AFF))*1.E-7
*
  RETURN
  END
*
*****
* SUBROUTINE DENSIT
*
*****
  COMMON/AREA2/N,MA,MF,MN,MO,MREF,PRES,RUGC,M,RHO(40),RHOE(40),
  1T(40),YF(40),YN(40),YO(40),TIME,DISTY(40),DISTOL(40),VAR(40),
  1VARM2(40),VAROLD(40),DISTPR(40),VARPR(40),YMF(40),YMO(40),
  1AVGM,YFAVG,VAROLM(40),VARPRM(40),ADT,BDT,VARVM2
  REAL M(40),MA,MF,MN,MO,MREF
*
* CALCULATE THE MIXTURE MOLECULAR WEIGHT AND DENSITY:
  DO 200 I=1,N

```

```

MOD07500
MOD07510
MOD07520
MOD07530
MOD07540
MOD07550
MOD07560
MOD07570
MOD07580
MOD07590
MOD07600
MOD07610
MOD07620
MOD07630
MOD07640
MOD07650
MOD07660
MOD07670
MOD07680
MOD07690
MOD07700
MOD07710
MOD07720
MOD07730
MOD07740
MOD07750
MOD07760
MOD07770
MOD07780
MOD07790
MOD07800
MOD07810
MOD07820
MOD07830
MOD07840
MOD07850
MOD07860
MOD07870
MOD07880
MOD07890
MOD07900
MOD07910
MOD07920
MOD07930
MOD07940
MOD07950
MOD07960
MOD07970
MOD07980
MOD07990
MOD08000
MOD08010
MOD08020
MOD08030
MOD08040
MOD08050
MOD08060
MOD08070
MOD08080
MOD08090
MOD08100
MOD08110
MOD08120
MOD08130
MOD08140
MOD08150
MOD08160
MOD08170
MOD08180

```

```

M(I)=YF(I)*DISTY(I)+YO(I)*MO+YN(I)*MN
RHO(I)=PRES/RUGC/T(I)
200 CONTINUE
AVGM = M(1)*M(N)/(2.*M(N)/3. + M(1)/3.)
MREF =2.*DISTY(1)/3. + DISTY(N)/3.
RETURN
END
*
*****
*
SUBROUTINE COEF
*
*****
*
COMMON/AREA1/TC, PC, W, R, TAVG, CP, CPL,
1CPF, CPAIR, RHOAVG, AL, BL, CL, DL, TR, DIFFUS, CONDK, DTIME, GO, RHOL, K, RCA,
2RCB, EA, DHF, PATM, YOAMB, YNAMB, GAMMA, ZETA(40), ZETA(40), ZE2DT(40),
3ZE3(40), ZE3D(40), VEL(40), RHOOLD(40), YFOLD(40), TOLD(40), VISCM, PCF
COMMON/AREA2/N, MA, MF, MN, MO, MREF, PRES, RUGC, M, RHO(40), RHOE(40),
1T(40), YF(40), YN(40), YO(40), TIME, DISTY(40), DISTOL(40), VAR(40),
1VARM2(40), VAROLD(40), DISTPR(40), VARPR(40), YMF(40), YMO(40),
1AVGM, YFAVG, VAROLM(40), VARPRM(40), ADT, BDT, VARVM2
COMMON/CCOEF/A0(40), DIF(40), WFO(40), DO(40), WFACT, WF, WEXP
REAL M(40), MF, MA, MO, MN, CONDK, K, MREF
*
* TEMPERATURE EQUATION COEFFICIENTS THAT ARE CONSTANT:
DO 300 I=1,N-1
DIF(I)=ZE2DT(I)/R**2
300 CONTINUE
DO 301 I=2,N-1
WEXP=EXP(-EA*503.5/TOLD(I))
WFACT=-K*MF*ZE3D(I)*DHF*DTIME/3./CP
IF (ABS(WFACT).LT.(1.0E-70/WEXP))GOTO 302
WFO(I)=WFACT*WEXP
GOTO 303
302 WFO(I)=0.
303 DO(I)=ZE3D(I)/3.*RHOOLD(I)
301 CONTINUE
RETURN
END
*
*****
*
SUBROUTINE TEMP
*
*****
*
COMMON/AREAL/TC, PC, W, R, TAVG, CP, CPL,
1CPF, CPAIR, RHOAVG, AL, BL, CL, DL, TR, DIFFUS, CONDK, DTIME, GO, RHOL, K, RCA,
2RCB, EA, DHF, PATM, YOAMB, YNAMB, GAMMA, ZETA(40), ZETA(40), ZE2DT(40),
3ZE3(40), ZE3D(40), VEL(40), RHOOLD(40), YFOLD(40), TOLD(40), VISCM, PCF
COMMON/AREA2/N, MA, MF, MN, MO, MREF, PRES, RUGC, M, RHO(40), RHOE(40),
1T(40), YF(40), YN(40), YO(40), TIME, DISTY(40), DISTOL(40), VAR(40),
1VARM2(40), VAROLD(40), DISTPR(40), VARPR(40), YMF(40), YMO(40),
1AVGM, YFAVG, VAROLM(40), VARPRM(40), ADT, BDT, VARVM2
COMMON/AREA3/RDOT, AMEANL, AMEANV, DTLDT, VARV
COMMON/AREA5/VISCA, VISCF, CONDAK, CONDFK, CVA, CVF, YAMOLE, YFMOLE,
1AAF, AFA, RAVG, CPN, CPO, AO, A1, A2, A3, A4, BO, B1, B2, B3, B4, AT, BT, CT, AP, BP,
1DP, DBAR, DTUITL, DHAT
COMMON/CCOEF/A0(40), DIF(40), WFO(40), DO(40), WFACT, WF, WEXP
COMMON/BLOCK/YFTHET(40), YFPSI(40), YFTOLD(40), YPSIOL(40)
DIMENSION A(40), B(40), C(40), D(40), FCNV(40), CONDIF(40)
DIMENSION P(40), Q(40), PEPOW(40), SUMM(40)
REAL M(40), MF, MA, MO, MN, CONDK, CONCPK, MREF
*
DTR=DTIME/R
GTRR = RDOT * DTR
CONCPK=CONDK/CP
ACP = AO + A1*TAVG + A2*TAVG**2 + A3*TAVG**3

```

```

BCP = BO + B1*TAVG + B2*TAVG**2 + B3*TAVG**3          MOD08890
ACP = RUGC*1000*ACP          MOD08900
BCP = RUGC*1000*BCP          MOD08910
*          MOD08920
* CALCULATE THE COEFFICIENTS FOR THE ENERGY EQUATION:  MOD08930
* FCNV,CONDIF AND PE CORRESPOND TO FE,DE AND PECLET IN PATANKAR MOD08940
DO 400 I=1,N-1          MOD08950
  SUMM(I)=GAMMA*(YF(I+1)-YF(I))*(ACP-CPAIR)          MOD08970
  SUMM(I)=SUMM(I)+RHOAVG*DTUITL*BCP*(YFTHET(I+1)-YFTHET(I)) MOD08980
  SUMM(I)=-1.*ZE2DT(I)/R**2*SUMM(I)/CP          MOD08990
  FCNV(I)=VEL(I)*DTR+SUMM(I)          MOD09000
  CONDIF(I)=CONCPK*DIF(I)          MOD09010
  PE=FCNV(I)/CONDIF(I)          MOD09020
  PEPOW(I)=(1.-0.1*ABS(PE))**5          MOD09030
400 CONTINUE          MOD09040
DO 401 I=2,N-1          MOD09050
  WF=WFO(I)*YF(I)**RCA*YO(I)**RCB*RHO(I)**(RCA+RCB) MOD09060
  B(I)=CONDIF(I)*AMAX1(0.,PEPOW(I))+AMAX1(-1.*FCNV(I),0.) MOD09070
  C(I)=CONDIF(I-1)*AMAX1(0.,PEPOW(I-1))+AMAX1(FCNV(I-1),0.) MOD09080
  A(I)=RHO(I)/3.*ZE3D(I)*(1.-3.*GTRR)-SUMM(I)+SUMM(I-1) MOD09090
  1 -WF*CP/DHF/MF          MOD09100
  A(I)=A(I)+B(I)+C(I)+(FCNV(I)-FCNV(I-1))          MOD09110
  D(I)=D0(I)*TOLD(I)-WF          MOD09120
401 CONTINUE          MOD09130
*          MOD09140
* TRIDIAGONAL-MATRIX ALGORITHM:          MOD09150
  A(1)=1.0          MOD09160
  B(1)=0.0          MOD09170
  C(1)=0.0          MOD09180
  D(1)=T(1)          MOD09190
  P(1)=B(1)/A(1)          MOD09200
  Q(1)=D(1)/A(1)          MOD09210
DO 403 I=2,N-1          MOD09220
  P(I)=B(I)/(A(I)-C(I)*P(I-1))          MOD09230
  Q(I)=(D(I)+C(I)*Q(I-1))/(A(I)-C(I)*P(I-1)) MOD09240
403 CONTINUE          MOD09250
DO 404 I=N-1,2,-1          MOD09260
  T(I)=P(I)*T(I+1)+Q(I)          MOD09270
404 CONTINUE          MOD09280
  RETURN          MOD09290
  END          MOD09300
*          MOD09310
*****          MOD09320
*          MOD09330
SUBROUTINE CONC          MOD09340
*          MOD09350
*****          MOD09360
*          MOD09370
COMMON/AREAL/TC,PC,W,R,TAVG,CP,CPL,          MOD09380
1CPF,CPAIR,RHOAVG,AL,BL,CL,DL,TR,DIFFUS,CONDK,DTIME,G0,RHOL,K,RCA, MOD09390
2RCB,EA,DHF,PATM,YOAMB,YNAMB,GAMMA,ZETA(40),ZETA(40),ZE2DT(40), MOD09400
3ZE3(40),ZE3D(40),VEL(40),RHOOLD(40),YFOLD(40),TOLD(40),VISCM,PCF MOD09410
COMMON/AREA2/N,MA,MF,MN,MO,MREF,PRES,RUGC,M,RHO(40),RHOE(40), MOD09420
1T(40),YF(40),YN(40),YO(40),TIME,DISTY(40),DISTOL(40),VAR(40), MOD09430
1VARM2(40),VAROLD(40),DISTPR(40),VARPR(40),YMF(40),YMO(40), MOD09440
1AVGM,YFAVG,VAROLM(40),VARPRM(40),ADT,BDT,VARVM2          MOD09450
COMMON/AREA3/RDOT,AMEANL,AMEANV,DTLDT,VARV          MOD09460
COMMON/CCOEF/A0(40),DIF(40),WFO(40),D0(40),WFACT,Wf,WEXP          MOD09470
DIMENSION A(40),B(40),C(40),D(40),FCNV(40),P(40),Q(40)          MOD09480
DIMENSION GAMDIF(40),PEPOW(40)          MOD09490
REAL M(40),MF,MA,MO,MN,MREF          MOD09500
*          MOD09510
C          MOD09520
  GTRR=0.0          MOD09530
  DTR=DTIME/R          MOD09530
  GTRR = RDOT * DTR          MOD09540
*          MOD09550
* CALCULATE THE COEFFICIENTS FOR THE DIFFUSION EQUATION: MOD09560
* FCNV,GAMDIF AND PE CORRESPOND TO FE,DE AND PECLET IN PATANKAR MOD09570
DO 100 I=1,N-1          MOD09580

```

```

FCNV(I)=VEL(I)*DTR
GAMDIF(I)=GAMMA*DIF(I)
PE=FCNV(I)/GAMDIF(I)
PEPOW(I)=(1.-0.1*ABS(PE))**5
100 CONTINUE
DO 101 I=2,N-1
  B(I)=GAMDIF(I)*AMAX1(0.,PEPOW(I))+AMAX1(-1.*FCNV(I),0.)
  C(I)=GAMDIF(I-1)*AMAX1(0.,PEPOW(I-1))+AMAX1(FCNV(I-1),0.)
  A(I)=B(I)+C(I)+RHO(I)/3.*ZE3D(I)*(1.-3.*GTRR)
  A(I)=A(I)+(FCNV(I)-FCNV(I-1))
  D(I)=D0(I)*YFOLD(I)
101 CONTINUE
*
*
* TRIDIAGONAL-MATRIX ALGORITHM:
  A(1)=1.0
  B(1)=0.0
  C(1)=0.0
  D(1)=YF(1)
  P(1)=B(1)/A(1)
  Q(1)=D(1)/A(1)
  DO 103 I=2,N-1
    P(I)=B(I)/(A(I)-C(I)*P(I-1))
    Q(I)=(D(I)+C(I)*Q(I-1))/(A(I)-C(I)*P(I-1))
103 CONTINUE
DO 104 I=N-1,2,-1
  YF(I)=P(I)*YF(I+1)+Q(I)
104 CONTINUE
DO 199 I=1,N
  YMF(I)=YF(I)*AMEANV/M(I)
199 CONTINUE
DO 105 I=1,N-1
  YO(I)=YOAMB*(1.-YF(I))
  YN(I)=YO(I)*YNAMB/YOAMB
105 CONTINUE
RETURN
END
*
*****
*
SUBROUTINE CONCI
*
*****
*
COMMON/AREA1/TC,PC,W,R,TAVG,CP,CPL,
1CPF,CPAIR,RHOAVG,AL,BL,CL,DL,TR,DIFFUS,CONDK,DTIME,G0,RHOL,K,RCA,
2RCB,EA,DHF,PATM,YOAMB,YNAMB,GAMMA,ZETA(40),ZETA(40),ZE2DT(40),
3ZE3(40),ZE3D(40),VEL(40),RHOOLD(40),YFOLD(40),TOLD(40),VISC,PCF
COMMON/AREA2/N,MA,MF,MN,MO,MREF,PRES,RUGC,M,RHO(40),RHOE(40),
1T(40),YF(40),YN(40),YO(40),TIME,DISTY(40),DISTOL(40),VAR(40),
1VARM2(40),VAROLD(40),DISTPR(40),VARPR(40),YMF(40),YMO(40),
1AVGM,YFAVG,VAROLM(40),VARPRM(40),ADT,BDT,VARVM2
COMMON/AREA3/RDOT,AMEANL,AMEANV,DTLDT,VARV
COMMON/AREA5/VISCA,VISCF,CONDAK,CONDFK,CVA,CVF,YAMOLE,YFMOLE,
1AAF,AFA,RAVG,CPN,CPO,AO,A1,A2,A3,A4,BO,B1,B2,B3,B4,AT,BT,CT,AP,BP,
1DP,DBAR,DTUITL,DHAT
COMMON/CCOEF/A0(40),DIF(40),WF0(40),D0(40),WFACT,Wf,WEXP
COMMON/BLOCK/YFTHET(40),YFPSI(40),YFTOLD(40),YFSIOL(40)
COMMON/BLOCK1/GAMDIT(40),GAMDIP(40),PET(40),PEP(40),PEPOT(40),
1ATH(40),BTH(40),CTH(40),APS(40),BPS(40),CPS(40)
DIMENSION A(40),B(40),C(40),DI(40),FCNV(40),PI(40),QI(40)
DIMENSION DV(40),FV(40),QV(40)
DIMENSION GAMDIF(40),PEPOW(40)
REAL M(40),MF,MA,MO,MN,MREF
DTR=DTIME/R
GTRR = RDOT * DTR
*
* CALCULATE THE COEFFICIENTS FOR THE DISTRIBUTION EQUATION:
* FCNV,GAMDIF AND PE CORRESPOND TO FE,DE AND PECLET IN PATANKAR

```

```

MOD09590
MOD09600
MOD09610
MOD09620
MOD09630
MOD09640
MOD09650
MOD09660
MOD09670
MOD09680
MOD09690
MOD09700
MOD09710
MOD09720
MOD09730
MOD09740
MOD09750
MOD09760
MOD09770
MOD09780
MOD09790
MOD09800
MOD09810
MOD09820
MOD09830
MOD09840
MOD09850
MOD09860
MOD09870
MOD09880
MOD09890
MOD09900
MOD09910
MOD09920
MOD09930
MOD09940
MOD09950
MOD09960
MOD09970
MOD09980
MOD09990
MOD10000
MOD10010
MOD10020
MOD10030
MOD10040
MOD10050
MOD10060
MOD10070
MOD10080
MOD10090
MOD10100
MOD10110
MOD10120
MOD10130
MOD10140
MOD10150
MOD10160
MOD10170
MOD10180
MOD10190
MOD10200
MOD10210
MOD10220
MOD10230
MOD10240
MOD10250
MOD10260
MOD10270

```

```

DO 501 I = 1,N-1
FCNV(I) = VEL(I)*DTR
GAMDIT(I) = RHOAVG*DTUITL*DIF(I)
GAMDIP(I) = RHOAVG*DHTAT*DIF(I)
PET(I) = FCNV(I)/GAMDIT(I)
PEP(I) = FCNV(I)/GAMDIP(I)
PEPOT(I) = (1. - 0.1*ABS(PET(I)))**5
PEPOW(I) = (1. - 0.1*ABS(PEP(I)))**5
501 CONTINUE
DO 502 I = 2,N-1
BTH(I) = GAMDIT(I)*AMAX1(0.,PEPOT(I)) + AMAX1(-1*FCNV(I),0.)
CTH(I) = GAMDIT(I-1)*AMAX1(0.,PEPOT(I-1)) + AMAX1(FCNV(I-1),0.)
ATH(I) = BTH(I)+CTH(I)+RHO(I)/3.*ZE3D(I)*(1.-3.*GTRR)
ATH(I) = ATH(I) + FCNV(I) - FCNV(I-1)
BPS(I) = GAMDIP(I)*AMAX1(0.,PEPOW(I)) + AMAX1(-FCNV(I),0.)
CPS(I) = GAMDIP(I-1)*AMAX1(0.,PEPOW(I-1)) + AMAX1(FCNV(I-1),0.)
APS(I) = BPS(I)+CPS(I) + RHO(I)/3.*ZE3D(I)*(1.-3.*GTRR)
APS(I) = APS(I) + FCNV(I) - FCNV(I-1)
DI(I) = DO(I)*YFTOLD(I)
DV(I) = DO(I)*YFSIOL(I)
502 CONTINUE
*
*
* TRIDIAGONAL-MATRIX ALGORITHM:
ATH(1) = 1.0
BTH(1) = 0.0
CTH(1) = 0.0
APS(1) = 1.0
BPS(1) = 0.0
CPS(1) = 0.0
* MEAN I TIMES YF
DI(1) = YFTHET(1)
PI(1) = BTH(1)/ATH(1)
QI(1) = DI(1)/ATH(1)
* PSI TIMES YF
DV(1) = YFPSI(1)
PV(1) = BPS(1)/APS(1)
QV(1) = DV(1)/APS(1)
*
DO 503 I = 2,N-1
PI(I)=BTH(I)/(ATH(I)-CTH(I)*PI(I-1))
QI(I)=(DI(I)+CTH(I)*QI(I-1))/(ATH(I)-CTH(I)*PI(I-1))
PV(I)=BPS(I)/(APS(I)-CPS(I)*PV(I-1))
QV(I)=(DV(I)+CPS(I)*QV(I-1))/(APS(I)-CPS(I)*PV(I-1))
503 CONTINUE
*
DO 504 I=N-1,2,-1
YFTHET(I)=PI(I)*YFTHET(I+1)+QI(I)
YFPSI(I)=PV(I)*YFPSI(I+1)+QV(I)
504 CONTINUE
IFLAG = 0
DO 106 I = 2,N
IF (IFLAG.EQ.1) GOTO 107
IF (YF(I)*1.0E38.LT.1.0E-40) THEN
IFLAG = 1
NFLAG = I
GOTO 107
ENDIF
DISTY(I) = YFTHET(I)/YF(I)
VARM2(I) = YFPSI(I)/YF(I)
VAR(I) = VARM2(I) - DISTY(I)**2
GOTO 106
107 DISTY(I) = DISTY(NFLAG-1)
VARM2(I) = VARM2(NFLAG-1)
VAR(I) = VARM2(I) - DISTY(I)**2
106 CONTINUE
RETURN
END
*

```

```

*
*
*****MOD11170
*****MOD11190
*****MOD11200
SUBROUTINE BOILIN
*****MOD11210
*****MOD11220
COMMON/AREAI/TC, PC, W, R, TAVG, CP, CPL,
MOD11230
1CPF, CPAIR, RHOAVG, AL, BL, CL, DL, TR, DIFFUS, CONDK, DTIME, GO, RHOL, K, RCA,
MOD11240
2RCB, EA, DHF, PATM, YOAMB, YNAMB, GAMMA, ZETA(40), ZETA(40), ZE2DT(40),
MOD11250
3ZE3(40), ZE3D(40), VEL(40), RHOOLD(40), YFOLD(40), TOLD(40), VISCM, PCF
MOD11260
COMMON/AREA3/RDOT, AMEANL, AMEANV, DTLDT, VARV
MOD11270
COMMON/AREA4/A, B, SFG, ALPHAL, BETAL, VLGAMA, YFR, TBOIL, DT, TSTART,
MOD11280
1ALPHAV, BETAV
MOD11290
COMMON/AREA5/VISCA, VISCF, CONDAK, CONDFK, CVA, CVF, YAMOLE, YFMOLE,
MOD11300
1AAF, AFA, RAVG, CPN, CPO, AO, A1, A2, A3, A4, BO, B1, B2, B3, B4, AT, BT, CT, AP, BP,
MOD11310
1DP, DBAR, DTUIT, DHAT
MOD11320
INTEGER N
MOD11330
REAL TMID, A, B, VLGAMA, BETAL, ALPHAL, SFG
MOD11340
DIMENSION T(1000), F(1000)
MOD11350
N = 1000
MOD11360
YFA = 1.
MOD11370
RUGC = 8.314
MOD11380
SFGR=SFG/RUGC
MOD11390
TC = AT + BT*AMEANL
MOD11400
TO = 200.
MOD11410
TF = TC
MOD11420
DT = (TC-TO)/N
MOD11430
T(1) = TO
MOD11440
DO 5 I=2,N
MOD11450
T(I) = T(I-1) + DT
MOD11460
5 CONTINUE
MOD11470
DO 10 I=1,N
MOD11480
F(I) = YFA - EXP(SFGR *(1.- (A + VLGAMA*B)/T(I)))/
MOD11490
((1.+SFGR*B*BETAL/T(I))**ALPHAL)
MOD11500
1 IF(I.EQ.1) GOTO 10
MOD11510
J = 0
MOD11520
3 P=F(I)*F(I-1)
MOD11530
J = J+1
MOD11540
IF (J.EQ.1000) GOTO 4
MOD11550
IF(P.LT.0.0) THEN
MOD11560
TSTART = T(I-1)
MOD11570
TSTOP = T(I)
MOD11580
TMID = (TSTART + TSTOP)/2
MOD11590
DIF = ABS(TSTOP - TSTART)
MOD11600
IF (DIF.LE.0.01) THEN
MOD11610
TBOIL = TSTART
MOD11620
GOTO 4
MOD11630
ELSEIF (P.LT.0.0) THEN
MOD11640
F(I) = YFA - EXP(SFGR *(1. - (A + VLGAMA*B)/TMID))/
MOD11650
((1.+SFGR*B*BETAL/TMID)**ALPHAL)
MOD11660
1 T(I) = TMID
MOD11670
GOTO 3
MOD11680
ELSE
MOD11690
F(I-1) = YFA - EXP(SFGR *(1. - (A + VLGAMA*B)/TMID))/
MOD11700
((1.+SFGR*B*BETAL/TMID)**ALPHAL)
MOD11710
1 T(I-1) = TMID
MOD11720
GOTO 3
MOD11730
ENDIF
MOD11740
10 ENDIF
MOD11750
CONTINUE
MOD11760
4 RETURN
MOD11770
END
MOD11780

```